Application of Mirror-image Screening Technology by Expansion of Bioassay Systems and Chiral Resources

Keitou Shu
Graduate School of Advanced Integrated Studies in Human Survivability, Kyoto University

Contents

Preface

In several decades, the need to find effective therapeutic agents for a variety of targets has pushed the process of drug discovery towards traditional small molecules, or larger molecule and alternative therapeutic modalities including biologics, antibodies, and oligonucleotides.[1] Compounds with chiralities occupy a certain part of the therapeutic agents and this chirality in life science is undoubtedly essential with respect to their therapeutic, toxicological, and pharmacokinetic properties. Especially, thalidomide-induced teratogenicity implied the importance of therapeutic efficacy and safety of chiral drugs.[2] This well-known tragedy gave impetus to consider that the opposite enantiomer of bioactive molecule, that is supposed to be inactive or nontoxic, might have an unexpected bioactivity (Figure 1).[3] For instance, Levomethorphan is a morphine analog with strong respiratory depression as an opioid analgesic effect, whereas Dextromethorphan, its mirror-image compound, is widely used as over-the-counter cough and cold medicine.[4] (−)-Propranolol is a β-Adrenoceptor blocker and used to treat high blood pressure, whereas (+)-enantiomer is hyperthyroidism.[5] Based on these observation, mirror-image compounds of library resources including chemical compounds, natural products, and biomolecules could have potential bioactivities as valuable resources in drug discovery. Therefore, development of novel approach to disclosure the unevaluated value of chiral compounds and expansion of the number of chiral compounds in the library would accelerate an efficient isolation of potent therapeutic agents.

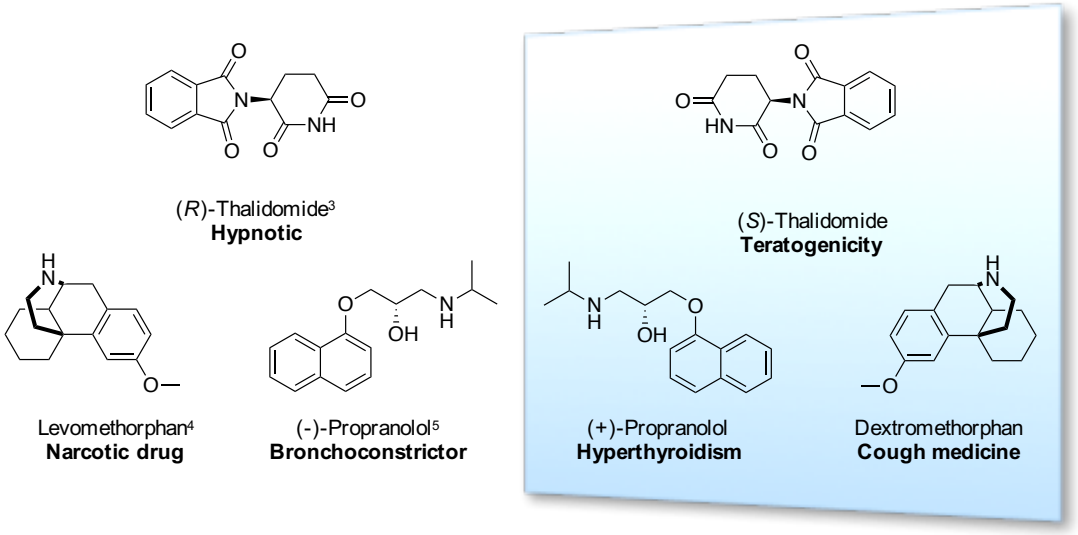

Figure 1. Representative mirror-image pairs of synthetic compounds and their unique bioactivities.

Besides an accidental discovery of these unprecedented bioactivities of mirror-image synthetic compounds (Figure 1), several groups successfully established the screening technology to identify mirror-image biomolecules such as peptides and oligonucleotides with physiological activity and many potential compounds have been isolated (Figure 2). Major advantage of mirror-image biomolecules is their ability to resist against in vivo proteolysis and escape immunoreactivity so that they would enjoy a native biostability. In 1996, Schumacher et al have developed mirror-image phage display to identify bioactive D-peptides.[6a] They focused on the fact that the three-dimensional structure of proteins composed of D-amino acids are the exact mirror image of the corresponding naturally occurring L-proteins. In this process, D-peptide with binding affinity against L-protein can be identified by mirror-image phage display using synthetic D-protein. They identified D-peptide agents that targets Src homology 3 (SH3) domain of c-Src in a proof-of-concept experiment. Other groups have also identified potent D-peptide inhibitors through mirror-image phage display for important targets such as the MDM2−p53 interaction,[6b] or HIV entry binding to the N-terminal pocket of gp41.[6c] At the same year as the first report of mirror-image phage display, Klussmann demonstrated mirror-image screening system to isolate nuclease-resistant L-RNA aptamers, called Spiegelmers, from an RNA library.[7a] Some of L-RNA identified by mirror-image platform are now in clinical trials and demonstrated a good safety profile as well as inhibition of their respective targets.[7b,c] Despite the accessibility of mirror-image biomolecules is a great advance, several innate limitations of biomolecules still remain, such as lack of oral availability, poor membrane permeability, and limited delivery methods. To identify attractive therapeutic agents by taking advantage of novel mirror-image screening technology, the author's group (Oishi's group) focused on the application of mirror-image screening system to chiral natural products because natural products generally have favorable drug-like properties including the appropriate molecular size, bioavailability, and many interactive moieties for binding to the target proteins.

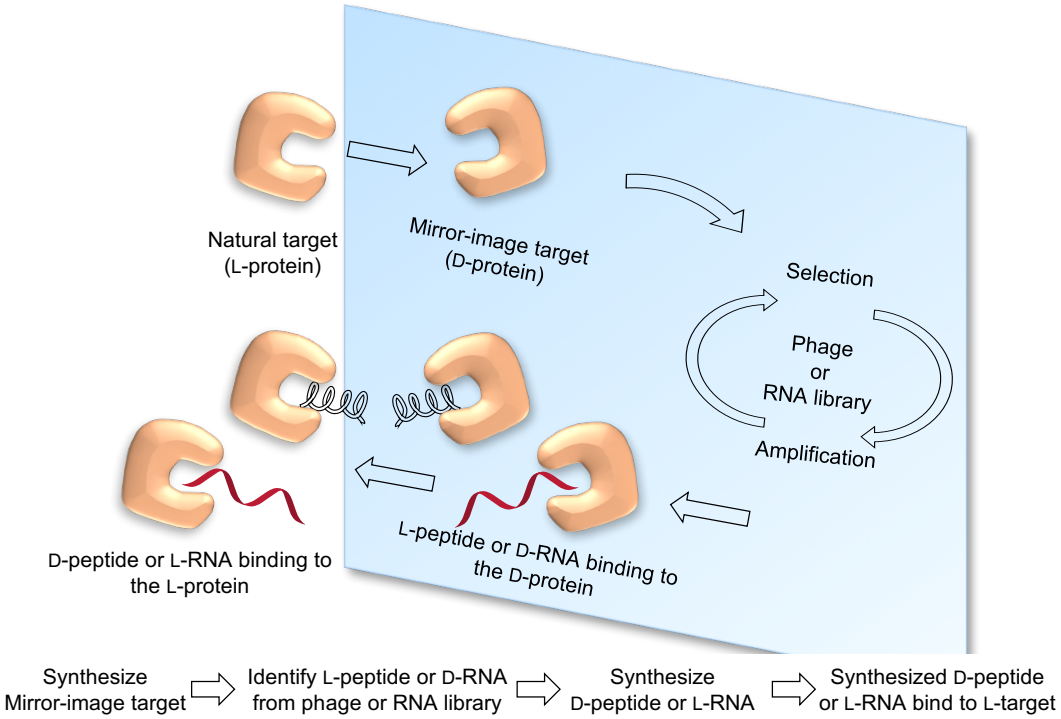

Figure 2. Identification of D-peptide and/or L-RNA ligands through the screening platform using synthetic D-protein. The identification of selected L-peptides and/or D-RNAs that bind to D-protein also provides the sequence of D-peptides and/or L-RNA bind to the L-protein.

Mirror-image library of natural products and its derivatives have identical drug-like properties to natural products[8] with the unique, complex, and sp^3-carbon-rich scaffold providing attractive biological activities. In addition, there are many reports demonstrating that the enantiomer of natural products exhibits unusual bioactivities (Figure 3). Based on these unique stereochemistry-bioactivity relationship, mirror-image natural products and its derivatives are expected to be the valuable chemical resources for a screening campaign. However, enantiomers of chiral natural products as screening resources are rarely obtained neither from natural resources, nor chemical synthesis of individual compounds. To overcome limited availability of mirror-image natural products and evaluate those compounds as an unexplored screening resources, Noguchi et al. have developed screening strategy using synthetic D-protein (Figure 4).[21a] In this approach, the bioactivity of existing chiral natural products was evaluated using a synthetic mirror-image MDM2 protein (D-MDM2). After mirror-image screening campaign from 22,293 compounds including chiral natural products, an a-tocopherol derivative was identified as a D-MDM2–D-p53 inhibitor. The mirror-image structure of the hit compound reproduced the inhibitory activity against the native L-MDM2–L-p53 interaction. It was demonstrated that just two chemical syntheses of mirror- image molecules of a target D-protein and hit compound(s) allow us to discover novel MDM2–p53 inhibitors without syntheses of

numerous unavailable mirror-image natural products. This approach has also been applied to screen systems for novel Grb2 SH2 domain inhibitors.[21b] The overarching goal of the author's project is to identify a variety of novel therapeutic agents through mirror-image screening technology and hopefully unveil the potential value of mirror-image library of natural products. To this end, the author decided to extends the applicability of this screening platform to another therapeutic target for cancer treatment. Establishment of facile synthetic protocol for preparation of target proteins with different tags enables us to develop several in vitro assay systems and rapid discovery of promising hits.

In addition to extension of the variety of bioassays using D-protein technology, the author also develops the methodology of synthetic library construction with chiralities on the solid-phase to complement the natural products library as a screening recourse. Particularly, one bead one compound library (OBOC library) facilitates to isolate hit molecule with high target-selectivity by incubating unlabeled or differentially labeled off targets in vitro assay. OBOC libraries is a promising approach for the rapid and inexpensive synthesis of a large number of synthetic libraries of potential protein ligands or therapeutic agents by a split and pool synthesis (Figure 5A).[22] In this synthetic approach, several kinds of oligomers with chirality and different functions can be prepared easily including incorporation of unnatural amino acids such as D-amino acids for high stability in plasma and low immunogenicity (Figure 5B)[22a] and N-alkylation of glycine appending further cell permeability than peptide (Figure 5C).[22b] Recently, Kodadek's group designed chiral oligomers of pentenoic acids (COPAs) providing 3-dimention space and constrained conformation (Figure 5D).[22c] The major obstacle for making OBOC library so far was the limitation of chemical strategy available for library construction on the beads. Because of high dependence on MS-MS sequencing for hit identification of the hit structures after screening, iterative employment of isomer unit is inoperable and synthetic option to ligate each monomer units was limited to an amide bond.[23] To overcome this defect, recently, the Paegel laboratory has extended DNA-encoding technology to the OBOC platform (Figure 6A).[24] This important advance eliminates the need for direct MS-based characterization of hit compounds, which had largely limited OBOC libraries to oligomers, such as peptides and peptoids, therefore DNA encoding allows us to create any kind of molecule on the beads. Additional advantage that the library can be constructed and screened on 10 μm TentaGel beads, which are small enough to pass through a flow cytometer (Figure 6B). Isolation of hit beads by using a fluorescent activated cell sorter (FACS) is far more convenient than manual picking and facilitates two-color screens that demand selectivity for a target over one or more off-targets.[25]

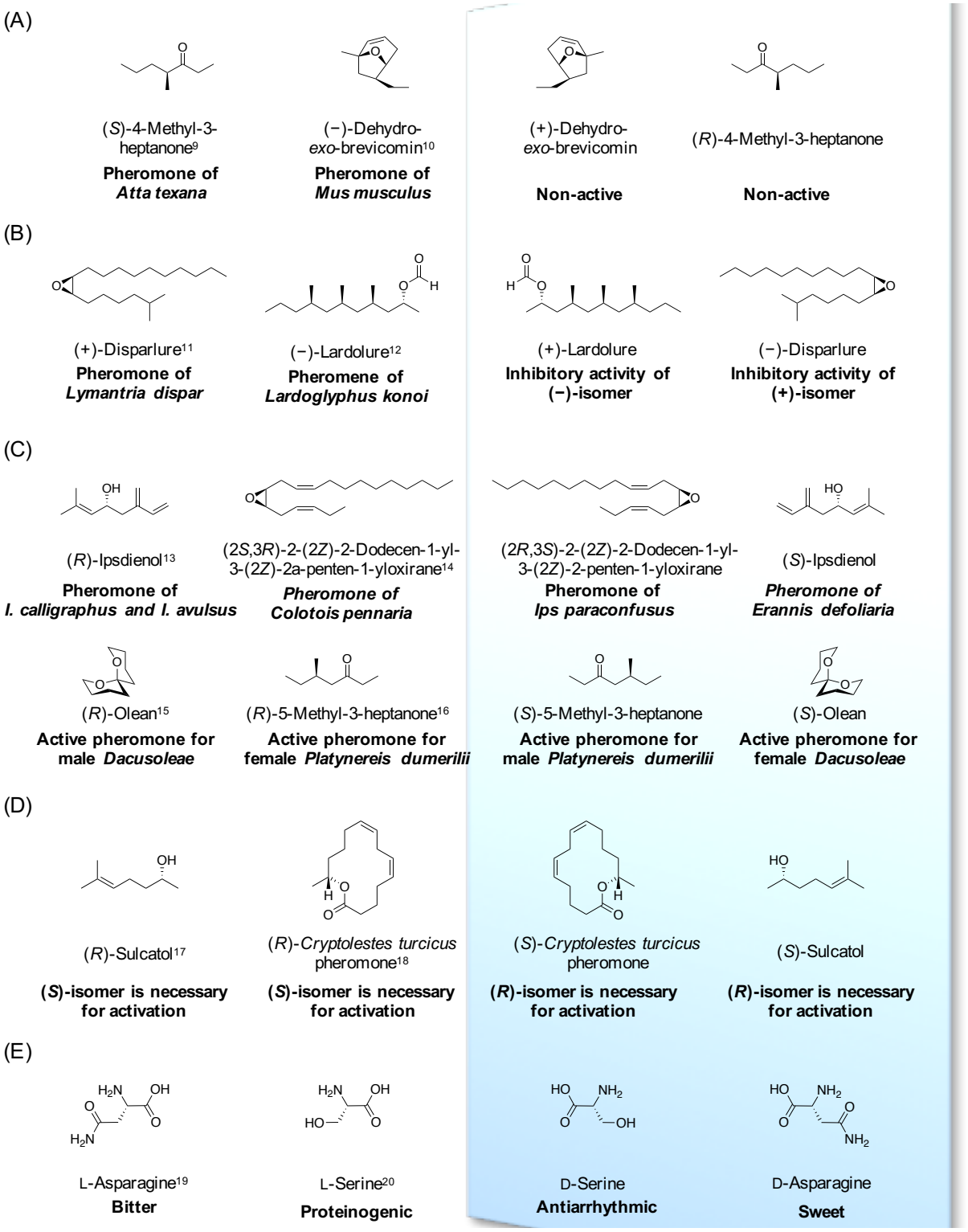

Figure 3. Classification of different biological activities of chiral natural products. Mirror-image pairs are divided into five categories. (A) Only a single enantiomer is bioactive, and its opposite enantiomer does not inhibit the response. (B) Only a single enantiomer is bioactive and its enantiomer inhibits the response. (C) Different enantiomers are employed by different sex or species. (D) Both enantiomers are essential for bioactivity. (E) Two enantiomers exhibit irreverent bioactivities.

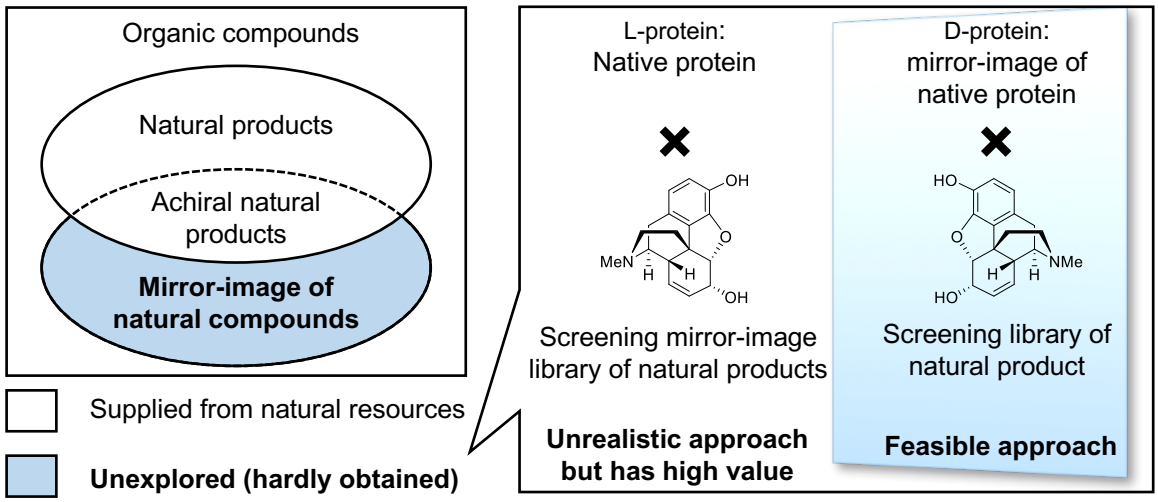

Figure 4. Unevaluated chemical space of mirror-image natural products and our screening approach to evaluate mirror-image library of natural products using D-protein.

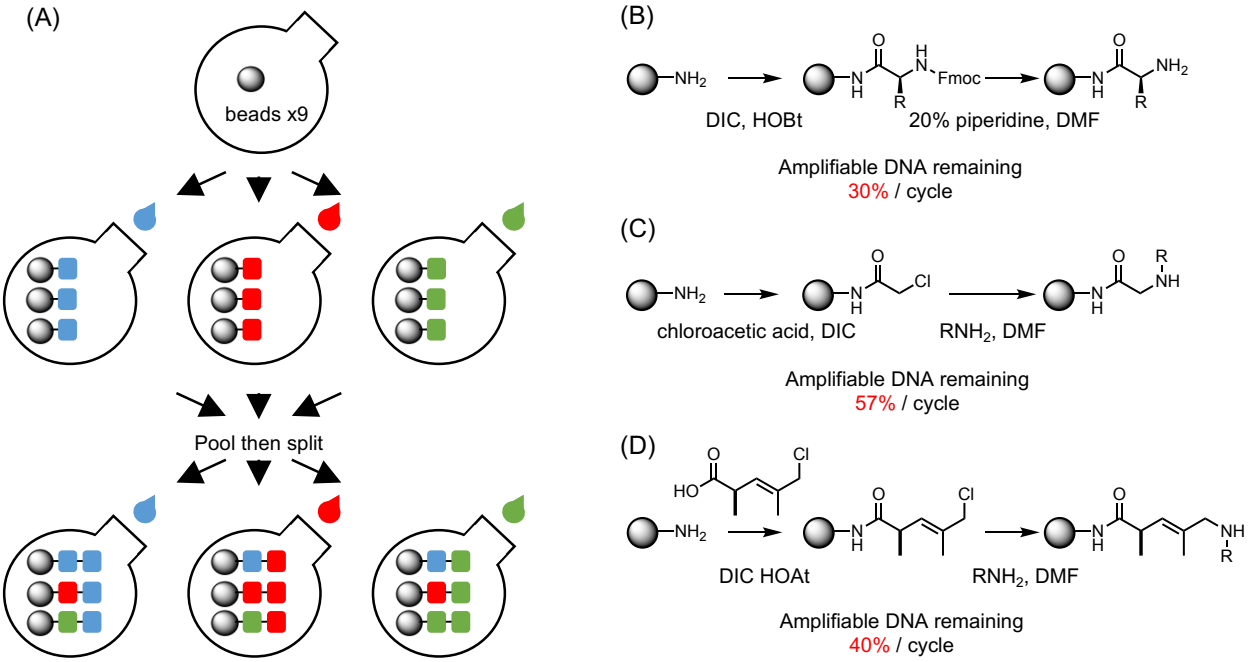

Figure 5. (A) Schematic depiction of the split and pool synthesis of combinatorial library synthesis. (B) Peptide library synthesis on the solid phase. (C) Halide substitution for peptoide library synthesis. (D) Chiral oligomers of pentenoic acids (COPAs) library synthesis on the solid phase.

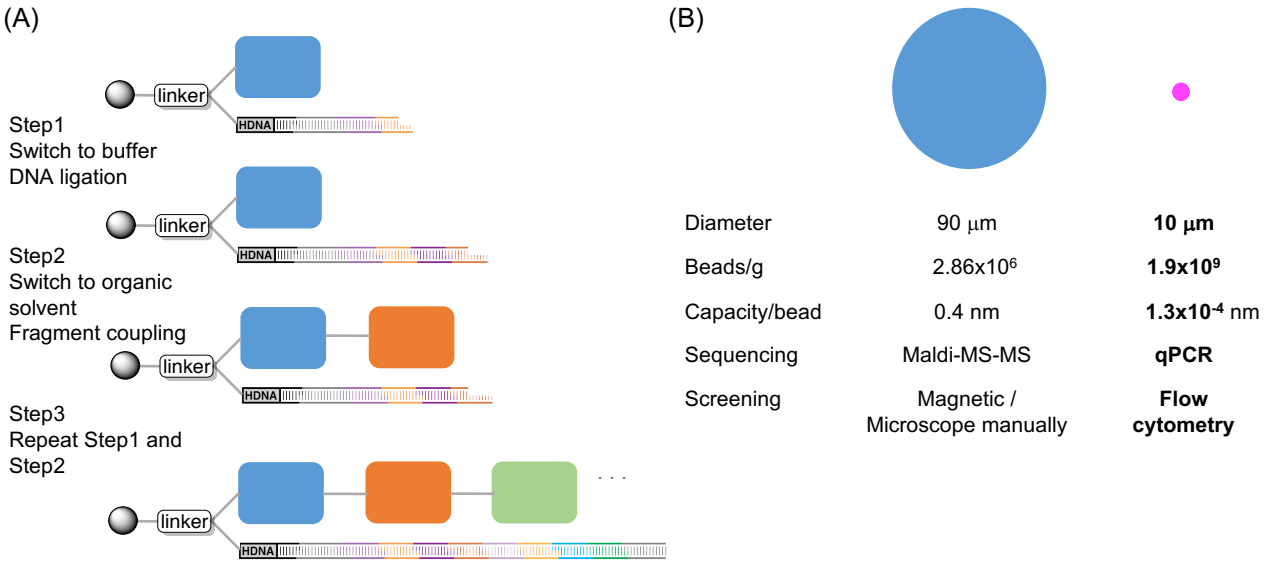

Figure 6. (A) Schematic process of fragment construction and its encoding DNA. (B) Beads comparison between previous macro beads (blue) and 10 μm Tentagel beads (magenta).

With this powerful technology now established, the author decided to expand the repertoire of chemical reactions that can be used to make OBOC libraries. Reactions that create chiral centers are of particular interest, since there is a general feeling in the screening community that molecules with a high level of "three-dimensionality" and natural product-like character would tend to bind their targets with higher selectivity than the flat, largely aromatic compounds that dominate most current screening collections. Another important consideration in developing reactions for the synthesis of DNA-encoded libraries is to evaluate the level of chemical damage suffered by the encoding DNA that would compromise it amplifiability. For example, routine amino acid or peptoid couplings are known to degrade encoding tags to some degree.[26]

In this thesis, the author describes practical application of mirror-image screening process by expansion of the repertoire of bioassays using D-protein technology and chemical reactions for OBOC library construction.

In Chapter 1, Section 1, the author describes the chemical synthesis of both enantiomers of Src SH2 domains and development of the screening platform using several in vitro assays.

In Chapter 1, Section 2, the author reports the chemical synthesis of both enantiomers of XIAP BIR3 domains and development of the screening platform using several in vitro assays

In Chapter 2, the author describes the chemical synthesis of efficient solid-phase synthesis of β-hydroxy ketones *via* the organocatalytic aldol reaction in a DNA compatible fashion.

References

1. Valeur, E., Guéret, S.M., Adihou, H., Gopalakrishnan, R., Lemurell, M., Waldmann, H., Grossmann, T.N. & Plowright, A.T. 2017, "New modalities for challenging targets in drug discovery", *Angewandte Chemie International Edition,* vol. 56, no. 35, pp. 10294-10323.
2. (a) Blaschke, G. 1979, "Chromatographische racemattrennung von thalidomid und teratogene wirkung der enantiomere", *Arzneimittelforschung,* vol. 29, no. 10, pp. 1640-1642. (b) Fabro, S., Smith, R.L. & Williams, R. 1967, "Toxicity and teratogenicity of optical isomers of thalidomide", *Nature,* vol. 215, no. 5098, pp. 296-296.
3. Ariens, E. 1991, "Racemic therapeutics—ethical and regulatory aspects", *European Journal of Clinical Pharmacology,* vol. 41, no. 2, pp. 89-93.
4. Benson, W.M., Stefko, P.L. & Randall, L.O. 1953, "Comparative pharmacology of levorphan, racemorphan and dextrorphan and related methyl ethers", *The Journal of Pharmacology and Experimental Therapeutics,* vol. 109, no. 2, pp. 189-200.
5. (a) Howe, R. & Shanks, R. 1966, "Optical isomers of propranolol", *Nature,* vol. 210, no. 5043, pp. 1336-1338. (b) Barrett, A. & Cullum, V.A. 1968, "The biological properties of the optical isomers of propranolol and their effects on cardiac arrhythmias", *British Journal of Pharmacology,* vol. 34, no. 1, pp. 43-55. (c) Stoschitzky, K., Lindner, W., Egginger, G., Brunner, F., Obermayer-Pietsch, B., Passath, A. & Klein, W. 1992, "Racemic (*R*, *S*)-propranolol versus half-dosed optically pure (*S*)-propranolol in humans at steady state: Hemodynamic effects, plasma concentrations, and influence on thyroid hormone levels", *Clinical Pharmacology & Therapeutics,* vol. 51, no. 4, pp. 445-453.
6. (a) Schumacher, T.N., Mayr, L.M., Minor, D.L.,Jr, Milhollen, M.A., Burgess, M.W. & Kim, P.S. 1996, "Identification of D-peptide ligands through mirror-image phage display", *Science,* vol. 271, no. 5257, pp. 1854-1857. (b) Liu, M., Li, C., Pazgier, M., Li, C., Mao, Y., Lv, Y., Gu, B., Wei, G., Yuan, W., Zhan, C., Lu, W.Y. & Lu, W. 2010, "D-peptide inhibitors of the p53-MDM2 interaction for targeted molecular therapy of malignant neoplasms", *Proceedings of the National Academy of Sciences of the United States of America,* vol. 107, no. 32, pp. 14321-14326. (c) Eckert, D.M., Malashkevich, V.N., Hong, L.H., Carr, P.A. & Kim, P.S. 1999, "Inhibiting HIV-1 entry: discovery of D-peptide inhibitors that target the gp41 coiled-coil pocket", *Cell,* vol. 99, no. 1, pp. 103-115.

7. (a) Klussmann, S., Nolte, A., Bald, R., Erdmann, V.A. & Fürste, J.P. 1996, "Mirror-image RNA that binds D-adenosine", *Nature Biotechnology,* vol. 14, no. 9, pp. 1112-1115. (b) Vater, A. & Klussmann, S. 2015, "Turning mirror-image oligonucleotides into drugs: the evolution of Spiegelmer® therapeutics", *Drug Discovery Today,* vol. 20, no. 1, pp. 147-155. (c) Boisgard, R., Kuhnast, B., Vonhoff, S., Younes, C., Hinnen, F., Verbavatz, J., Rousseau, B., Fürste, J.P., Wlotzka, B. & Dollé, F. 2005, "In vivo biodistribution and pharmacokinetics of ^{18}F-labelled Spiegelmers: a new class of oligonucleotidic radiopharmaceuticals", *European Journal of Nuclear Medicine and Molecular Imaging,* vol. 32, no. 4, pp. 470-477.

8. (a) Butler, M.S., Robertson, A.A. & Cooper, M.A. 2014, "Natural product and natural product derived drugs in clinical trials", *Natural Product Reports,* vol. 31, no. 11, pp. 1612-1661. (b) Harvey, A.L., Edrada-Ebel, R. & Quinn, R.J. 2015, "The re-emergence of natural products for drug discovery in the genomics era", *Nature Reviews Drug Discovery,* vol. 14, no. 2, pp. 111-129. (c) Newman, D.J. & Cragg, G.M. 2016, "Natural products as sources of new drugs from 1981 to 2014", *Journal of Natural Products,* vol. 79, no. 3, pp. 629-661.

9. Riley, R.G., Silverstein, R.M. & Moser, J.C. 1974, "Biological responses of *Atta texana* to its alarm pheromone and the enantiomer of the pheromone", *Science,* vol. 183, no. 4126, pp. 760-762.

10. Novotny, M., Xie, T., Harvey, S., Wiesler, D., Jemiolo, B. & Carmack, M. 1995, "Stereoselectivity in mammalian chemical communication: male mouse pheromones", *Experientia,* vol. 51, no. 7, pp. 738-743.

11. Iwaki, S., Marumo, S., Saito, T., Yamada, M. & Katagiri, K. 1974, "Synthesis and activity of optically active disparlure", *Journal of the American Chemical Society,* vol. 96, no. 25, pp. 7842-7844.

12. Kuwahara, Y., Matsumoto, K., Wada, Y. & Suzuki, T. 1991, "Chemical ecology on astigmatid mites. XXIX. Aggregation pheromone and kairomone activity of synthetic lardolure (1*R*, 3*R*, 5*R*, 7*R*)-1, 3, 5, 7-tetramethyldecyl formate and its optical isomers to *Lardoglyphus konoi* and *Carpoglyphus lactis* (Acari: Astigmata)", *Applied Entomology and Zoology,* vol. 26, no. 1, pp. 85-89.

13. Mori, K. & Kuwahara, S. 1986, "Synthesis of both the enantiomers of lardolure, the aggregation pheromone of the acarid mite, *Lardoglyphus konoi*", *Tetrahedron,* vol. 42, no. 20, pp. 5539-5544.

14. Szöcs, G., Tóth, M., Francke, W., Schmidt, F., Philipp, P., König, W., Mori, K., Hansson, B. & Löfstedt, C. 1993, "Species discrimination in five species of winter-flying geometrids (Lepidoptera) based on chirality of semiochemicals and flight season", *Journal of Chemical Ecology,* vol. 19, no. 11, pp. 2721-2735.
15. Haniotakis, G., Francke, W., Mori, K., Redlich, H. & Schurig, V. 1986, "Sex-specific activity of (*R*)-(−)- and (*S*)-(+)-1,7-dioxaspiro[5.5]undecane, the major pheromone of *Dacus oleae*", *Journal of Chemical Ecology,* vol. 12, no. 6, pp. 1559-1568.
16. Zeeck, E., Hardege, J., Willig, A., Krebber, R. & König, W. 1992, "Preparative separation of enantiomeric polychaete sex pheromones", *Naturwissenschaften,* vol. 79, no. 4, pp. 182-183.
17. (a) Borden, J.H., Chong, L., McLean, J.A., Slessor, K.N. & Mori, K. 1976, "*Gnathotrichus sulcatus*: synergistic response to enantiomers of the aggregation pheromone sulcatol", *Science,* vol. 192, no. 4242, pp. 894-896. (b) Bordon, J., Handley, J., McLean, J., Silverstein, R., Chong, L., Slessor, K., Johnston, B. & Schuler, H. 1980, "Enantiomer-based specificity in pheromone communication by two sympatric*Gnathoirichus* species (Coleoptera: Scolytidae)", *Journal of Chemical Ecology,* vol. 6, no. 2, pp. 445-456.
18. Millar, J., Pierce, H., Pierce, A., Oehlschlager, A. & Borden, J. 1985, "Aggregation pheromones of the grain beetle, *Cryptolestes turcicus* (Coleoptera: Cucujidae)", *Journal of Chemical Ecology,* vol. 11, no. 8, pp. 1071-1081.
19. Schiffman, S.S., Sennewald, K. & Gagnon, J. 1981, "Comparison of taste qualities and thresholds of D-and L-amino acids", *Physiology & Behavior,* vol. 27, no. 1, pp. 51-59.
20. Wolosker, H., Dumin, E., Balan, L. & Foltyn, V.N. 2008, "D-amino acids in the brain: D-serine in neurotransmission and neurodegeneration", *The FEBS Journal,* vol. 275, no. 14, pp. 3514-3526.
21. (a) Noguchi, T., Oishi, S., Honda, K., Kondoh, Y., Saito, T., Ohno, H., Osada, H. & Fujii, N. 2016, "Screening of a virtual mirror-image library of natural products", *Chemical Communications,* vol. 52, no. 49, pp. 7653-7656. (b) Noguchi, T., Ishiba, H., Honda, K., Kondoh, Y., Osada, H., Ohno, H., Fujii, N. & Oishi, S. 2016, "Synthesis of Grb2 SH2 Domain Proteins for Mirror-image Screening Systems", *Bioconjugate Chemistry,* vol. 28, no. 2, pp. 609-619.
22. (a) Houghten, R.A., Pinilla, C., Blondelle, S.E., Appel, J.R., Dooley, C.T. & Cuervo, J.H. 1991, "Generation and use of synthetic peptide combinatorial libraries for basic research and drug discovery", *Nature,* vol. 354, no. 6348, pp. 84-86. (b) Alluri, P.G., Reddy, M.M.,

Bachhawat-Sikder, K., Olivos, H.J. & Kodadek, T. 2003, "Isolation of protein ligands from large peptoid libraries", *Journal of the American Chemical Society,* vol. 125, no. 46, pp. 13995-14004. (c) Aquino, C., Sarkar, M., Chalmers, M.J., Mendes, K., Kodadek, T. & Micalizio, G.C. 2012, "A biomimetic polyketide-inspired approach to small-molecule ligand discovery", *Nature Chemistry,* vol. 4, no. 2, pp. 99. (d) Lian, W., Upadhyaya, P., Rhodes, C.A., Liu, Y. & Pei, D. 2013, "Screening bicyclic peptide libraries for protein–protein interaction inhibitors: discovery of a tumor necrosis factor-α antagonist", *Journal of the American Chemical Society,* vol. 135, no. 32, pp. 11990-11995.

23. (a) Paulick, M.G., Hart, K.M., Brinner, K.M., Tjandra, M., Charych, D.H. & Zuckermann, R.N. 2006, "Cleavable hydrophilic linker for one-bead-one-compound sequencing of oligomer libraries by tandem mass spectrometry", *Journal of Combinatorial Chemistry,* vol. 8, no. 3, pp. 417-426. (b) Thakkar, A., Cohen, A.S., Connolly, M.D., Zuckermann, R.N. & Pei, D. 2009, "High-throughput sequencing of peptoids and peptide-peptoid hybrids by partial Edman degradation and mass spectrometry", *Journal of Combinatorial Chemistry,* vol. 11, no. 2, pp. 294-302.

24. (a) Liu, R., Marik, J. & Lam, K.S. 2002, "A novel peptide-based encoding system for “one-bead one-compound” peptidomimetic and small molecule combinatorial libraries", *Journal of the American Chemical Society,* vol. 124, no. 26, pp. 7678-7680. (b) MacConnell, A.B., McEnaney, P.J., Cavett, V.J. & Paegel, B.M. 2015, "DNA-encoded solid-phase synthesis: encoding language design and complex oligomer library synthesis", *ACS Combinatorial Science,* vol. 17, no. 9, pp. 518-534.

25. Mendes, K.R., Malone, M.L., Ndungu, J.M., Suponitsky-Kroyter, I., Cavett, V.J., McEnaney, P.J., MacConnell, A.B., Doran, T.M., Ronacher, K. & Stanley, K. 2016, "High-throughput identification of DNA-encoded IgG ligands that distinguish active and latent Mycobacterium tuberculosis infections", *ACS Chemical Biology,* vol. 12, no. 1, pp. 234-243.

26. Malone, M.L. & Paegel, B.M. 2016, "What is a “DNA-compatible” reaction?", *ACS Combinatorial Science,* vol. 18, no. 4, pp. 182-187.

Chapter 1. Development of Mirror-image screening systems

Section 1. Synthesis of the Src SH2 Domain and Its Application in Bioassays for Mirror-image Screening

Summary

The Src SH2 domain was synthesized via native chemical ligation of two fragment peptides. In this section, the facile protocol was used to prepare the mirror-image SH2 domain (D-Src SH2 domain) and tetramethylrhodamine-labeled SH2 domains. The synthesized SH2 domains were correctly folded and showed activity, and using these proteins the author established bioassays to identify novel Src SH2 domain inhibitors from an unexplored mirror-image library of natural products.

The Src SH2 domain is a noncatalytic module involved in cellular signaling and is ~100 amino acids in length.[1] This domain binds to a phosphorylated tyrosine (pTyr) peptide motif found within target proteins such as FAK, p68, p130 and Hapv middle T antigen (HmT).[2] To characterize SH2 domain-mediated protein–protein interactions as well as to identify specific pTyr containing peptide(s) towards the SH2 domain, proteomics approaches and screening campaigns using a combinatorial pTyr peptide library have been conducted.[3] The crystal structure of the Src SH2 domain–pYEEI motif-containing peptide complex revealed valuable information about the interaction interface between the peptide and SH2 domain.[4] Since Src is expressed highly in a variety of disease tissues, inhibitors that target Src's function represent promising pharmaceutical agents for cancers and osteoporosis treatment.[5] Considerable effort has been devoted to the development of Src SH2 domain inhibitors, which are mainly based on structure-based approaches starting from native peptide pYEEI sequences.[6] For example, Nam et al. investigated the structure–activity relationships of pYEEI tetrapeptide ligands.[6h,i] N-terminal modification and incorporation of a conformationally constrained substructure led to the identification of novel potent peptidomimetics with a pYEEI motif. Alternatively, rosmarinic acid (RosA; derived from *Prunella vulgaris*) inhibits the interaction between the Src SH2 domain and the pYEEI-containing peptide.[6j] Salvianolic acids A and B, and caftaric acid also exhibit inhibitory activity against the Src SH2 domain in the micromolar range (Figure 1).[7] As such, both structure-based design from the pTyr-containing peptides and screening of natural products are promising strategies for the identification of novel Src SH2 domain inhibitors.

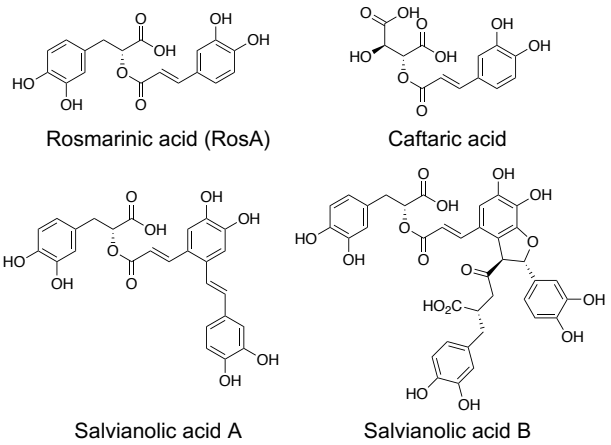

Figure 1. Structures of Src SH2 domain inhibitors from natural products.

Recently Noguchi et al reported the chemical synthesis of Grb2 SH2 domain and application to the development of mirror-image screening process. For the preparation of the native (L-protein) and mirror-image (D-protein) Grb2 SH2 domain, two synthetic procedures using native chemical ligation(s) (NCLs) of two or three segments were established. The resulting synthetic proteins with an appropriate labeling group were used to develop bioassays to evaluate the inhibitory activity against the interaction between the Grb2 SH2 domain and the counterpart phosphotyrosine (pTyr)-containing peptide. Additionally, Virdee et al. reported the semisynthesis of Src SH2 domain from three peptide fragments including two recombinant proteins and one synthetic peptides.[8] In this section, to extend mirror-image screening approach to other SH2 domain proteins, the author investigated the chemical synthesis of the Src SH2 domain and the development of several bioassays for mirror-image screening of chiral natural products.

For the synthesis of the Src SH2 domain, $Src^{145–251}$ (Figure 2), an NCL strategy was designed, in which two fragment peptides would be ligated at the Tyr187–Cys188 peptide bond.[9] Initially, the N-terminal fragment $Src^{145–187}$ (**L-1a**) was prepared on H-Rink amide ChemMatrix resin with a Dawson linker using 2-(1*H*-benzotriazol-1-yl)-1,1,3,3-tetramethyluroniuim hexauorophosphate (HBTU)/(*i*-Pr)$_2$NEt activation by an Fmoc-based solid-phase peptide synthesis (Fmoc-SPPS) protocol, according to our previous report.[10] The more reactive *O*-(7-azabenzotriazol-1-yl)-*N*,*N*,*N*^{0},*N*^{0}-tetramethyluronium hexauorophosphate (HATU)/(*i*-Pr)$_2$NEt was used for coupling of Arg158, Arg159, Arg163, Leu164, and Arg172, because of the less efficient coupling of Fmoc-protected amino acids using HBTU activation. The resin **L-1a** was subjected to the *N*-acylurea approach,[11] in which the C-terminal Dawson linker was activated by treatment with *p*-nitrophenyl chloroformate to

form the Nbz (*N*-acyl benzimidazolinone) leaving group of **L-2a**. Trifluoroacetic acid (TFA)-mediated total deprotection and cleavage from the resin followed by treatment of the crude peptide with 4-mercaptophenylacetic acid (MPAA) afforded the expected L-Src$^{145–187}$ thioester (**L-3a**). For the synthesis of the C-terminal fragment, L-Src$^{188–251}$ (**L-4**), the identical Fmoc-SPPS protocol on H-Rink amide ChemMatrix resin followed by TFA-mediated final deprotection gave the expected fragment. The resulting L-Src$^{145–187}$ thioester (**L-3a**) and L-Src$^{188–251}$ (**L-4**) were subjected to native chemical ligation conditions to provide the full-length L-Src$^{145–251}$ (**L-5a**) in 17% yield in good purity (Figure 3A). To avoid the undesirable intramolecular and intermolecular disulfide bond formation *via* the three Cys residues, an increase in the concentration of tris(2-carboxyethyl)phosphine (TCEP, 100 mM) was used during ligation.

The Src SH2 domain with a labeling group required for bioassays was designed and synthesized. The previous report on the crystal structure of the Src SH2 domain in complex with the cognate pTyr-containing peptide revealed that the binding site of the pTyr-containing peptide is located distal from the N-terminus of the Src SH2 domain.[5] On the basis of this information, the author designed a labeled Src SH2 domain that possessed a single modification with tetramethylrhodamine (TMR) or biotin at the N-terminus. The N-terminal TMR or biotin group was introduced on the resin after solid-phase synthesis of the N-terminal fragment L-Src$^{145–187}$ (**L-1b** or **L-1c**). The N-terminally modified fragment **L-3b** or **L-3c** was then used in the identical ligation protocol to afford the TMR-labeled Src^{TMR} (**L-5b**) and biotinylated L-Src^{biotin} (**L-5c**) (Figure 3B,C). The mirror-image Src SH2 domains (**D-5a**, **D-5b**, and **D-5c**) were synthesized by the same procedure.

With the different full-length Src SH2 domains in hand, the author investigated the refolding conditions based on a previously reported protocol.[8] Since the three Cys residues (Cys188, Cys241 and Cys248) in Src SH2 are not involved in disulfide bond formation,[5] the synthetic proteins were subjected to refolding under reducing conditions in the presence of 0.5 mM TCEP to prevent dimer formation. Dialysis of denatured Src$^{145–251}$ (**L-5a**) against HEPES buffer (20 mM HEPES, 100 mM NaCl, 0.5 mM TCEP, pH 7.4) resulted in a homogenous solution of Src$^{145–251}$. Circular dichroism (CD) was used to confirm the tertiary structure of the folded Src SH2 domains (L-Src$^{145–251}$ and D-Src$^{145–251}$) (Figure 4). CD spectra of L-Src$^{145-251}$ was similar to those of other SH2 domains, including the N-terminal SH2 domain of the p85α subunit of the phosphatidylinositol 3-kinase (PI3K) and Btk SH2 domain,[12] which displayed a broad minimum over the range of 210–220 nm. In addition, the symmetry CD spectra of L-Src$^{145–251}$ and D-Src$^{145–251}$ confirmed the mirror-image nature of the structures. The CD results indicated that the Src SH2 domains are correctly folded and should have

biological activity.

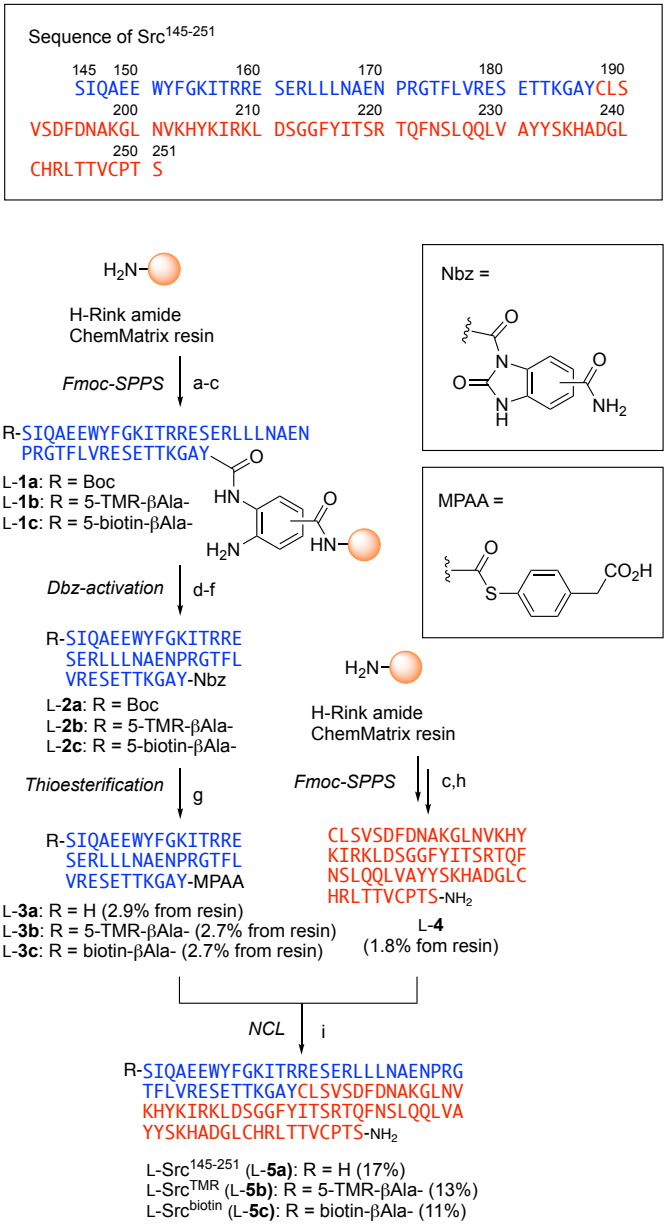

Figure 2. Synthesis of the Src SH2 domain. Reagents and conditions: (a) Fmoc-Dbz-OH, HBTU, 1-hydroxybenzotriazole (HOBt), (*i*-Pr)$_2$NEt, DMF, and then 20% piperidine/DMF; (b) Fmoc-Xaa-OH, HBTU, HOBt, (*i*-Pr)$_2$NEt, DMF, and then 20% piperidine/DMF; [repeat (b) until the sequence was completed] (c) Boc-Ser(*t*-Bu)-OH, HBTU, HOBt, (*i*-Pr)$_2$NEt, and DMF; (d) 4-nitrophenyl chloroformate, and DCM; (e) (*i*-Pr)$_2$NEt, and DMF; (f) TFA/H$_2$O/*m*-cresol/thioanisole (80:10:5:5); (g) MPAA, tris(2-carboxyethyl)phosphine (TCEP), 6 M guanidine, and phosphate buffered saline (PBS, pH 7.0); (h) TFA/H$_2$O/*m*-cresol/thioanisole/1,2-ethanedithiol (EDT) (80:5:5:5:5); (i) MPAA, TCEP, 6 M guanidine, and PBS (pH 7.0). Abbreviation: Dbz = 3,4-diaminobenzoic acid.

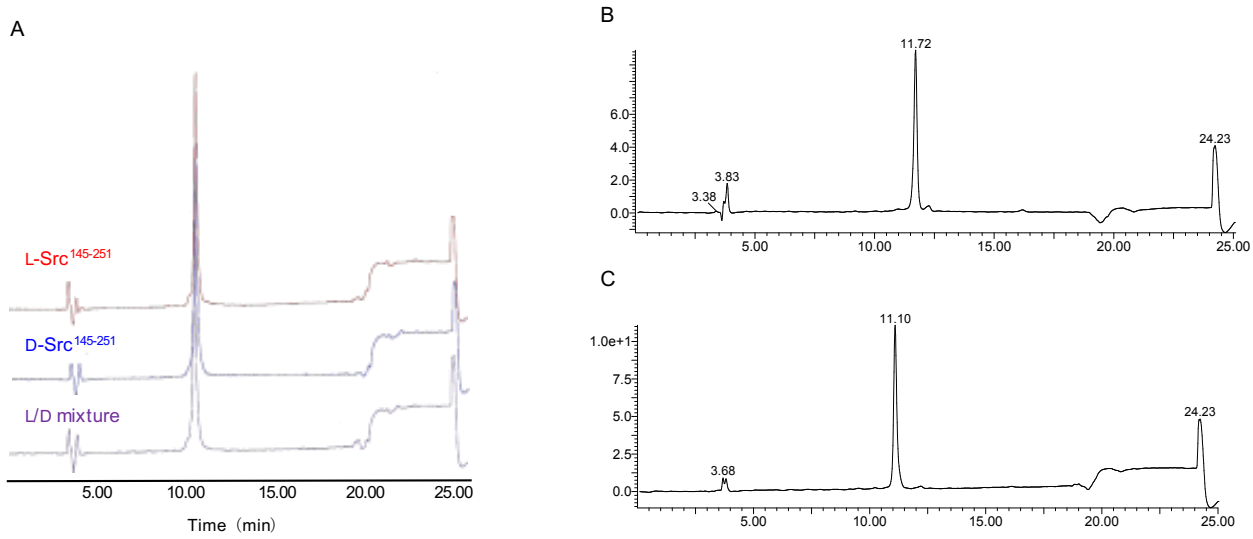

Figure 3. Analytical HPLC chromatograms of purified **L-5a**, **L-5b**, L/D mixture (A) and **L-5b** (B), and **L-5c** (C). HPLC analysis was performed at 25 °C with a linear gradient of 30–45% CH_3CN containing 0.1% TFA at a flow rate of 1mL/min over 15 min.

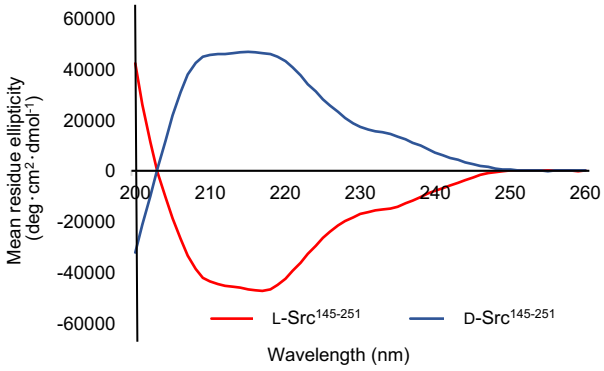

Figure 4. CD spectra of folded L-$Src^{145–251}$ and D-$Src^{145–251}$

Next the binding affinity of the synthetic Src SH2 domains toward a pTyr-containing peptide was evaluated by surface plasmon resonance (SPR) analysis. The author chose hmT pY324 (H-EPQpYEEIPIYL-NH_2) as a target sequence, which is derived from the hamster polyoma middle-sized tumor antigen (hmT antigen).[1] After the biotinylated hmT pY324 was immobilized on the streptavidin coated sensor chip, interaction between the immobilized hmT pY324 ligand and a Src SH2 domain analyte was evaluated. L-$Src^{145–251}$ bound the L-peptide form of hmT pY324 (**L-7**) with high affinity [K_D (L-$Src^{145–251}$–L-hmT pY324 peptide): 42.8 nM], whereas no interaction with the D-peptide (**D-7**) was observed. In a similar manner, D-$Src^{145–251}$ showed potent affinity toward D-hmT pY324 selectively [K_D (D-$Src^{145–251}$– D-hmT pY324 peptide): 55.1 nM] (Figure 5A). The bioactivity of the synthetic Src SH2 domains was also evaluated by a fluorescence polarization assay using a fluorescent peptide FMT1 (FAM- GpYEEIA-NH_2).[13] L-$Src^{145–251}$ and D- $Src^{145–251}$ interacted with L-

FMT1 (**L-8**) and D-FMT1 (**D-8**) peptides, respectively, with submicromolar affinities [K_D (L-Src$^{145–251}$–L-FMT1): 162 nM; K_D (D-Src$^{145–251}$–D-FMT1): 182 nM] (Figure 6). These results suggested the synthetic Src SH2 domains after an appropriate refolding process reproduced biological functions, and exhibited stereoselective interaction with the counterpart pTyr-containing sequence.

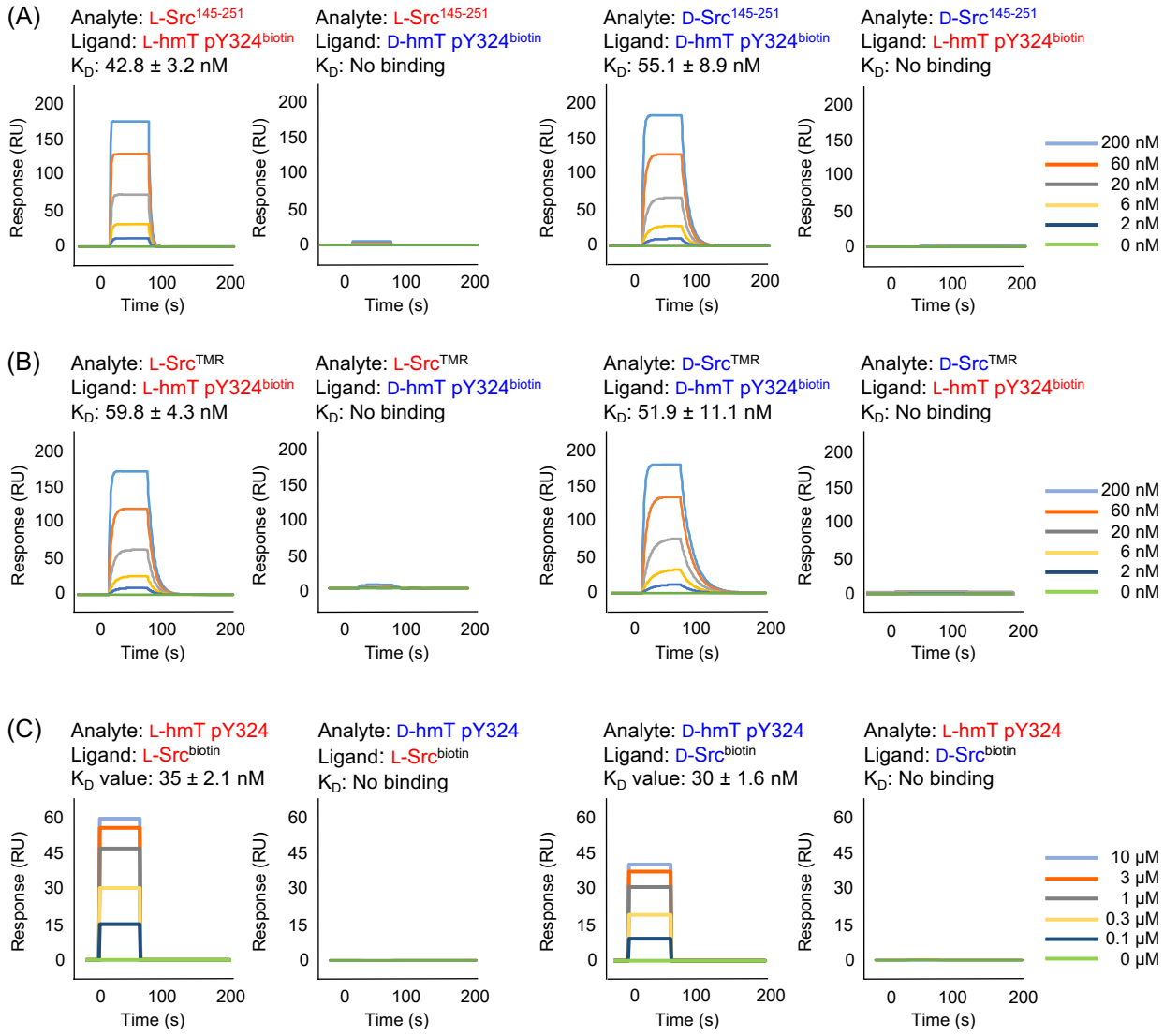

Figure 5. Representative data of SPR analysis of folded Src SH2 derivatives binding to the hmT pY324 peptide. (A, B) Binding kinetics were evaluated by immobilizing a biotinylated hmT on an NCL sensor chip. (C) Binding kinetics were evaluated by immobilizing Src^{biotin} on an NCL sensor chip.

The SPR analysis was carried out using the TMR-labeled Src SH2 domains. L-Src^{TMR} had similar binding affinity for L-hmT pY324 peptide (**L-7**) when compared with that of unlabeled L-Src$^{145–251}$ [K_D (L-Src^{TMR}–L-hmT pY324 peptide): 59.8 nM]. The mirror-image interaction between D-Src^{TMR} and D-hmT pY324 peptide (**D-7**) was also similarly observed with high affinity [K_D (D-Src^{TMR}–D-

hmT pY324 peptide): 51.9 nM] (Figure 5B). Binding affinity of the biotinylated Src SH2 domain was assessed by SPR analysis by immobilizing Src^{biotin} on the sensor chip and flushing unlabeled hmT pY324 peptide as an analyte. L-Src^{biotin} showed the stereoselective binding towards hmT pY324 peptide (**L-6**) [K_D (L-Src^{biotin}–L-hmT pY324 peptide): 35 nM]. Similarly, the mirror-image interaction also showed the comparable binding kinetics towards **D-6** [K_D (D-Src^{biotin}–D-hmT pY324 peptide): 30 nM]. These results with a point modified proteins indicates that the N-terminal TMR modification or biotin had no effect on either the folding of the Src SH2 domain or the interaction with the target pTyr peptide. Thus, N-terminal labeled proteins should be suitable in a number of in vitro bioassays for screening campaigns.

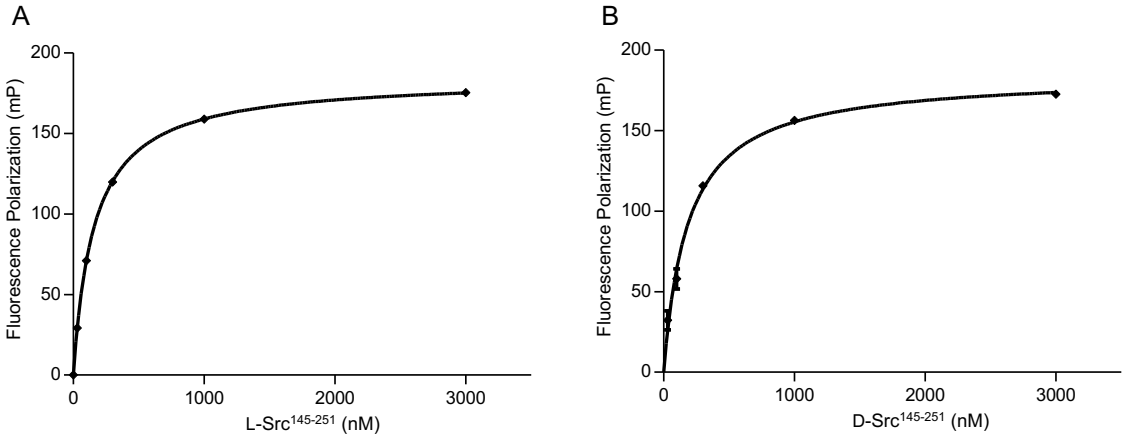

Figure 6. Binding of Src SH2 to pTyr-containing peptides. (A) Binding curve of the L-FMT–L-Src SH2 complex. K_D (L-Src–L-FMT1): 162 ± 5 nM. (B) Binding curve of the D-FMT1–D-Src SH2 complex. K_D (D-Src– D-FMT1): 182 ± 3 nM. K_D values were determined from the saturation curves generated from triplicate experiments of the fluorescence polarization assay using the FMT1 peptide (20 nM). Representative saturation curves of the binding experiments are shown.

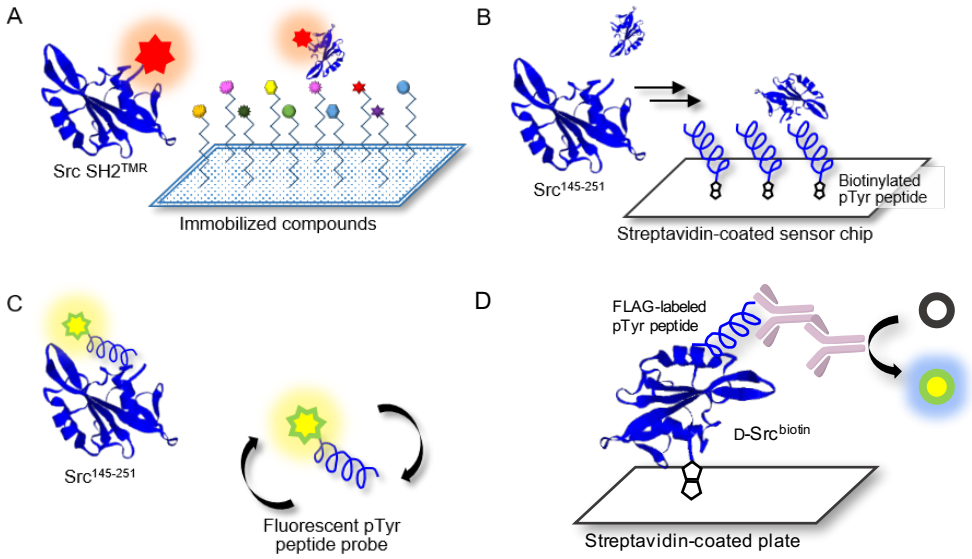

Figure 7. Design of the bioassay systems using synthetic proteins. (A) Chemical array analysis for the first screening. Binding with immobilized compound(s) on glass slides is detected by fluorescence signal of Src $SH2^{TMR}$. (B) Surface plasmon resonance (SPR) analysis of Src SH2 domain binding with hmT pY324 (a pTyr-containing peptide) immobilized on the streptavidin-coated sensor chip. The Src SH2 binding to hmT pY342 is detected by the increased SPR signal. The inhibitory activity is evaluated in the presence of the potential inhibitor as an analyte. (C) Fluorescence polarization (FP) assay for Src SH2 domain binding with fluorescent FMT1 peptide probe. The FMT1 binding to Src SH2 binding is detected by the increased FP signal, which is derived from the impaired mobility of the fluorescent probe. The inhibitory activity is evaluated in the presence of the potential inhibitor. (D) ELISA for Src SH2 domain binding with FLAG-labeled pTyr peptide. Biotylylated Src SH2 is immobilized on a streptavidin-coated plats. The binding of pTyr peptide with a FLAG tag is detected by primary antibody (anti-FLAG mouse IgG), secondary antibody (HRP-conjugated anti-mouse antibody) and TMB substrate. Abbreviations: HRP = horseradish peroxidase, TMB = 3,3',5,5'-tetramethylbenzidin.

The author established several in vitro assay systems using $Src^{145–251}$ and its modified derivatives to identify compounds that bind to the pTyr peptide binding pocket in the Src SH2 domain. First, competitive binding assay using SPR was established (Fig. 7B). In the SPR analysis, specific and stereoselective binding of the Src SH2 domain ($Src^{145–251}$) to the pTyr-containing peptide (biotinylated hmT pY324) was observed, which was immobilized on the streptavidin-coated sensor chip (Figure 5A).[16] Using this system in the presence of a potential inhibitor(s), the inhibitory effect against the Src SH2 domain–pTyr peptide interaction could be measured. Since the detection of the Src SH2 domain–pTyr peptide interaction by SPR does not involve a colored material(s), the possibility of observing false-positives and false-negatives was minimized. The SPR response of L-$Src^{145–251}$ onto the immobilized L-pTyr peptide (L-**7**) decreased in the presence of the unlabeled L-hmT pY234 peptide (**L-6**) in a dose-dependent manner (IC_{50}: 323 nM) (Figure 8A). The inhibitory

activity of D-hmT pY324 peptide (**D-6**) against the D-Src$^{145–251}$–D-pTyr peptide interaction was determined as well (IC_{50}: 387 nM). Second, the author investigated the development of a competitive inhibition assay for Src SH2 domain inhibitors using fluorescence polarization (FP) based on a reported protocol (Figure 7C and 8B).[13] The homogeneous assay by FP experiments provides an alternative high-throughput screening approach using non-labeled protein.[17] The fluorescent pTyr-peptide probe (FMT1, 20 nM) and unlabeled Src protein (Src$^{145–251}$, 300 nM) were used for the inhibition experiment. Dose-dependent inhibition against the L-Src$^{145–251}$–L-pTyr peptide interaction by the unlabeled L-hmT pY324 peptide (**L-6**) was observed (IC_{50}: 860 nM). The mirror-image interaction between D-Src$^{145–251}$ and D-pTyr peptide was also inhibited by the D-hmT pY324 peptide (**D-6**) (IC_{50}: 946 nM). Third, an ELISA (enzyme-linked immunosorbent assay) was established based on the previous report of Grb2 using the biotin-labeled Src SH2 domain (Figure 7D). After initial immobilization of Src^{biotin} on a streptavidin-coated 96well plates, and FLAG-labelled pTyr containing peptide (**L-9**) was incubated with the immobilized Src^{biotin}. The binding of Src SH2 with the pTyr containing peptide was detected by using a commercially available anti-FLAG mouse IgG, HRP-conjugated anti-mouse antibody, and the TMB substrate. The stereoselective binding of L-Src^{biotin} and D-Src^{biotin} towards pTyr peptides (**L-9** or **D-9**) were inhibited under the condition with the inhibitor peptide (Figure 8C). Unlabeled L-hmT pY324 peptide (**L-6**) showed inhibitory activity to L-Src^{biotin}–L-pTyr peptide interaction in a dose-depending fashion (IC_{50}: 121 nM). Likewise, D-Src^{biotin}–D-pTyr peptide interaction was inhibited by D-pY324 peptide (**D-6**) (IC_{50}: 166 nM). These three complementary bioassay systems to determine the inhibitory activity should be suitable for identifying potential inhibitors that bind to the pTyr binding pocket in the Src SH2 domain following the primary comprehensive chemical array-based screening to explore and identify compounds that bind to the Src SH2 domain.

Chemical array screening is an ultrahigh-throughput screening technology for drug discovery (Figure 7A).[14] The affinity-based selection by microarray technology facilitates the identification of potential inhibitors against a protein–protein interaction(s) from a library of small molecules. In our previous mirror-image screening studies for MDM2 inhibitors and Grb2 SH2 domain inhibitors, this chemical array analysis was employed as the initial screening of natural products, which were immobilized *via* carbene-mediated covalent bond formation.[15] Using this unique chemical array technique, the binding compound(s) for the alternative or unprecedented pockets as well as previously recognized binding pockets of the target protein were identified. To demonstrate the applicability of the TMR-labeled Src SH2 domains to chemical array screening, binding with the target hmT pY324 peptide

on a chemical array was assessed. The L-peptide and D-peptide of hmT pY324 (**L-6** and **D-6**) were immobilized on a chemical array by carbene-mediated covalent bond formation at different concentrations. When the array was treated with TMR-labeled Src SH2 domains, L-Src^{TMR} and D-Src^{TMR} bound to L-hmT pY324 and D-hmT pY324, respectively (Fig. 9). In contrast, no significant binding to the mismatch target peptides was observed, indicating the enantioselective recognition by the synthetic TMR-labeled proteins. Thus, the synthetic TMR- labeled Src SH2 domains should be applicable to mirror- image screening using the chemical array technology.

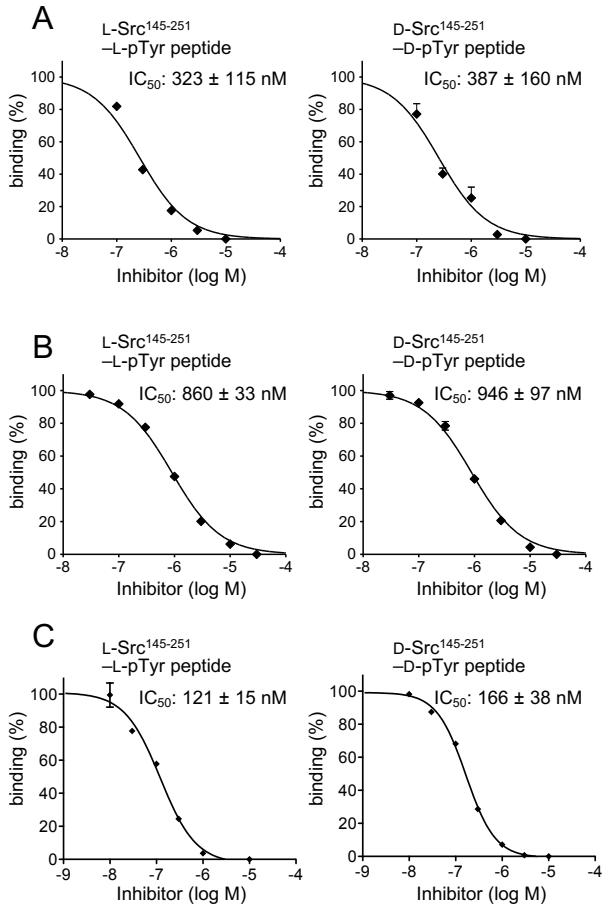

Figure 8. Inhibitory activity of the hmT pY324 peptide against the Src SH2 domain–pTyr-containing peptide interaction. (A) SPR analysis was carried out by Src$^{145–251}$ (200 nM) in the presence of the inhibitor as an analyte on the pTyr peptide-immobilized NLC sensor chip. (B) FP assay was carried out using the fluorescent FMT1 peptide probe (20 nM) and Src$^{145–251}$ (300 nM). IC_{50} values were derived from the dose–response curves generated from triplicate experiments. Representative dose–response curves of the inhibition experiments are shown.

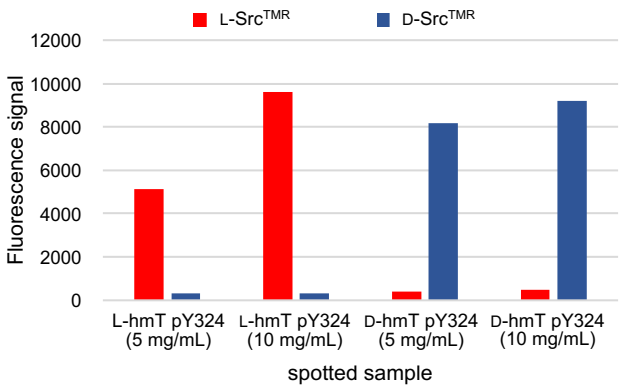

Figure 9. Binding activities of the Src SH2 domain towards hmT pY324 peptides immobilized on a chemical array. The binding of L-Src^{TMR} and D-Src SH2^{TMR} were assessed using a chemical array, where L-hmT pY324 or D-hmT pY324 peptides were spotted at various concentrations.

Finally, the author conducted chemical array screening in mirror-image platform of natural products and its derivatives from the Natural Products Depository, NPDepo in RIKEN by (Figure 10). From 22,097 compounds, 1269 hits (L-Src bound to 949 compounds, D-Src bound to 890 compounds) are identified in primary chemical array screening. Competitive inhibitory activity of these primary hits are evaluated by ELISA resulting in 45 hits. 21 compounds exhibited inhibitory activity of L-Src–L-pTyr peptide interaction, whereas 33 compounds exhibited inhibition of D-Src–D-pTyr peptide interaction. Further investigations of these hit compounds including determination of each IC_{50} and specificity evaluations are currently in progress.

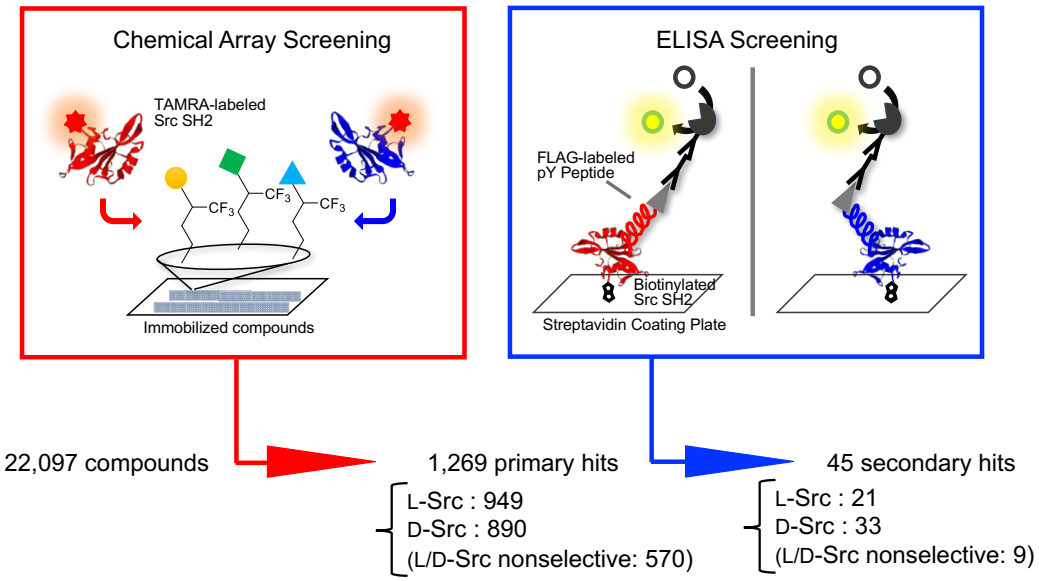

Figure 10. Mirror-image screening campaign of Src SH2 by two-step in vitro assay systems

In conclusion, the author accomplished total synthesis of the Src SH2 domain by conjugating two fragment peptides by native chemical ligation at Cys188. The TMR-labeled or biotinylated Src SH2 domain was also synthesized using the same procedure with the N-terminal peptide fragment ligated to a fluorescent group or a biotin at the N-terminus. The synthetic L-Src SH2 and D-Src SH2 domains were converted into functional proteins under appropriate conditions and were found to recognize the target pTyr sequence in a stereoselective manner. Taking advantage of the resulting domain prepared, the author established four bioassays, namely SPR analysis, chemical array analysis, and fluorescence polarization (FP), and ELISA to detect the interaction between the Src SH2 domain and the counterpart pTyr peptide. Additionally, three competitive inhibition assays were established using SPR analysis and FP, and ELISA to identify Src SH2 domain inhibitors, which bound into the pTyr-binding pocket. As a result of the screening campaign by chemical array and competitive ELISA from natural products and their derivatives provided from RIKEN, a number of chiral compounds were identified to show inhibitory activity to L-Src SH2 or D-Src SH2 domain. These mirror-image bioassays should facilitate efficient screening of potential Src SH2 inhibitors from unexplored mirror-image compounds of natural product resources.

Experimental Section

Peptide synthesis

All peptide fragments were prepared by standard Fmoc-based solid phase peptide synthesis (Fmoc-SPPS) using an automatic peptide synthesizer (PSSM-8, Shimadzu) unless otherwise stated.[32] For side chain protection: *t*-Bu ester was used for Asp and Glu; 2,2,4,6,7-pentamethyldihydrobenzofuran-5-sulfonyl (Pbf) was used for Arg; *t*-Bu was used for Thr, Tyr and Ser; Boc was used for Lys and Trp; Trt was used for Gln, Asn, His and Cys; and mono Bzl for pTyr. Fmoc-amino acids were coupled using HBTU (5 eq)/HOBt·H_2O (5 eq)/(*i*-Pr)$_2$NEt (10 eq) activation to free the amino group in DMF for 45 min twice. Fmoc deprotection was performed by 20% piperidine in DMF for 6 min twice. The resulting protected resin was treated with TFA/H_2O/thioanisole/*m*-cresol/1,2-ethandithiol (80:5:5:5:5) at room temperature for 2 h. After removal of the resin by filtration, the filtrate was poured into ice-cold dry Et_2O. The resulting powder was collected by centrifugation and washed with ice-cold dry Et_2O. Crude peptide fragments and ligand peptides were purified by preparative HPLC on a Cosmosil 5C18-AR300 preparative column (Nacalai Tesque, 20 × 250 mm, flow rate 8 mL/min). For analytical HPLC of peptide fragments, a Cosmosil 5C18-AR300 column (4.6 × 250 mm, Nacalai Tesque) was employed with a linear gradient of CH_3CN containing 0.1% (v/v) TFA at a flow rate of 1 mL/min. For analytical HPLC of the ligand peptides, a Cosmosil 5C18-ARII column (4.6 × 250 mm, Nacalai Tesque) was employed with a linear gradient of CH_3CN containing 0.1% (v/v) TFA at a flow rate of 1 mL/min. All peptides were characterized by ESI-MS (micromass ZQ, Waters) or MALDI-TOF-MS (AXIMA-CFR plus, Shimadzu).

L-Src$^{145–187}$ (L-3a)

3-[(9-Fluorenylmethyloxycarbonyl)amino]-4-aminobenzoic acid (Fmoc-Dbz-OH, 37.4 mg, 0.1 mmol) was manually coupled on H-Rink Amide-ChemMatrix resin (0.4-0.6 mmol/g, 40 mg, 0.016-0.024 mmol) using HBTU (37.8 mg, 0.1 mmol), HOBt·H_2O (15.2 mg, 0.1 mmol), and (*i*-Pr)$_2$NEt (0.0348 mL, 0.2 mmol) in DMF for 2.5 h. This treatment was repeated four times. The peptide sequence was constructed by the standard protocol. Because of the less efficient coupling of Arg158, Arg159, Arg163, Leu164, and Arg172, HATU (38.0 mg, 0.1 mmol) and (*i*-Pr)$_2$NEt (0.0348 mL, 0.2 mmol) were employed for activation and the coupling reactions for these amino acids were repeated three times. A solution of *p*-nitrophenyl chloroformate (22.5 mg, 0.11 mmol) in CH_2Cl_2 (0.38 mL)

was added to the protected peptide resin **L-1a**, and the mixture was agitated for 40 min at room temperature. Then, the resin was treated with a solution of 0.5 M (*i*-Pr)$_2$NEt in DMF (0.38 mL) for 15 min. Three portions of the resulting peptide resin were combined and the total peptide resin **L-2a** (0.048-0.072 mmol) was treated with TFA/H_2O/thioanisole/*m*-cresol (80:10:5:5) at room temperature for 2 h. After removal of the resin by filtration, the filtrate was poured into ice-cold dry Et_2O. The precipitate was washed with ice-cold dry Et_2O three times. The crude peptide was dissolved in 1 M phosphate buffer (pH 7.0) containing 6 M GuHCl, 200 mM, 4-mercaptophenyl acetic acid (MPAA), and 20 mM TCEP. The solution was kept at 37 °C for 30 min and purified by preparative HPLC (a linear gradient of 25–55% CH_3CN in H_2O containing 0.1% (v/v) TFA over 90 min) to afford the thioester L-**3a** (10.5 mg, 2.9 % yield). MS(ESI): Calcd for $C_{231}H_{357}N_{64}O_{71}S$ (MH^+): 5198.83; observed: $[M+6H]^{6+}$ *m/z* = 867.2, $[M+5H]^{5+}$ *m/z* = 1040.7, $[M+4H]^{4+}$ *m/z* = 1300.4, $[M+3H]^{3+}$ *m/z* = 1733.3.

L-Src^{TMR} (L-3b)

By the identical procedure described for the synthesis of peptide **L-3a**, thioester **L-3b** was synthesized (3.5 mg, 2.7% yield) from H-Rink Amide-ChemMatrix resin (40 mg, 0.016-0.024 mmol). TMR (43 mg, 0.1 mmol) was coupled by using *N*,*N*'-diisopropylcarbodiimide (DIC) (15.5 mL, 0.1 mmol)/HOBt·H_2O (15.3 mg, 0.1 mmol) in DMF for 4 h. MS(ESI): Calcd for $C_{259}H_{382}N_{67}O_{76}S$: 5682.36 ($MH^+$); observed: $[M+7H]^{7+}$ *m/z* = 812.7 $[M+6H]^{6+}$ *m/z* = 948.0, $[M+5H]^{5+}$ *m/z* = 1137.4, $[M+4H]^{4+}$ *m/z* = 1421.3.

L-Src^{biotin} (L-3c)

By the identical procedure described for the synthesis of peptide **L-3a**, thioester **L-3c** was synthesized (3.4 mg, 2.7% yield) from H-Rink Amide-ChemMatrix resin (40 mg, 0.016-0.024 mmol). D-Biotin (43 mg, 0.1 mmol) was coupled by using DIC (15.5 mL, 0.1 mmol)/HOBt·H_2O (15.3 mg, 0.1 mmol) in DMF for 4 h. MS(ESI): Calcd for $C_{244}H_{375}N_{67}O_{74}S_2$: 5493.71 ($MH^+$); observed: $[M+6H]^{6+}$ m/z = 917.2, $[M+5H]^{5+}$ m/z = 1100.3, $[M+4H]^{4+}$ m/z = 1374.4, $[M+3H]^{3+}$ m/z = 1832.6.

L-Src$^{145–187}$ (D-3a)

By the identical procedure described for the synthesis of peptide **L-3a**, thioester **D-3a** was synthesized (7.8 mg, 2.1% yield) from H-Rink Amide-ChemMatrix resin (40 mg × 3 portions, 0.048-0.072 mmol).

MS(ESI): Calcd for $C_{231}H_{357}N_{64}O_{71}S$: 5198.83 ($MH^+$); observed: $[M+6H]^{6+}$ *m/z* = 867.4, $[M+5H]^{5+}$ *m/z* = 1040.7, $[M+4H]^{4+}$ *m/z* = 1300.4, $[M+3H]^{3+}$ *m/z* = 1733.4.

L-Src^{TMR} (D-3b)

By the identical procedure described for the synthesis of peptide **L-3b**, thioester **D-3b** was synthesized (3.8 mg, 2.9% yield) from H-Rink Amide-ChemMatrix resin (40 mg, 0.016-0.024 mmol). MS(ESI): Calcd for $C_{259}H_{382}N_{67}O_{76}S$: 5682.36 ($MH^+$); observed: $[M+7H]^{7+}$ *m/z* = 812.6, $[M+6H]^{6+}$ *m/z* = 947.9, $[M+5H]^{5+}$ *m/z* = 1137.3, $[M+4H]^{4+}$ *m/z* = 1421.4.

L-Src^{biotin} (D-3c)

By the identical procedure described for the synthesis of peptide **L-3c**, thioester **D-3c** was synthesized (5.2 mg, 2.0% yield) from H-Rink Amide-ChemMatrix resin (40 mg, 0.016-0.024 mmol). MS(ESI): Calcd for $C_{244}H_{375}N_{67}O_{74}S_2$: 5493.71 ($MH^+$); observed: $[M+6H]^{6+}$ m/z = 916.9, $[M+5H]^{5+}$ m/z = 1100.2, $[M+4H]^{4+}$ m/z = 1374.8, $[M+3H]^{3+}$ m/z = 1832.7

L-Src$^{188–251}$ (L-4)

By the standard protocol for peptide synthesis, peptide **L-4** was synthesized (8.91 mg, 1.8% yield) from H-Rink Amide-ChemMatrix resin (40 mg × 3 portions, 0.048-0.072 mmol). MS(ESI): Calcd for $C_{318}H_{500}N_{91}O_{94}S_3$ (MH^+): 7198.22; observed: $[M+8H]^{8+}$ *m/z* = 900.7, $[M+7H]^{7+}$ *m/z* = 1029.1, $[M+6H]^{6+}$ *m/z* = 1200.4, $[M+5H]^{5+}$ *m/z* = 1440.4, $[M+4H]^{4+}$ *m/z* = 1800.0.

L-Src$^{188–251}$ (D-4)

By the standard protocol for peptide synthesis, peptide **D-4** was synthesized (5.5 mg, 1.6% yield) from H-Rink Amide-ChemMatrix resin (40 mg × 2 portions, 0.032-0.048 mmol). MS(ESI): Calcd for $C_{318}H_{500}N_{91}O_{94}S_3$: 7198.22 ($MH^+$); observed: $[M+8H]^{8+}$ *m/z* = 900.7, $[M+7H]^{7+}$ *m/z* = 1029.1, $[M+6H]^{6+}$ *m/z* = 1200.1, $[M+5H]^{5+}$ *m/z* = 1440.2, $[M+4H]^{4+}$ *m/z* = 1799.7.

Native chemical ligation: synthesis of L-Src$^{145–251}$ (L-5a)

The L-Src$^{145–187}$ thioester (**L-3a**, 4.5 mg) and L-Src$^{188–251}$ (**L-4**, 4.8 mg) were dissolved in 0.200 mL of ligation buffer [1 M phosphate buffer (pH 7.0) containing 6 M Gu·HCl, 200 mM MPAA, 100 mM TCEP], and the ligation reaction was continued for 1 h at 37 °C. Then, 1.80 mL of TCEP solution (6 M Gu·HCl and 100 M TCEP) was added to the mixture and the reaction was continued for 15 min

at room temperature. The crude product was purified by preparative HPLC (a linear gradient of 25–55% CH_3CN in H_2O containing 0.1% (v/v) TFA over 90 min) to provide peptide **L-5a** (1.4 mg, 17 % yield). MS(ESI): Calcd for $C_{541}H_{848}N_{155}O_{163}S_3$ (MH^+): 12227.84; observed (ESI): $[M+14H]^{14+}$ *m/z* = 874.4, $[M+13H]^{13+}$ *m/z* = 941.7, $[M+12H]^{12+}$ *m/z* = 1020.1, $[M+11H]^{11+}$ *m/z* = 1112.7, $[M+10H]^{10+}$ *m/z* = 1223.9, $[M+9H]^{9+}$ *m/z* = 1359.7, $[M+8H]^{8+}$ *m/z* = 1529.8, $[M+7H]^{7+}$ *m/z* = 1747.8.

L-Src^{TMR} (L-5b)

By the identical procedure described for the synthesis of peptide **L-5a**, peptide **L-5b** was synthesized (0.45 mg, 13% yield). MS(ESI): Calcd for $C_{569}H_{873}N_{158}O_{168}S_3$: 12711.36 ($MH^+$); observed: $[M+15H]^{15+}$ *m/z* = 848.5, $[M+14H]^{14+}$ *m/z* = 909.1, $[M+13H]^{13+}$ *m/z* = 978.9, $[M+12H]^{12+}$ *m/z* = 1060.5, $[M+11H]^{11+}$ *m/z* = 1156.7, $[M+10H]^{10+}$ *m/z* = 1272.3, $[M+9H]^{9+}$ *m/z* = 1413.3, $[M+8H]^{8+}$ *m/z* = 1590.2, $[M+7H]^{7+}$ *m/z* = 1760.0.

L-Src^{biotin} (L-5c)

By the identical procedure described for the synthesis of peptide **L-5a**, peptide **L-5c** was synthesized (0.2 mg, 11% yield). MS(ESI): Calcd for Calcd for $C_{554}H_{866}N_{158}O_{166}S_4$: 12521.32 ($MH^+$); observed: $[M+15H]^{15+}$ m/z = 835.1, $[M+14H]^{14+}$ m/z = 895.7, $[M+13H]^{13+}$ m/z = 964.6, $[M+12H]^{12+}$ m/z = 1044.8, $[M+11H]^{11+}$ m/z = 1139.7, $[M+10H]^{10+}$ m/z = 1253.5, $[M+9H]^{9+}$ m/z = 1392.9, $[M+8H]^{8+}$ m/z = 1566.5, $[M+7H]^{7+}$ m/z = 1790.4.

D-Src$^{145–251}$ (D-5a)

By the identical procedure described for the synthesis of peptide **L-5a**, peptide **D-5a** was synthesized (1.1 mg, 18% yield). MS(ESI): Calcd for $C_{541}H_{848}N_{155}O_{163}S_3$: 12227.84 ($MH^+$); observed: $[M+15H]^{15+}$ *m/z* = 813.9, $[M+14H]^{14+}$ *m/z* = 874.5, $[M+13H]^{13+}$ *m/z* = 941.6, $[M+12H]^{12+}$ *m/z* = 1020.0, $[M+11H]^{11+}$ *m/z* = 1112.8, $[M+10H]^{10+}$ *m/z* = 1223.9, $[M+9H]^{9+}$ *m/z* = 1359.8, $[M+8H]^{8+}$ *m/z* = 1529.5, $[M+7H]^{7+}$ *m/z* = 1747.5.

D-Src^{TMR} (D-5b).

By the identical procedure described for the synthesis of peptide **L-5a**, peptide **D-5b** was synthesized (0.25 mg, 14% yield). MS(ESI): Calcd for $C_{569}H_{873}N_{158}O_{168}S_3$: 12711.36 ($MH^+$); observed: $[M+15H]^{15+}$ *m/z* = 848.6, $[M+14H]^{14+}$ *m/z* = 909.0, $[M+13H]^{13+}$ *m/z* = 978.9, $[M+12H]^{12+}$ *m/z* =

1060.4, $[M+11H]^{11+}$ *m/z* = 1156.7, $[M+10H]^{10+}$ *m/z* = 1272.2, $[M+9H]^{9+}$ *m/z* = 1413.4, $[M+8H]^{8+}$ *m/z* = 1588.1.

D-Src^{biotin} (D-5c)

By the identical procedure described for the synthesis of peptide **L-5a**, peptide **D-5c** was synthesized (0.31 mg, 9% yield). MS(ESI): Calcd for Calcd for $C_{554}H_{866}N_{158}O_{166}S_4$: 12521.32 ($MH^+$); observed: $[M+15H]^{15+}$ m/z = 834.0, $[M+14H]^{14+}$ m/z = 895.7, $[M+13H]^{13+}$ m/z = 964.5, $[M+12H]^{12+}$ m/z = 1044.7, $[M+11H]^{11+}$ m/z = 1139.6, $[M+10H]^{10+}$ m/z = 1253.4, $[M+9H]^{9+}$ m/z = 1393.0, $[M+8H]^{8+}$ m/z = 1566.3, $[M+7H]^{7+}$ m/z = 1790.0

L-hmT pY324 (L-6, H-EPQpYEEIPIYL-NH_2)

The peptide resin was manually constructed by by Fmoc-SPPS on Rink-amide resin (0.6 mmol/g, 75 mg, 0.03 mmol). Fmoc-protected amino acids (3 eq) were coupled by using DIC (0.209 mL, 0.135 mmol) and HOBt·H_2O (21.2 mg, 0.135 mmol) in DMF. For coupling of the N-terminal Glu, Pro, Gln and pTyr, Fmoc-protected amino acid (5 eq), HATU (85.5 mg, 0.225 mmol) and (*i*-Pr)$_2$NEt (0.783 mL, 0.45 mmol) were employed. Fmoc-protecting group was removed by treatment of the resin with 20% piperidine in DMF. The resulting protected peptide resin was treated with TFA/thioanisole/*m*-cresol/1,2-ethanedithiol/H_2O (80:5:5:5:5) at room temperature for 2 h. After removal of the resin by filtration, the filtrate was poured into ice-cold dry Et_2O. Purification by preparative HPLC on a Cosmosil 5C18-ARII column (Nacalai Tesque, 20 × 250 mm, a linear gradient of 20–50% CH_3CN containing 0.1% (v/v) TFA aq. over 90 min) provided the peptide **L-6** (22.4 mg, 31% yield). MS(ESI): Calcd for $C_{66}H_{99}N_{13}O_{23}P$: 1473.56; observed: $[M+H]^+$ *m/z* = 1473.0.

D-hmT pY324 (D-6)

By the identical procedure described for the synthesis of peptide **L-6**, peptide **D-6** was synthesized (14.5 mg, 30% yield). MS(ESI): Calcd for $C_{66}H_{99}N_{13}O_{23}P$: 1473.56 ($MH^+$); observed: $[M+H]^+$ *m/z* = 1473.0.

L-hmT pY324^{biotin} (L-7, biotin-Ahx-EPQpYEEIPIYL-NH_2)

By the identical procedure described for the synthesis of peptide **L-6**, peptide **L-7** was synthesized (38 mg, 35% yield). D-Biotin was coupled with HBTU (73.3 mg, 0.3 mmol), HOBt·H_2O (45.9 mg,

0.3 mmol) and (*i*-Pr)$_2$NEt (0.104 mL, 0.6 mmol) in DMF. MS(ESI): Calcd for $C_{82}H_{124}N_{16}O_{26}PS$: 1813.01 ($MH^+$); observed: $[M+H]^+$ *m/z* = 1812.7.

D-hmT pY324^{biotin} (D-7)

By the identical procedure described for the synthesis of peptide **L-7**, peptide **D-7** was synthesized using D-biotin (24.2 mg, 44% yield). MS(ESI): Calcd for $C_{82}H_{124}N_{16}O_{26}PS$: 1813.01 ($MH^+$); observed: $[M+H]^+$ *m/z* = 1813.0.

L-FMT1^{FAM} (L-8, 5-FAM-GpYEEIA-NH$_2$)

By the identical procedure described for the synthesis of peptide **L-6**, peptide **L-8** was synthesized (7.9 mg, 23% yield). Labeling of 5-carboxyfluorecein (33.9 mg, 0.090 mmol) was carried out with DIC (0.0139 mL, 0.090 mmol) and HOBt·H_2O (13.8 mg, 0.090 mmol) in DMF. MS(MALDI-TOF): Calcd for $C_{51}H_{57}N_7O_{20}P$: 1119.02 (MH^+); observed: $[M+H]^+$ *m/z* = 1118.7, $[M+Na]^+$ *m/z* = 1141.7, $[M+K]^+$ *m/z* = 1156.6.

D-FMT1^{FAM} (D-8)

By the identical procedure described for the synthesis of peptide **L-8**, peptide **D-8** was synthesized (11.6 mg, 33% yield). MS(MALDI-TOF): Calcd for $C_{51}H_{57}N_7O_{20}P$: 1119.02 (MH^+); observed: $[M+H]^+$ *m/z* = 1118.7, $[M+Na]^+$ *m/z* = 1141.7, $[M+K]^+$ *m/z* = 1156.7.

L-hmT pY324^{FLAG} (H-KDDDDKYDIDHDKYDGDHDKYD-EPQpYEEIPIYL-NH$_2$) (L-9)

By the identical procedure described for the synthesis of peptide **L-6**, peptide **L-9** was synthesized (120 mg, 28% yield). FLAG sequence was manually constructed with Fmoc-protected amino acid (5 eq), HBTU (151 mg, 0.4 mmol), HOBt·H_2O (61.2 mg, 0.4 mmol) and (*i*-Pr)$_2$NEt (0.14 mL, 0.8 mmol) in DMF. The peptide was purified by preparative HPLC on a Cosmosil 5C18-AR300 column (Nacalai Tesque, 20 × 250 mm, a linear gradient of 15–45% CH_3CN containing 0.1% (v/v) TFA aq. over 90 min). MS(ESI): Calcd for $C_{181}H_{256}N_{43}O_{70}P$: 4183.76; observed: $[M+4H]^{4+}$ *m/z* = 1047.4, $[M+3H]^{7+}$ *m/z* = 1396.1.

D-hmT pY324^{FLAG} (D-9). By the identical procedure described for the synthesis of peptide **L-6**, peptide **D-6** was synthesized (108 mg, 25% yield). MS(ESI): Calcd for $C_{181}H_{256}N_{43}O_{70}P$: 4183.76; observed: $[M+4H]^{4+}$ *m/z* = 1047.2, $[M+3H]^{7+}$ *m/z* = 1395.9.

Folding of synthetic Src SH2 domains

Folding of synthetic Src SH2 derivatives were carried out by dialysis using Slide-A-Lyzer G2 dialysis cassette (cutoff 3.5 kDa, Thermo).[8] Lyophilized polypeptide (1 mg/mL) was dissolved in guanidine solution (6 M Gu·HCl, 20 mM HEPES, 100 mM NaCl, pH 8.5) and the solution was dialyzed against a 200-fold volume of dialysis buffer (20 mM HEPES, 100 mM NaCl, and 0.5 mM TCEP, pH 7.4) for 1.5 h at 4 °C. The additional dialysis was repeated against the dialysis buffer for an additional 1.5 h at 4 °C and overnight at 4 °C.

CD spectra of L-Src$^{145–251}$ and D-Src$^{145–251}$

Using the identical procedure for the folding of the protein, synthetic proteins were dialyzed in HEPES buffer against PBS buffer [1 M phosphate buffer (pH 7.4) containing 1 mM DTT]. CD spectra of L-Src$^{145–251}$ and D-Src$^{145–251}$ were recorded on a JASCO J-720 circular dichroism spectrometer at 20 °C.

Surface plasmon resonance analysis

SPR analysis was carried out using a ProteOnXPR36 surface plasmon resonance (SPR) system (BioRad) in the running buffer [10 mM HEPES (pH 7.4), 150 mM NaCl containing 0.005 % Tween-20] at 25 °C. For binding analysis of synthetic Src$^{145–251}$ (0–200 nM and Src SH2^{TMR} (0–200 nM) proteins, hmT pY324^{biotin} (5 nM, 5 min) was immobilized on a ProteOn NLC sensor chip. All analytes were evaluated for 60 s as contact time, followed by 600 s dissociation at a flow rate of 0.050 mL min^{-1}. For competitive experiments, Src SH2 (200 nM) in the presence of varying concentrations of unlabeled hmT pY324 (0–10 μM) in running buffer were injected onto the ProteOn NLC sensor chip, where hmT pY324^{biotin} was immobilized. The data were analyzed using GraphPad Prism software.

Fluorescence polarization assay

Fluorescence polarization (FP) assays were carried out in the assay buffer (PBS containing 2 mM DTT, 0.1% bovine gamma globulin, and 2% DMSO) using FMT1^{FAM} (20 nM) in 96-well non-binding surface black assay plates (Corning).[13] For binding titration analysis, probe FMT1^{FAM} (20 nM) was incubated with the synthetic Src SH2 domain at increasing concentrations (0–30 μM) in 0.10 mL of assay buffer. The K_D was obtained by nonlinear least-squares fitting to a single site binding model and Scatchard plot. For the competitive inhibition experiment, the hmT pY324

(inhibitor) and FMT1^{FAM} were diluted five-fold with PBS in advance. The Src SH2 domain (300 nM, 0.090 mL well^{-1}) was incubated with hmT pY324 (0.005 mL) for 30 min. Then, FMT1^{FAM} (0.005 mL) was added and the mixture was incubated for 30 min. FP signals were detected using an EnVision Xcite plate reader (Perkin Elmer) with a 480 nm excitation filter and a 535 nm emission filter. The data were analysed using GraphPad Prism software.

Competitive Binding Inhibition experiments by a Standard ELISA

ELISA competitive binding inhibition experimet were carried out in HEPES buffer [20 mM HEPES (pH7.4), 100 mM NaCl, 0.05 % Tween-20, 0,1% BSA]]. Precoated streptavidin 96-well plated (Nunc) were incubated with HEPES buffer containing 0.15% Tween-20 (300 μl/ well) for 1h. After three washes, 1 nM Src^{biotin} (100 μl/ well) was added and incubated for 2 h. After three washes, 100 nM FLAG-labeled hmT pY324 peptide in the presence of varying concentration of hmT pY324 peptide in HEPES buffer containing 1% DMSO (100 μl/ well) was added and incubated for 1 h. After three washes, 1: 5000 dilution of primary antibody (Anti DYKDDDK tag Monoclonal Antibody, WAKO) in HEPES buffer (100 μl/ well) was added and incubated for 1 h. After three washes, 1: 5000 dilution of secondary antibody (Blotting Grade Affinity Purified Goat Anti-Mouse IgG(H+L) Horseradish Peroxidase Conjugate, Bio-Rad) in HEPES buffer (100 μl/ well) was added and incubated for 1 h. After three washes, TMB (3,3',5,5'-Tetramethylbenzidine) solution (WAKO, 100 μl/ well) was added and incubated for 1 h. Then aqueous 1M H_2SO_4 (100 μl/ well) was added. Absorbance at 450 nm was measured for each well sing EnVision Xcite plate reader (Perkin Elmer).

Chemical array analysis

Photoaffinity linker-coated (PALC) slides were prepared according to previous reports[10,15a,15c] using amine-coated slides and the photoaffinity PEG linker. A solution of compounds in DMSO was spotted onto the PALC glass slides with a chemical arrayer equipped with 24 stamping pins or a MultiSPRinter spotter (Toyobo) equipped with a single stamping pin. The slides were exposed to UV irradiation of 4 J cm^{-2} at 365 nm using a CL-1000L UV crosslinker (UVP, CA) for immobilization. The slides were washed successively with DMSO, DMF, acetonitrile, THF, dichloromethane, EtOH, and ultra-pure water (5 min, three times each), and dried. L-Src SH2^{TMR} or D-Src SH2^{TMR} (3 μM in 1% skimmed-milk-TBS-T) was incubated with the glass slide for 1 h and then washed with TBS-T [10 mM Tris-HCl (pH 8.0), 150 mM NaCl, 0.05% Tween-20] (5 min, three

times). The slides were dried and scanned at 532 nm on a GenePix scanner. The fluorescence signals were quantified with GenePixPro.

References

1. (a) Zhou, S., Shoelson, S.E., Chaudhuri, M., Gish, G., Pawson, T., Haser, W.G., King, F., Roberts, T., Ratnofsky, S. & Lechleider, R.J. 1993, "SH2 domains recognize specific phosphopeptide sequences", *Cell,* vol. 72, no. 5, pp. 767-778. (b) Schwartzberg, P.L., Xing, L., Hoffmann, O., Lowell, C.A., Garrett, L., Boyce, B.F. & Varmus, H.E. 1997, "Rescue of osteoclast function by transgenic expression of kinase-deficient Src in src-/- mutant mice", *Genes & Development,* vol. 11, no. 21, pp. 2835-2844. (c) Kaplan, K.B., Swedlow, J.R., Morgan, D.O. & Varmus, H.E. 1995, "c-Src enhances the spreading of src-/- fibroblasts on fibronectin by a kinase-independent mechanism", *Genes & Development,* vol. 9, no. 12, pp. 1505-1517. (d) Fukui, Y., O'Brien, M.C. & Hanafusa, H. 1991, "Deletions in the SH2 domain of p60v-src prevent association with the detergent-insoluble cellular matrix", *Molecular and Cellular Biology,* vol. 11, no. 3, pp. 1207-1213.
2. (a) Schaller, M.D., Hildebrand, J.D., Shannon, J.D., Fox, J.W., Vines, R.R. & Parsons, J.T. 1994, "Autophosphorylation of the focal adhesion kinase, pp125FAK, directs SH2-dependent binding of pp60src", *Molecular and Cellular Biology,* vol. 14, no. 3, pp. 1680-1688. (b) Taylor, S.J. & Shalloway, D. 1994, "An RNA-binding protein associated with Src through its SH2 and SH3 domains in mitosis", *Nature,* vol. 368, no. 6474, pp. 867-871. (c) Petch, L.A., Bockholt, S.M., Bouton, A., Parsons, J.T. & Burridge, K. 1995, "Adhesion-induced tyrosine phosphorylation of the p130 src substrate", *Journal of Cell Science,* vol. 108, pp. 1371-1379. (d) Courtneidge, S.A., Goutebroze, L., Cartwright, A., Heber, A., Scherneck, S. & Feunteun, J. 1991, "Identification and characterization of the hamster polyomavirus middle T antigen", *Journal of Virology,* vol. 65, no. 6, pp. 3301-3308.
3. (a) Majkut, P., Claußnitzer, I., Merk, H., Freund, C., Hackenberger, C.P. & Gerrits, M. 2013, "Completion of proteomic data sets by Kd measurement using cell-free synthesis of site-specifically labeled proteins", *PloS One,* vol. 8, no. 12, pp. e82352. (b) Beebe, K.D., Wang, P., Arabaci, G. & Pei, D. 2000, "Determination of the binding specificity of the SH2 domains of protein tyrosine phosphatase SHP-1 through the screening of a combinatorial phosphotyrosyl peptide library", *Biochemistry,* vol. 39, no. 43, pp. 13251-13260. (c) Machida, K., Thompson, C.M., Dierck, K., Jablonowski, K., Kärkkäinen, S., Liu, B., Zhang, H., Nash, P.D., Newman, D.K. & Nollau, P. 2007, "High-throughput phosphotyrosine profiling using SH2 domains", *Molecular Cell,* vol. 26, no. 6, pp. 899-915.

4. Waksman, G., Shoelson, S.E., Pant, N., Cowburn, D. & Kuriyan, J. 1993, "Binding of a high affinity phosphotyrosyl peptide to the Src SH2 domain: crystal structures of the complexed and peptide-free forms", *Cell,* vol. 72, no. 5, pp. 779-790.
5. Brown, M.T. & Cooper, J.A. 1996, "Regulation, substrates and functions of src", *Biochimica et Biophysica Acta (BBA)-Reviews on Cancer,* vol. 1287, no. 2, pp. 121-149.
6. (a) Plummer, M.S., Holland, D.R., Shahripour, A., Lunney, E.A., Fergus, J.H., Marks, J.S., McConnell, P., Mueller, W.T. & Sawyer, T.K. 1997, "Design, synthesis, and cocrystal structure of a nonpeptide Src SH2 domain ligand", *Journal of Medicinal Chemistry,* vol. 40, no. 23, pp. 3719-3725. (b) Buchanan, J.L., Bohacek, R.S., Luke, G.P., Hatada, M., Lu, X., Dalgarno, D.C., Narula, S.S., Yuan, R. & Holt, D.A. 1999, "Structure-based design and synthesis of a novel class of Src SH2 inhibitors", *Bioorganic & Medicinal Chemistry Letters,* vol. 9, no. 16, pp. 2353-2358. (c) Shakespeare, W., Yang, M., Bohacek, R., Cerasoli, F., Stebbins, K., Sundaramoorthi, R., Azimioara, M., Vu, C., Pradeepan, S., Metcalf, C.,3rd, Haraldson, C., Merry, T., Dalgarno, D., Narula, S., Hatada, M., Lu, X., van Schravendijk, M.R., Adams, S., Violette, S., Smith, J., Guan, W., Bartlett, C., Herson, J., Iuliucci, J., Weigele, M. & Sawyer, T. 2000, "Structure-based design of an osteoclast-selective, nonpeptide src homology 2 inhibitor with in vivo antiresorptive activity", *Proceedings of the National Academy of Sciences of the United States of America,* vol. 97, no. 17, pp. 9373-9378. (d) Sundaramoorthi, R., Siedem, C., Vu, C.B., Dalgarno, D.C., Laird, E.C., Botfield, M.C., Combs, A.B., Adams, S.E., Yuan, R.W. & Weigele, M. 2001, "Selective inhibition of Src SH2 by a novel thiol-targeting tricarbonyl-modified inhibitor and mechanistic analysis by $^{1}H/^{13}C$ NMR spectroscopy", *Bioorganic & Medicinal Chemistry Letters,* vol. 11, no. 13, pp. 1665-1669. (e) Davidson, J.P., Lubman, O., Rose, T., Waksman, G. & Martin, S.F. 2002, "Calorimetric and structural studies of 1, 2, 3-trisubstituted cyclopropanes as conformationally constrained peptide inhibitors of Src SH2 domain binding", *Journal of the American Chemical Society,* vol. 124, no. 2, pp. 205-215. (f) Park, S., Won, J. & Lee, K. 2002, "Design and characterization of non-phosphopeptide inhibitors for Src family SH2 domains", *Bioorganic & Medicinal Chemistry Letters,* vol. 12, no. 19, pp. 2711-2714. (g) Lange, G., Lesuisse, D., Deprez, P., Schoot, B., Loenze, P., Bénard, D., Marquette, J., Broto, P., Sarubbi, E. & Mandine, E. 2002, "Principles governing the binding of a class of non-peptidic inhibitors to the SH2 domain of src studied by X-ray analysis", *Journal of Medicinal Chemistry,* vol. 45, no. 14, pp. 2915-2922. (h) Nam, N., Pitts, R.L., Sun, G., Sardari, S.,

Tiemo, A., Xie, M., Yan, B. & Parang, K. 2004, "Design of tetrapeptide ligands as inhibitors of the Src SH2 domain", *Bioorganic & Medicinal Chemistry,* vol. 12, no. 4, pp. 779-787. (i) Nam, N., Ye, G., Sun, G. & Parang, K. 2004, "Conformationally constrained peptide analogues of pTyr-Glu-Glu-Ile as inhibitors of the Src SH2 domain binding", *Journal of Medicinal Chemistry,* vol. 47, no. 12, pp. 3131-3141. (j) Won, J., Hur, Y., Hur, E.M., Park, S., Kang, M., Choi, Y., Park, C., Lee, K. & Yun, Y. 2003, "Rosmarinic acid inhibits TCR-induced T cell activation and proliferation in an Lck-dependent manner", *European Journal of Immunology,* vol. 33, no. 4, pp. 870-879.

7. Sperl, B., Seifert, M.H. & Berg, T. 2009, "Natural product inhibitors of protein–protein interactions mediated by Src-family SH2 domains", *Bioorganic & Medicinal Chemistry Letters,* vol. 19, no. 12, pp. 3305-3309.
8. Virdee, S., Macmillan, D. & Waksman, G. 2010, "Semisynthetic Src SH2 domains demonstrate altered phosphopeptide specificity induced by incorporation of unnatural lysine derivatives", *Chemistry & Biology,* vol. 17, no. 3, pp. 274-284.
9. Dawson, P.E., Muir, T.W., Clark-Lewis, I. & Kent, S.B. 1994, "Synthesis of proteins by native chemical ligation", *Science,* vol. 266, pp. 776-776.
10. Noguchi, T., Oishi, S., Honda, K., Kondoh, Y., Saito, T., Kubo, T., Kaneda, M., Ohno, H., Osada, H. & Fujii, N. 2013, "Affinity-based screening of MDM2/MDMX–p53 interaction inhibitors by chemical array: Identification of novel peptidic inhibitors", *Bioorganic & Medicinal Chemistry Letters,* vol. 23, no. 13, pp. 3802-3805.
11. Blanco-Canosa, J.B. & Dawson, P.E. 2008, "An efficient Fmoc-SPPS approach for the generation of thioester peptide precursors for use in native chemical ligation", *Angewandte Chemie International Edition,* vol. 47, no. 36, pp. 6851-6855.
12. (a) Panayotou, G., Bax, B., Gout, I., Federwisch, M., Wroblowski, B., Dhand, R., Fry, M.J., Blundell, T.L., Wollmer, A. & Waterfield, M.D. 1992, "Interaction of the p85 subunit of PI 3-kinase and its N-terminal SH2 domain with a PDGF receptor phosphorylation site: structural features and analysis of conformational changes", *The EMBO Journal,* vol. 11, no. 12, pp. 4261-4272. (b) Mattsson, P.T., Lappalainen, I., Backesjo, C.M., Brockmann, E., Lauren, S., Vihinen, M. & Smith, C.I. 2000, "Six X-linked agammaglobulinemia-causing missense mutations in the Src homology 2 domain of Bruton's tyrosine kinase: phosphotyrosine-binding and circular dichroism analysis", *Journal of Immunology,* vol. 164, no. 8, pp. 4170-4177.

13. Lynch, B.A., Loiacono, K.A., Tiong, C.L., Adams, S.E. & MacNeil, I.A. 1997, "A fluorescence polarization based Src-SH2 binding assay", *Analytical Biochemistry,* vol. 247, no. 1, pp. 77-82.
14. Foong, Y.M., Fu, J., Yao, S.Q. & Uttamchandani, M. 2012, "Current advances in peptide and small molecule microarray technologies", *Current Opinion in Chemical Biology,* vol. 16, no. 1, pp. 234-242.
15. (a) Kanoh, N., Kumashiro, S., Simizu, S., Kondoh, Y., Hatakeyama, S., Tashiro, H. & Osada, H. 2003, "Immobilization of natural products on glass slides by using a photoaffinity reaction and the detection of protein–small-molecule interactions", *Angewandte Chemie International Edition,* vol. 42, no. 45, pp. 5584-5587. (b) Kanoh, N., Asami, A., Kawatani, M., Honda, K., Kumashiro, S., Takayama, H., Simizu, S., Amemiya, T., Kondoh, Y. & Hatakeyama, S. 2006, "Photo-cross-linked small-molecule microarrays as chemical genomic tools for dissecting protein–ligand interactions", *Chemistry–An Asian Journal,* vol. 1, no. 6, pp. 789-797. (c) Kondoh, Y., Honda, K. & Osada, H. 2015, "Construction and application of a photo-cross-linked chemical array", *Methods in Molecular Biology*, vol. 1263, pp. 29-41.
16. Bravman, T., Bronner, V., Lavie, K., Notcovich, A., Papalia, G.A. & Myszka, D.G. 2006, "Exploring “one-shot” kinetics and small molecule analysis using the ProteOn XPR36 array biosensor", *Analytical Biochemistry,* vol. 358, no. 2, pp. 281-288.
17. Labbé, C.M., Laconde, G., Kuenemann, M.A., Villoutreix, B.O. & Sperandio, O. 2013, "iPPI-DB: a manually curated and interactive database of small non-peptide inhibitors of protein–protein interactions", *Drug Discovery Today,* vol. 18, no. 19, pp. 958-968.
18. Ettmayer, P., France, D., Gounarides, J., Jarosinski, M., Martin, M., Rondeau, J., Sabio, M., Topiol, S., Weidmann, B. & Zurini, M. 1999, "Structural and conformational requirements for high-affinity binding to the SH2 domain of Grb2 1", *Journal of Medicinal Chemistry,* vol. 42, no. 6, pp. 971-980.

Chapter 1. Development of Mirror-image screening systems

Section 2. Synthesis of XIAP BIR3 Domain for Mirror-Image Screening System

Summary

The X-linked inhibitor of apoptosis protein baculovirus IAP repeat (XIAP BIR3) domain is a promising therapeutic target for cancer treatment. For the mirror-image screening campaign to identify drug candidates from an unexplored mirror-image natural product library, in this section, a facile synthetic protocol for XIAP BIR3 domain synthesis was established by a native chemical ligation strategy using conserved cysteines present among BIR domains. The native and mirror-image XIAP BIR3 domains with an appropriate functional group for labeling were prepared using the established protocol. Taking advantage of the resulting synthetic proteins, several bioassay systems were developed to characterize inhibitors of the protein-protein interaction between the XIAP BIR3 domain and the second mitochondria-derived activator of caspases (SMAC).

Inhibitor of apoptosis proteins (IAPs) are a class of proteins that prevent apoptotic signaling *via* caspase inhibition.[1] Because caspases play an important role in the execution of programed cell death,[2] overexpression of IAPs leads to dysregulation of the process for eliminating unwanted cells. IAPs are characterized by highly conserved sequences with one or multiple baculovirus IAP repeat (BIR) domains that are approximately 70 amino acids in length (Figure 1).[3] BIR domains contain the characteristic motif $CX_2CX_{16}HX_6C$, in which the three conserved Cys and single conserved His coordinate a zinc ion to adopt a classical zinc finger-like structure.[4] X-linked IAP (XIAP), a human IAP, has three tandem BIR domains[5] that are responsible for caspase inhibition *via* distinct interactions.[6] The linker region between BIR1 and BIR2 inhibits the catalytic activity of caspase-3 and caspase-7 by binding to the substrate binding pockets in caspase-3 and caspase-7.[7] The BIR3 domain binds to the N-terminal sequence of the small subunit of caspase-9 to prevent formation of active caspase-9 homodimers.[8] These observations are supported by X-ray crystal structures of the XIAP–caspase complexes.[9] The XIAP BIR3 domain also recognizes the N-terminal sequence of the second mitochondria-derived activator of caspases (SMAC), which is released in response to cell death signaling.[10] The direct binding of SMAC with the XIAP BIR3 domain relieves XIAP-mediated inhibition of caspase 9 to promote apoptosis.[11]

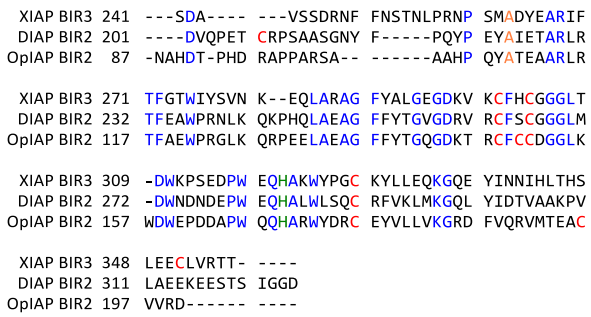

Figure 1. Sequences of BIR domains. Red-colored letters: cysteines; other colored letters: conserved amino acids.

The N-terminal four residues (Ala-Val-Pro-Ile) of SMAC bind to the XIAP BIR3 domain.[10] The N-terminal Ala of SMAC forms multiple hydrogen bonds with Glu314, Gln319 and Trp323, whereas the four hydrophobic residues have van der Waals interactions with hydrophobic residues (Leu292, Leu307, Trp310, Gln319, Trp323 and Tyr 324) in a surface groove located on the XIAP BIR3 domain. On the basis of these findings, considerable medicinal chemistry efforts by structure-based approaches from the native SMAC peptide sequence have been devoted to the development of small molecule inhibitors that target the XIAP BIR3 domain.[12] Currently, several clinical studies of SMAC mimetics including LCL161, Debio1143 and Birinapant have been performed for patients with solid tumors and leukemia (Figure 2).[13] Accordingly, IAP antagonists including SMAC mimetics represent promising therapeutic agents for treatment of cancers with deregulation of cell death pathways.[14]

To extend the applicability of the mirror-image screening process, the author focused on the XIAP BIR3 domain as an initial trial among a number of BIR domains. In this section, the author investigated the efficient preparation of the XIAP BIR3 domain and labeled derivatives. Bioassay systems using the synthetic proteins were also established to identify potential drug candidates from an unexplored chemical space of chiral natural products.

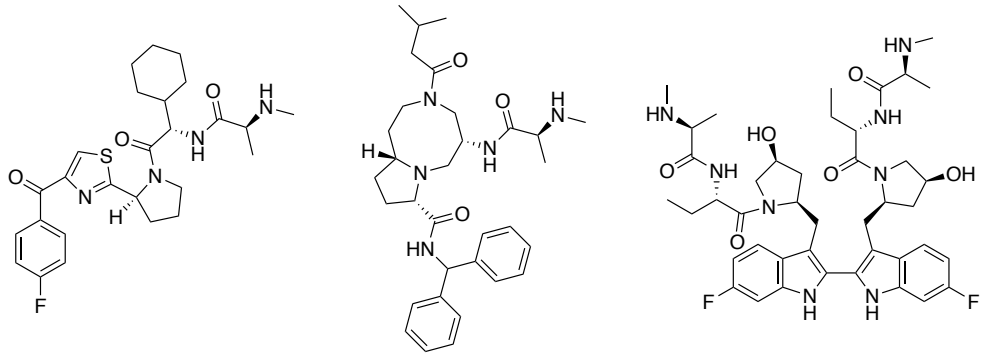

Figure 2. Structures of XIAP BIR3 domain inhibitors in clinical trials.

The author designed a synthetic process for XIAP BIR3 domain ($XIAP^{241–356}$) production by using a NCL strategy. In this strategy, the author hypothesized that three peptide segments can be ligated at two cysteines, Cys300 and Cys327. The NCL strategy developed should be applicable for the synthesis of a variety of BIR domains because these Cys residues are conserved among BIR domains (Figure 1). Initially, the author investigated the synthesis of these three segments for NCL (Figure 3). The peptide segments [L-$XIAP^{241–299}$ (**L-1a**), L-$XIAP^{300–326}$ (**L-2**) and L-$XIAP^{327–356}$ (**L-3**)] were prepared by standard Fmoc-SPPS using HBTU/(i-Pr)$_2$NEt activation on Rink amide ChemMatrix resin. For the preparation of N-terminal and middle thioester segments (N-segment **L-1a** and M-segment **L-2**), the Dbz linker was used according to the same procedure described in section 1 (Figure 3). After construction of the peptide sequences on the resins, the Dbz linker was activated by treatment with p-nitrophenyl chloroformate and (i-Pr)$_2$NEt to give the Nbz form. TFA-mediated final deprotection followed by treatment with MPAA afforded the expected peptide thioester **L-1a** in very low yield (0.2%). The low yield is supposed to be low conversion of coupling during construction of the protected peptide fragment by solid-phase synthesis. The author investigated the reaction conditions using other resins and coupling reagents; however, the author failed to improve the yield of **L-1a**. The M-segment **L-2** with the C-terminal Nbz active ester was obtained in a similar manner *via* activation of the Dbz linker in good purity. The C-segment **L-3** was also synthesized by the identical Fmoc-SPPS protocol followed by TFA-mediated final deprotection. The resulting M-segment **L-2** and C-segment **L-3** were subjected to NCL conditions. The subsequent thiazolidine deprotection of the N-terminal thioproline (Thz) using methoxyamine[15] provided L-$XIAP^{300–356}$ (M+C-segment, **L-4**) in 35% yield.

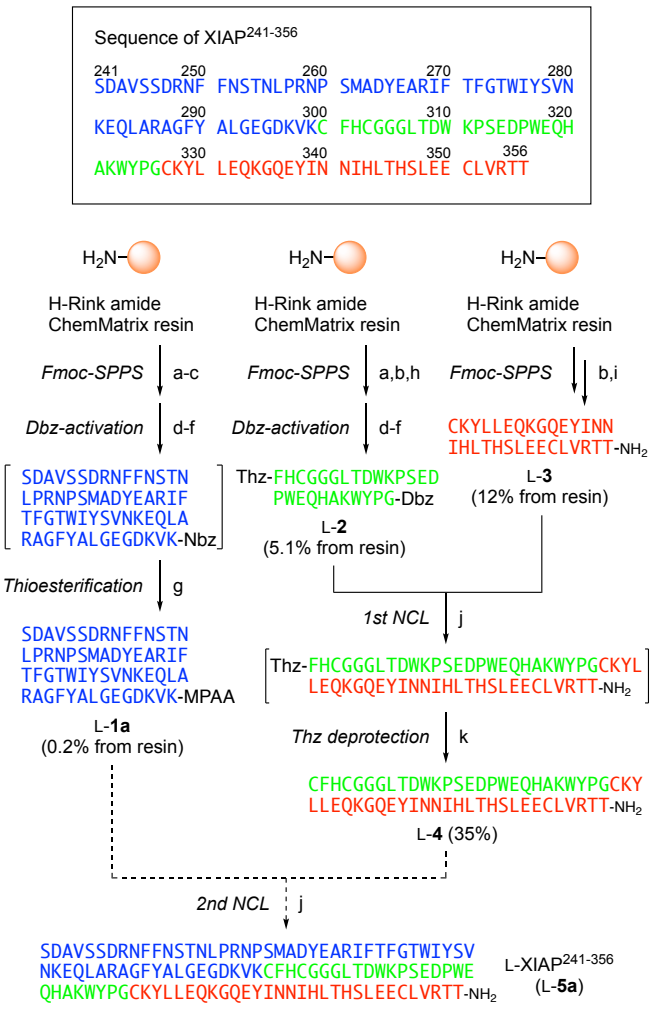

Figure 3. Synthesis of L-XIAP$^{241–356}$ using three segments. (a) Fmoc-Dbz-OH, HBTU, 1-hydroxybenzotriazole (HOBt), (*i*-Pr)$_2$NEt, DMF, and then 20% piperidine/DMF; (b) Fmoc-Xaa-OH, HBTU, HOBt, (*i*-Pr)$_2$NEt, DMF, and then 20% piperidine/DMF; [repeat (b) until the sequence was completed] (c) Boc-Ser(*t*-Bu)-OH, HBTU, HOBt, (*i*-Pr)$_2$NEt, and DMF; (d) 4-nitrophenyl chloroformate, and DCM; (e) (*i*-Pr)$_2$NEt, and DMF; (f) TFA/H$_2$O/*m*-cresol/thioanisole (80:10:5:5); (g) MPAA, 20 mM tris(2-carboxyethyl)phosphine (TCEP), 6 M guanidine, and phosphate buffered saline (PBS, pH 7.0); (h) Boc-Thz-OH, HBTU, HOBt, (*i*-Pr)$_2$NEt, and DMF; (i) TFA/H$_2$O/*m*-cresol/thioanisole/1,2-ethanedithiol (EDT) (80:5:5:5:5); (j) MPAA, 100 mM TCEP, 6 M guanidine, and PBS (pH 7.0); (k) methoxyamine.

To improve the preparation yield of the N-segment **L-1a**, an alternative synthetic process for **L-1a** from two short segments was designed (Figure 4). The author focused on Ala263, which is shared among many BIR domains at this position (Figure 1), for the additional NCL site in the N-segment (Figure 4). The author expected that Ala263 could be constructed by desulfurization of Cys263 after NCL between N^1-segment XIAP$^{241–262}$ (**L-6a**) and N^2-segment XIAP$^{263–299}$ (**L-7**). The N^1-segment **L-6a** was obtained by the identical procedure used to synthesize thioester **L-1a** on the Dbz linker. For

the synthesis of N^2-segment **L-7**, a hydrazide linker was attached to Wang-PEG resin by treatment with 4-nitrophenyl chloroformate and hydrazine.[16] When the resulting thioester **L-6a** and hydrazide **L-7** were subjected to NCL conditions, the expected [Cys^{263}]-L-XIAP$^{241–299}$ (**L-8a**) was obtained in 49% yield. The subsequent VA-044-mediated metal-free desulfurization (MFD)[17] of **L-8a** provided the N-segment L-XIAP$^{241–299}$ (**L-9a**). This process including an additional NCL and desulfurization improved the overall yield of the N-segment compared with the stepwise synthesis. The hydrazide moiety at the C-terminus of **L-9a** was employed for the next N-to-C-directed NCL, in which $NaNO_2$-mediated activation of **L-9a** followed by ligation with M+C segment **L-4** in the presence of MPAA provided the desired L-XIAP$^{241–356}$ (**L-5a**) in 33% yield (Figure 5A).

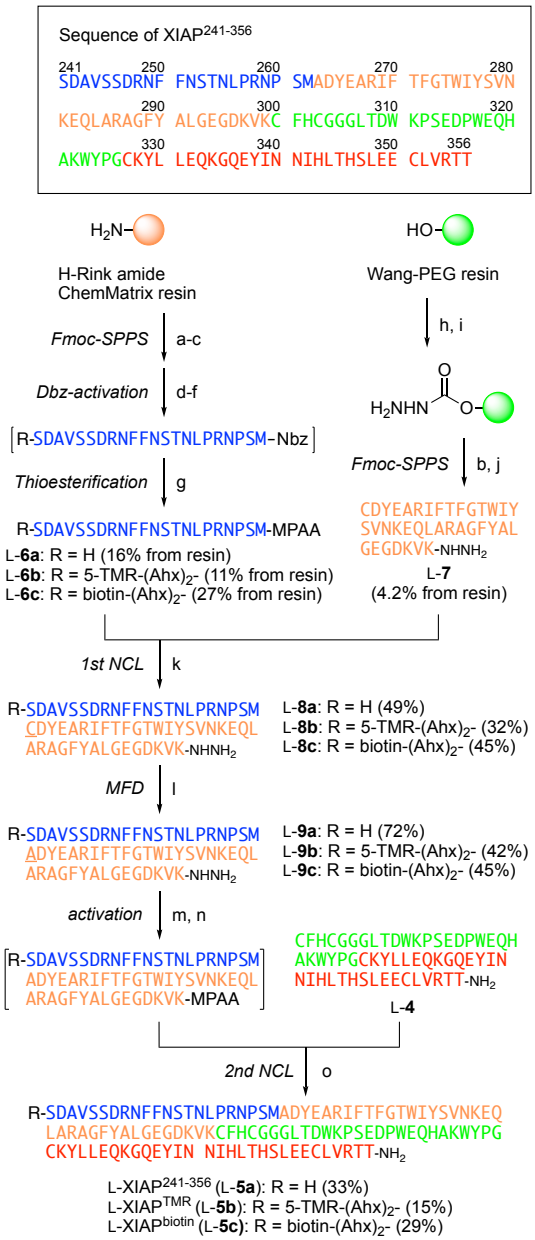

Figure 4. Synthesis of L-XIAP$^{241–356}$, L-XIAP^{TMR}, and L-XIAP^{biotin} using four fragments. (a) Fmoc-Dbz-OH, HBTU, HOBt, (*i*-Pr)$_2$NEt, DMF, and then 20% piperidine/DMF; (b) Fmoc-Xaa-OH, HBTU, HOBt, (*i*-Pr)$_2$NEt, DMF, and then 20% piperidine/DMF; [repeat (b) until the sequence was completed] (c) Boc-Ser(*t*-Bu)-OH, HBTU, HOBt, (*i*-Pr)$_2$NEt, and DMF (for **L-6a**); 5-Carboxytetramethylrhodamine (5-TMR), DIC, HOBt, and DMF (for **L-6b**); D-Biotin, HBTU, HOBt, (*i*-Pr)$_2$NEt, and DMF (for **L-6c**); (d) 4-nitrophenyl chloroformate, and DCM; (e) (*i*-Pr)$_2$NEt, and DMF; (f) TFA/H_2O/*m*-cresol/thioanisole (80:10:5:5); (g) MPAA, 20 mM TCEP, 6 M guanidine, and PBS (pH 7.0); (h) 4-nitrophenyl chloroformate, pyridine, and DCM; (i) $NH_2NH_2 \cdot H_2O$, and THF; (j) TFA/H_2O/*m*-cresol/thioanisole/EDT (80:5:5:5:5); (k) MPAA, 100 mM TCEP, 6 M guanidine, and PBS (pH 7.0); (l) VA-044, TCEP, sodium 2-mercaptoethanesulfonate (MESNa), 6 M guanidine, and 200 mM phosphate buffer (pH 6.5); (m) $NaNO_2$, 6 M guanidine, and phosphate buffer (pH 3.0); (n) MPAA, 6 M guanidine, and 150 mM phosphate buffer (pH 6.8); (o) MPAA, TCEP, 6 M guanidine, and 150 mM phosphate buffer (pH 6.8).

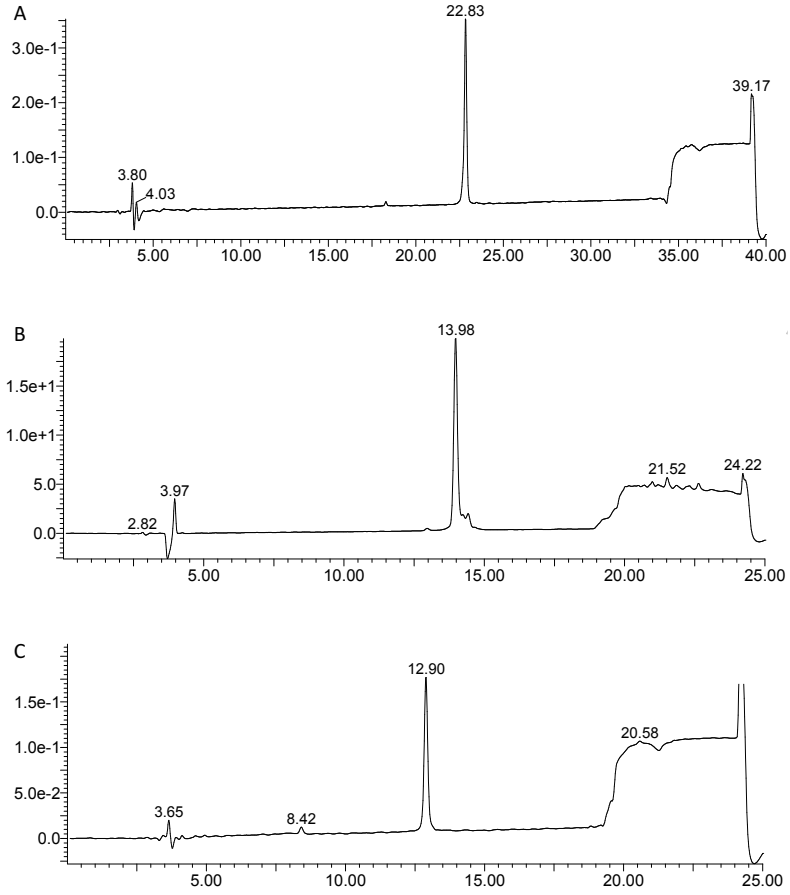

Figure 5. Analytical HPLC chromatograms of purified L-**5a** (A), L-**5b** (B), and L-**5c** (C). HPLC analysis was performed at 25 °C with a linear gradient of CH_3CN (for A: 20-50%, for B,C: 30–45%) containing 0.1% TFA at a flow rate of 1mL/min over 15 min.

XIAP BIR3 domains with a single fluorescent group or a biotin tag were designed and synthesized for bioassays including chemical array screening and an ELISA, which are suitable for identifying inhibitors of the XIAP BIR3 domain. A previous structural study revealed that the binding surface

on the XIAP BIR3 domain with the SMAC peptide is located distal from the N-terminus.[10b] Based on this structural information, the author hypothesized that a single modification with TMR or biotin at the N-terminus of the XIAP BIR3 domain should not disrupt bioactivity of the intact protein. The TMR group or biotin was conjugated by on-resin modification at the N-terminus of the N-segment *via* an Ahx_2 linker after peptide sequence elongation to provide TMR-labeled L-XIAP$^{241–262}$ **L-6b** and biotin-labeled L-XIAP$^{241–262}$ **L-6c** (Figue 5B,C). The modified XIAP BIR3 domains [L-XIAP^{TMR} (**L-5b**) and L-XIAP^{biotin} (**L-5c**)] were prepared by the same procedures used to prepare **L-6b** and **L-6c**, respectively. The mirror-image proteins (**D-5a–c**) were also synthesized from four mirror-image segments **D-2**, **D-3**, **D-6a–c** and **D-7** by the same process.

For the preparation of bioactive XIAP BIR3 domains, the resulting full-length proteins were subjected to refolding according to the protocol reported previously.[18] After synthetic L-XIAP$^{241–356}$ (**L-5a**) was denatured in 7 M urea, the solution was dialyzed against Tris buffer (20 mM Tris-HCl, 150 mM NaCl, 5 mM 2-mercaptoethanol, 0.01 mM $ZnCl_2$, pH 8.0) to give a homogenous solution of L-XIAP$^{241–356}$. CD spectra were recorded to confirm the secondary structure of the folded XIAP BIR3 domains (Figure 6). The CD spectrum of L-XIAP$^{241–356}$ was consistent with that of the recombinant XIAP BIR3 domain, in which the ellipticity minima around 209 and 228 nm supported the presence of the characteristic all α-helix structure.[19] The inverse but equivalent CD signal of D-XIAP$^{241–356}$ was also observed, suggesting that the mirror-image L- and D-proteins were appropriately generated by the folding process.

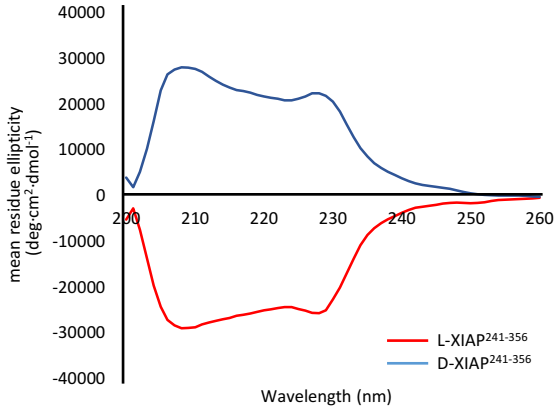

Figure 6. CD spectra of L-XIAP$^{241–356}$ and D-XIAP$^{241–356}$

Next, to confirm the bioactivity of the synthetic proteins, the binding affinity of the XIAP BIR3 domain to SMAC mimetics was assessed by SPR analysis (Figure 7). For the SPR experiments, the

SMAC-derived peptide with biotin modification [SMAC^{biotin}: H-Abu-Arg-Pro-Phe-Lys(Ahx-biotin)-NH_2, **10**] was immobilized on the streptavidin coated sensor chip. Homogenous solutions of the XIAP BIR3 domain at concentrations from 20 to 2000 nM were flushed into the flow system. Submicromolar binding affinity of L-XIAP$^{241–356}$ towards L-SMAC^{biotin} (**L-10**) was observed [K_D (L-XIAP$^{241–356}$–**L-10**): 0.37 μM], whereas no binding interaction was observed toward D-SMAC^{biotin} (**D-10**), indicating that satisfactory stereoselective molecular recognition was accomplished. In a similar manner, D-XIAP$^{241–356}$ had reasonable affinity towards D-SMAC^{biotin} (**D-10**) [K_D (D-XIAP$^{241–356}$–**D-10**): 0.28 μM] without binding to L-SMAC^{biotin} (**L-10**).

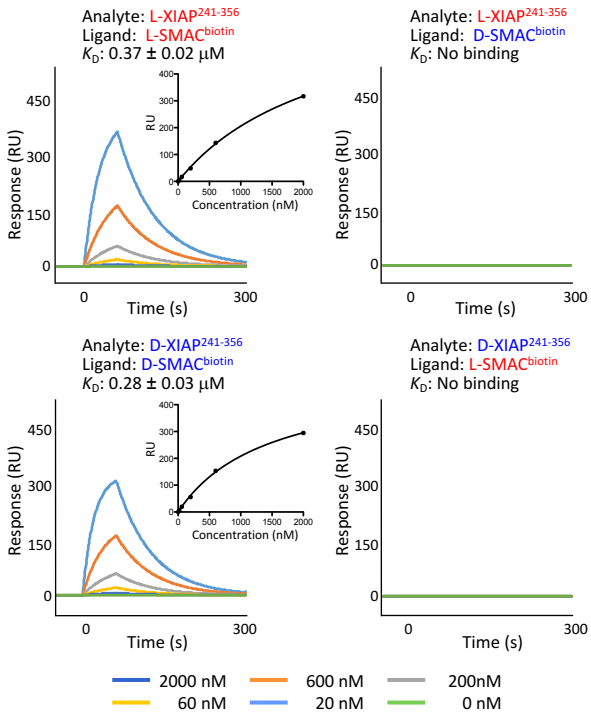

Figure 7. Representative data of the SPR analysis of folded L-XIAP$^{241–356}$ and D-XIAP$^{241–356}$ towards L-SMAC and D-SMAC-derived peptides. A Langmuir model was used for determining binding affinities from triplicate assays.

The binding affinity of the TMR-labeled XIAP BIR3 domains (XIAP^{TMR}) towards SMAC-derived peptides were assessed by SPR analysis. L-XIAP^{TMR} and D-XIAP^{TMR} possessed slightly higher binding affinity toward SMAC-derived peptides [K_D (L-XIAP^{TMR}–**L-10**): 0.13 μM] and [K_D (D-XIAP^{TMR}–**D-10**): 0.11 μM] when compared with that of the unlabeled XIAP BIR3 domain (Figure 8). Noteworthy, no binding with the respective mirror-image SMAC-derived peptides was observed. Similarly, the biotin-labeled XIAP BIR3 domain (L-XIAP^{biotin}) showed stereoselective binding towards the L-SMAC-derived peptide [K_D: (L-XIAP^{biotin}–**L-10**): 0.17 μM] without binding with the

D-SMAC-derived peptide (**D-10**) (Figure 9). These results suggested that N-terminal TMR and biotin modification *via* an Ahx_2 linker had minimal effect on the bioactivity of XIAP BIR3.

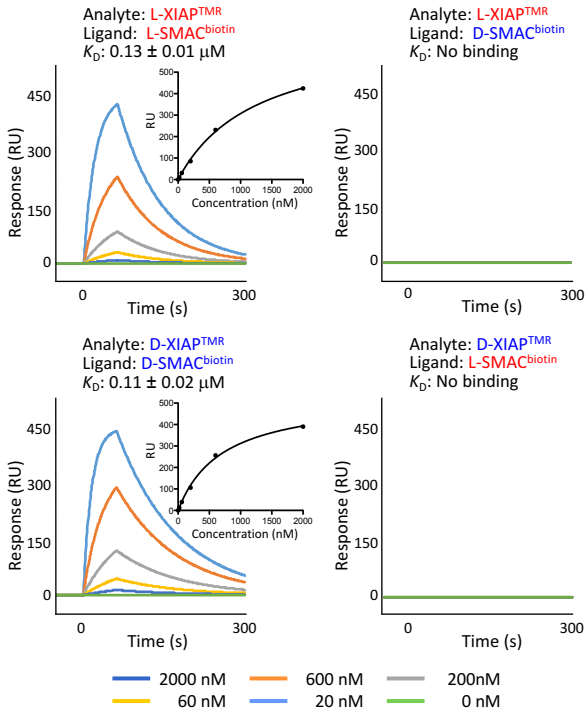

Figure 8. Representative data of the SPR analysis of folded L- and D-$XIAP^{TMR}$ towards L- and D-SMAC-derived peptides. A Langmuir model was used for determining binding affinities from triplicate assays.

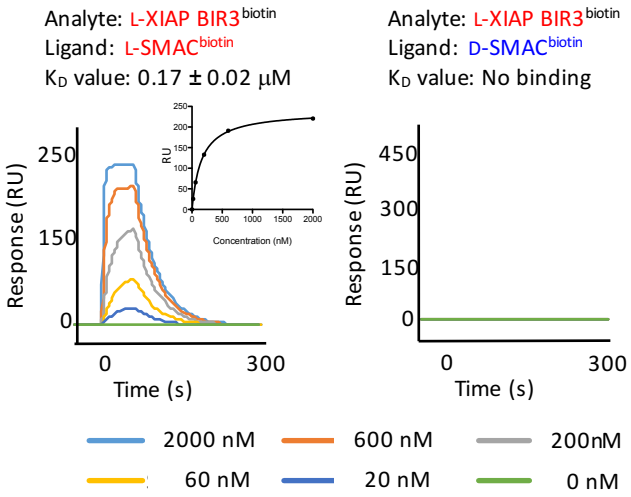

Figure 9. SPR analysis of the biotinylated XIAP BIR3 domain. Representative data of L-$XIAP^{biotin}$ towards L-$SMAC^{biotin}$ and D-$SMAC^{biotin}$ peptides. A Langmuir model was used for determining the binding affinities from triplicate assays.

The author also evaluated the apparent binding affinity between synthetic XIAP BIR3 domains and the fluorescent SMAC-derived peptide [SMAC^{FAM}: H-Abu-Arg-Pro-Phe-Lys(5-FAM)-NH_2, **11**: FAM] by a FP assay (Figure 10A,B).[20] L-XIAP$^{241–356}$ bound to L-SMAC^{FAM} with a submicromolar affinity [K_D (L-XIAP$^{241–356}$–L-SMAC^{FAM}): 0.12 ± 0.01 μM]. Identical binding was observed between the mirror-image pair D-XIAP$^{241–356}$ and D-SMAC^{FAM} [K_D (D-XIAP$^{241–356}$–D-SMAC^{FAM}): 0.12 ± 0.02 μM]. These SPR and FP experiments demonstrated that synthetic XIAP BIR3 proteins retained the appropriate structures and functions after the refolding process to show stereoselective interaction with the SMAC-derived peptides.

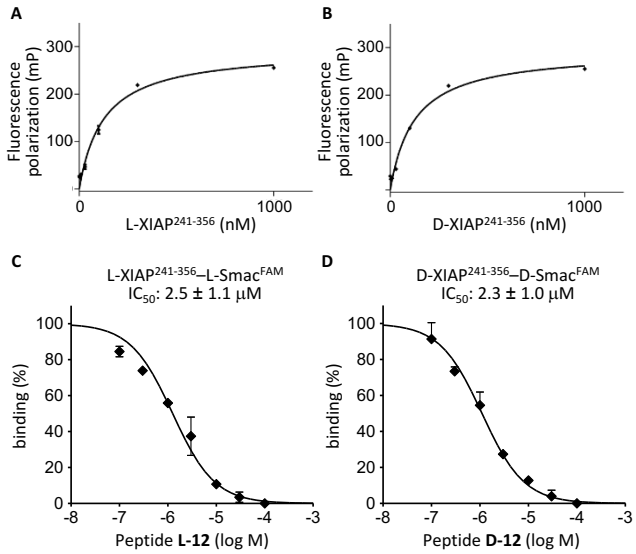

Figure 10. Fluorescence polarization analysis of XIAP BIR3 domain binding with SMAC mimetics. (A,B) Binding curves of the XIAP$^{241–356}$–SMAC^{FAM}. K_D values were determined from the saturation curves generated from triplicate experiments of the fluorescence polarization assay using FAM-labeled SMAC (L-XIAP$^{241–356}$–L-SMAC^{FAM}: 0.12 ± 0.01 μM; D-XIAP$^{241–356}$–D-SMAC^{FAM}: 0.12 ± 0.02 μM). (C,D) The representative dose-dependent curves of inhibition by unlabeled SMAC-derived peptides (**L-12** and **D-12**) against the L-XIAP$^{241–356}$–L-SMAC^{FAM} interaction (C) and the D-XIAP$^{241–356}$–D-SMAC^{FAM} interaction (D).

With functional XIAP BIR3 domains available, the author investigated the development of several types of in vitro bioassay systems for mirror-image screening. Initially, a competitive inhibition assay for XIAP BIR3 domain inhibitors by FP experiments was established based on a reported protocol (Figure 10C,D).[20] Detection of the protein-protein interaction by FP allows a homogeneous assay

using label-free proteins for high-throughput screening. When the fluorescent L-SMAC-derived peptide (L-SMAC^{FAM}, **L-11**, 5 nM) and unlabeled L-XIAP BIR domain (L-XIAP$^{241–356}$, 120 nM) were used for the experiment, dose-dependent inhibition of the unlabeled L-SMAC-derived peptide [**L-12**, H-Abu-Arg-Pro-Phe-Lys-NH_2: Abu: 2-aminobutyric acid][20] was observed (IC_{50}: 2.5 ± 1.1 μM). The mirror-image interaction between D-XIAP$^{241–356}$ and D-SMAC was inhibited by the D-SMAC-derived peptide (**D-12**, IC_{50}: 2.3 ± 1.0 μM) in a similar manner.

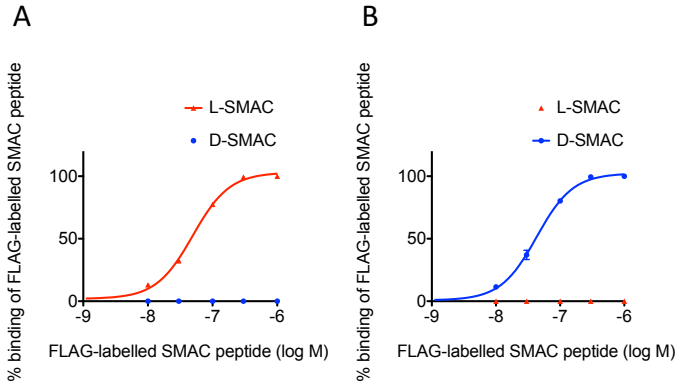

Figure 11. Binding curves of SMAC-derived peptides for the XIAP BIR3 domain in ELISA. XIAP^{biotin} (10 nM) in HEPES buffer (100 μL/well) was immobilized onto recoated streptavidin 96-well plates (Nunc) for 2 h. After thee washes, varying concentrations of SMAC^{FLAG} (**13**) in HEPES buffer (100 μL/well) was added and incubated for 1 h. K_D values were determined from the dose-response curves generated from triplicate experiments (**L-13**: 44 ± 6.2 nM, and **D-13**: 39 ± 4.4 nM).

Using the biotin-labeled XIAP BIR3 domain (XIAP^{biotin}), the author also established an ELISA based on the procedure described in section 1. XIAP^{biotin} was initially immobilized on a streptavidin-coated 96-well plate and the SMAC-derived peptide with the FLAG tag (SMAC^{FLAG}, **13**) was then incubated with the immobilized XIAP^{biotin}. The binding of the XIAP BIR3 domain with the SMAC-derived peptide was detected by using a commercially available HRP-conjugated anti-FLAG antibody and the TMB substrate. The stereoselective binding of L-SMAC^{FLAG} and D-SMAC^{FLAG} peptides with L-XIAP^{biotin} and D-XIAP^{biotin}, respectively, were observed in a dose-dependent manner. (Figure 11). Using these ELISA systems, the inhibitory activities of unlabeled SMAC-derived peptides (**L-12** and **D-12**) against XIAP^{biotin}–SMAC^{FLAG} interactions were assessed. Peptide **L-12** inhibited the native interaction between L-XIAP^{biotin} and L-SMAC^{FLAG} in the low micromolar range (IC_{50}: 2.3 μM), whereas no inhibition by peptide **D-12** was observed (Figure 12). The mirror image interaction between D-XIAP^{biotin} and D-SMAC^{FLAG} was inhibited similarly (IC_{50}: 2.0 μM). To identify potential inhibitors that target the SMAC/caspase binding pocket in the XIAP BIR3 domain, this mirror-image

ELISA assay would be an alternative to the FP assay, in which colored substances may often interfere with the analysis to cause false-positives or false-negatives.

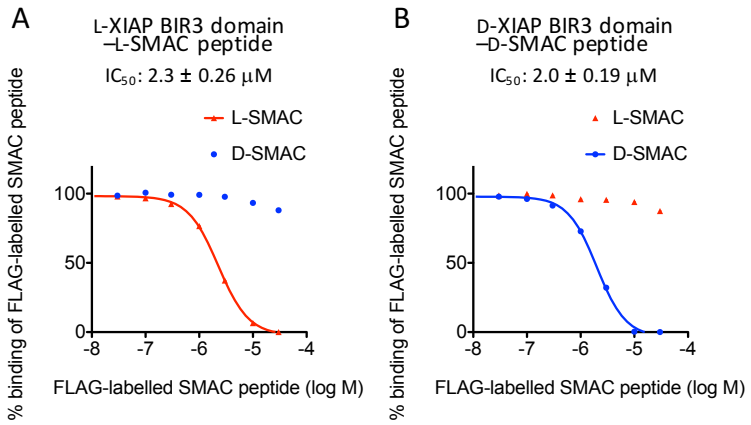

Figure 12. ELISA-based competition assays for XIAP BIR3 domain inhibitors. The representative dose-dependent curves of the inhibitory activity of the L-SMAC-derived peptide (**L-12**) against the $XIAP^{biotin}$–$SMAC^{FLAG}$ interaction (A) and the D-SMAC-derived peptide (**D-12**) against the $XIAP^{biotin}$–$SMAC^{FLAG}$ interaction (B). IC_{50} values were calculated from the dose-response curves generated from four independent experiments.

The synthetic fluorescence-labeled XIAP BIR3 domains (L-$XIAP^{TMR}$ and D-$XIAP^{TMR}$) were applied to chemical array analysis, which is a high-throughput affinity-based screening technology. To verify the specific and enantioselective binding of $XIAP^{TMR}$, binding analysis toward the counterpart SMAC-derived peptide on a chemical array was carried out. Each L-SMAC- or D-SMAC-derived peptide (**L-12** or **D-12**) was immobilized on the array surface *via* photoaffinity PEG or proline linker by spotting at the different concentrations (1.25–10 mg/mL). When the array was treated with L-$XIAP^{TMR}$ and D-$XIAP^{TMR}$ (1 μM), the fluorescent spots were observed at the positions of L-SMAC and D-SMAC-derived peptides, respectively (Figures 13 and 14). These results indicated that the synthetic XIAP BIR3 domains can distinguish the mirror-image structures of the target SMAC-derived peptide in the chemical array platform to facilitate the expected screening of virtual mirror-image natural products. Of note, the fluorescent intensities of bound $XIAP^{TMR}$ were dependent on the concentrations of the spotted SMAC-derived peptide. Additionally, relatively higher fluorescent intensities were observed when a proline linker was used for the immobilization of SMAC-derived peptides when compared with the results using the PEG linker.

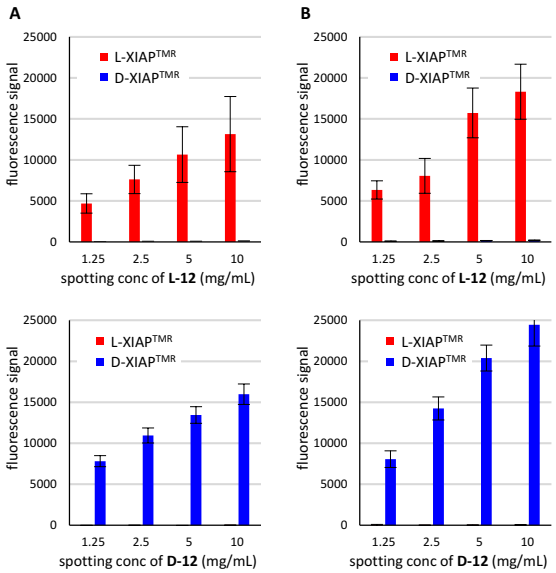

Figure 13. Binding of XIAP BIR3 domains with SMAC-derived peptides immobilized on a chemical array. The fluorescence intensities of L-XIAP^{TMR} or D-XIAP^{TMR} were measured using the chemical array, in which L-SMAC- or D-SMAC-derived peptides (**L-12** or **D-12**) were spotted at various concentrations *via* a PEG (A) or proline linker (B).

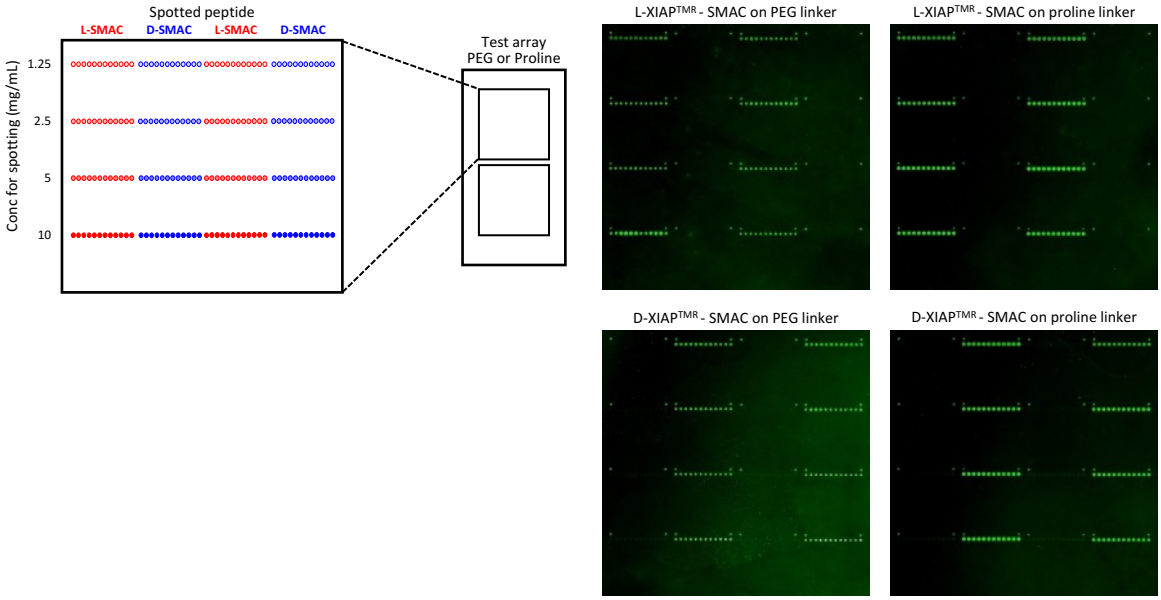

Figure 14. Representative results of chemical array analysis of TMR-labeled XIAP BIR3 domain binding with SMAC peptides. L-SMAC and D-SMAC derived peptides were immobilized on the array surface *via* PEG or proline linker at various concentrations (1.25, 2.5, 5 and 10 mg/mL). The array was treated wth L-XIAP^{TMR} and D-XIAP^{TMR} (1 μM).

Having established the facile screening platform by an array technology, the author conducted the mirror-image screening of natural products and derivatives (22,097 compounds) from the Natural

Products Depository, NPDepo in RIKEN. L-XIAP^{TMR} was observed to bind 451 compounds, whereas D-XIAP^{TMR} bound 281 compounds. Among the 579 total hit compounds, 53 chiral compounds with a single or multiple chiral center(s) exhibited selective binding with D-XIAP^{TMR}. Further investigations of these hit compounds including binding site analysis and specificity evaluations are currently in progress.

In the current study, the author have investigated the synthesis of XIAP BIR3 domains, which are attractive drug targets for cancer chemotherapy. The initial design strategy to produce synthetic XIAP BIR3 involved a stepwise NCL process using three peptide segments, in which two conserved Cys residues were used as the ligation sites; however, the 59-residue N-segment was obtained in low yield using a standard solid-phase synthesis protocol. Thus, the N-segment was prepared *via* an additional NCL from two short segments followed by VA-044-mediated desulfurization. The N-to-C ligation between the peptide hydrazide in the N-segment and the cysteine in the M+C-segment afforded the full-length XIAP BIR3 domain. After refolding the synthetic protein according to a reported procedure, the characteristic structure and biological function of the folded protein were verified by spectroscopic and physicochemical analyses. This is the first reported chemical synthesis of BIR domains. The established synthetic protocol should be applicable to the preparation of other BIR domains because the cysteine and alanine residues used as ligation sites are conserved across a number of BIR domains.

Exploiting the established synthetic protocol, TMR- and biotin-labeled XIAP BIR3 domains and their mirror-image proteins were prepared in the same manner. These synthetic proteins exhibited comparable affinity toward target SMAC-derived peptides when compared with that of unlabeled counterparts. Additionally, the L- and D-XIAP BIR3 domains displayed selective binding to L-SMAC- and D-SMAC-derived peptides, respectively, without cross-reactivity to the heterochiral mutated SMAC peptide, suggesting that the good chiral recognition of synthetic proteins facilitates novel mirror-image screening for XIAP BIR3 domain inhibitors. The author established three in vitro assays for mirror-image screening: (1) the FP assay using the unlabeled XIAP BIR3 domain and the FAM-labeled mutated SMAC peptide; (2) ELISA using the biotin-labeled XIAP BIR3 domain and the FLAG-labeled SMAC-derived peptide; and (3) chemical array analysis by the TMR-labeled XIAP BIR3 domain. In a screening campaign by chemical array analysis from natural products and their derivatives at RIKEN, a variety of compounds were identified to show binding to L-XIAP BIR3 and/or D-XIAP BIR3 domains. This established mirror-image bioassay platform for the XIAP BIR3 domain should contribute to the development of facile screening protocols for a number of IAP BIR

domains and for rapid discovery of potential BIR domain inhibitors.

Experimental Section

L-XIAP$^{241-299}$ (L-1a)

Fmoc-Dbz-OH was manually loaded onto Rink Amide-ChemMatrix resin (0.4–0.6 mmol/g, 40 mg, 0.016–0.024 mmol) by HBTU (37.8 mg, 0.1 mmol), HOBt·H_2O (15.2 mg, 0.1 mmol) and (*i*-Pr)$_2$NEt (34.8 μL, 0.2 mmol) in DMF for 2.5 h (four times). The peptide sequence was constructed by standard Fmoc-SPPS. Boc-Thz-OH (23.3 mg, 0.1 mmol) was employed for coupling of the N-terminal Thz. After solid-phase peptide synthesis, a solution of *p*-nitrophenyl chloroformate in CH_2Cl_2 (22.5 mg/mL, 0.38 mL, 0.11 mmol) was added to the protected peptide resin and the reaction was continued for 40 min at room temperature. Subsequently, the resin was treated with 0.5 M (*i*-Pr)$_2$NEt in DMF (0.38 mL) for 15 min. The resin was treated with TFA/H_2O/thioanisole/*m*-cresol (80:10:5:5) for 2 h at room temperature. After removal of the resin by filtration, the filtrate was poured into ice-cold dry Et_2O. Crude Dbz-ester cleaved from the resin was dissolved in MPAA solution [6 M guanidine·HCl, 200 mM MPAA, 20 mM TCEP in PBS (pH 7.0)]. The reaction was continued for 30 min at 37 °C. The mixture was purified by preparative HPLC (a linear gradient of 15–45% CH_3CN in H_2O containing 0.1% (v/v) TFA over 90 min) to provide thioester **L-1a** was synthesized (0.7 mg, 0.2% yield) from H-Rink Amide-ChemMatrix resin (40 mg, 0.016-0.024 mmol). MS(ESI): $[M+H]^+$ Calcd for $C_{301}H_{450}N_{81}O_{93}S_2$: 6755.50; observed: $[M+8H]^{8+}$ *m/z* = 845.5, $[M+7H]^{7+}$ *m/z* = 966.2, $[M+6H]^{6+}$ *m/z* = 1127.3, $[M+5H]^{5+}$ *m/z* = 1352.0, $[M+4H]^{4+}$ *m/z* = 1689.7.

L-XIAP$^{300–326}$ (L-2)

By the identical protocol for the synthesis of **L-1**, crude Dbz-ester cleaved from resin was purified by preparative HPLC (a linear gradient of 25–55% CH_3CN in H_2O containing 0.1% (v/v) TFA over 90 min) to afford **L-2** (31.2 mg,_5.1 % yield). MS(ESI): $[M+H]^+$ Calcd for $C_{152}H_{197}N_{40}O_{41}S_2$: 3304.61; observed: $[M+4H]^{4+}$ *m/z* = 827.0, $[M+3H]^{3+}$ *m/z* = 1102.2, $[M+2H]^{2+}$ *m/z* = 1652.5.

D-XIAP$^{300-326}$ (D-2)

By the identical procedure described for the synthesis of peptide **L-2**, peptide **D-2** was synthesized (55 mg, 8.9% yield) from H-Rink Amide-ChemMatrix resin (320 mg, 0.128-0.192 mmol). MS(ESI): $[M+H]^+$ Calcd for $C_{152}H_{197}N_{40}O_{41}S_2$: 3304.61; observed: $[M+4H]^{4+}$ *m/z* = 826.8, $[M+3H]^{3+}$ *m/z* = 1102.2.

L-XIAP$^{327–356}$ (L-3)

By the standard protocol for peptide synthesis, peptide **L-3** was synthesized (76.3 mg, 12% yield) from Rink Amide-ChemMatrix resin (40 mg × 8 portions, 0.128-0.196 mmol). MS(ESI): $[M+H]^+$ Calcd for $C_{156}H_{253}N_{44}O_{48}S_2$: 3577.12; observed: $[M+5H]^{5+}$ *m/z* = 716.1, $[M+4H]^{4+}$ *m/z* = 894.9, $[M+3H]^{3+}$ *m/z* = 1192.9.

D-XIAP$^{327-356}$ (D-3)

By the standard protocol for peptide synthesis, peptide **D-3** was synthesized (102 mg, 16% yield) from H-Rink Amide-ChemMatrix resin (40 mg × 8 portions, 0.128-0.192 mmol). MS(ESI): $[M+H]^+$ Calcd for $C_{156}H_{253}N_{44}O_{48}S_2$: 3577.12; observed: $[M+5H]^{5+}$ *m/z* = 716.1, $[M+4H]^{4+}$ *m/z* = 895.0, $[M+3H]^{3+}$ *m/z* = 1193.0.

L-XIAP$^{300–356}$ (L-4)

L-XIAP(300–326) (**L-2**, 14.3 mg) and L-XIAP(327–356) (**L-3**, 20.1 mg) were dissolved in ligation buffer [6 M guanidine·HCl, 200 mM 4-mercaptophenylacetic acid (MPAA), 100 mM TCEP in PBS (pH 7.0); 800 μL] and the reaction was continued for 2 h at 37 °C. Then, a 0.4 M methoxyamine solution (3.0 mL) was added and reaction mixture was incubated for 3 h at 37 °C. After 6 M guanidine·HCl solution (10 mL) was added, the mixture was purified by preparative HPLC (a linear gradient of 25–55% CH_3CN in H_2O containing 0.1% (v/v) TFA over 90 min) to provide peptide **L-4** (10.3 mg, 35% yield). MS(ESI): $[M+H]^+$ Calcd for $C_{299}H_{442}N_{81}O_{87}S_4$: 6691.54; observed: $[M+9H]^{9+}$ *m/z* = 744.3, $[M+8H]^{8+}$ *m/z* = 837.4, $[M+7H]^{7+}$ *m/z* = 956.9, $[M+6H]^{6+}$ *m/z* = 1116.2, $[M+5H]^{5+}$ *m/z* = 1339.3, $[M+4H]^{4+}$ *m/z* = 1673.6.

D-XIAP$^{300-356}$ (D-4)

By the identical procedure described for the synthesis of peptide **L-4**, peptide **D-4** was synthesized (17.2 mg, 49% yield). MS(ESI): $[M+H]^+$ Calcd for $C_{299}H_{442}N_{81}O_{87}S_4$: 6691.54; observed: $[M+9H]^{9+}$ *m/z* = 744.2, $[M+8H]^{8+}$ *m/z* = 837.2, $[M+7H]^{7+}$ *m/z* = 956.8, $[M+6H]^{6+}$ *m/z* = 1116.0, $[M+5H]^{5+}$ *m/z* = 1339.1, $[M+4H]^{4+}$ *m/z* = 1673.5.

L-XIAP$^{241–262}$ (L-6a). By the identical protocol for the synthesis of **L-1**, peptide thioester **L-6a** was synthesized (37.7 mg, 16% yield). MS(ESI): $[M+H]^+$ Calcd for $C_{106}H_{163}N_{32}O_{38}S_2$: 2557.78; observed: $[M+3H]^{3+}$ *m/z* = 853.1, $[M+2H]^{2+}$ *m/z* = 1279.2.

TMR-labeled L-XIAP$^{241-262}$ (L-6b)

By the identical procedure described for the synthesis of peptide **L-6a**, thioester **L-6b** was synthesized (3.2 mg, 11% yield) from H-Rink Amide-ChemMatrix resin (40 mg, 0.016-0.024 mmol). Two Fmoc-protected aminocaproic acid (Fmoc-Ahx-OH) were coupled as a linker by the identical HBTU/HOBt activation described for the synthesis of peptide **L-1a**. 5-Carboxytetramethylrhodamine (TMR, 43 mg, 0.1 mmol) was coupled by using *N*,*N*'-diisopropylcarbodiimide (DIC) (15.5 mL, 0.1 mmol)/HOBt·H_2O (15.3 mg, 0.1 mmol) in DMF for 4 h. MS(ESI): $[M+H]^+$ Calcd for $C_{143}H_{208}N_{36}O_{44}S_2$: 3196.55; observed: $[M+3H]^{3+}$ *m/z* = 1066.2.

Biotin-labeled L-XIAP$^{241-262}$ (L-6c)

By the identical procedure described for the synthesis of peptide **L-6a**, thioester **L-6c** was synthesized (8.0 mg, 27% yield) from H-Rink Amide-ChemMatrix resin (40 mg, 0.016-0.024 mmol). Two Fmoc-protected aminocaproic acids (Fmoc-Ahx-OH) were coupled as a linker by the identical HBTU/HOBt activation described for the synthesis of peptide **L-1a**. D-Biotin was coupled with HBTU (48.9 mg, 0.2 mmol), HOBt·H_2O (30.6 mg, 0.2 mmol) and (*i*-Pr)$_2$NEt (69 μL, 0.4 mmol) in DMF for 2 h. MS(ESI): $[M+H]^+$ Calcd for $C_{128}H_{198}N_{39}O_{42}S_2$: 3019.34; observed: $[M+3H]^{3+}$ *m/z* = 1007.3.

D-XIAP$^{241-262}$ (D-6a)

By the identical procedure described for the synthesis of peptide **L-6a**, thioester **D-6a** was synthesized (38 mg, 17% yield) from H-Rink Amide-ChemMatrix resin (120 mg, 0.048-0.072 mmol). MS(ESI): $[M+H]^+$ Calcd for $C_{106}H_{163}N_{32}O_{38}S_2$: 2557.78; observed: $[M+3H]^{3+}$ *m/z* = 853.2, $[M+2H]^{2+}$ *m/z* = 1279.3.

TMR-labeled D-XIAP$^{241-262}$ (D-6b)

By the identical procedure described for the synthesis of peptide **L-6b**, thioester **D-6b** was synthesized (3.5 mg, 12% yield) from H-Rink Amide-ChemMatrix resin (40 mg, 0.016-0.024 mmol). MS(ESI): $[M+H]^+$ Calcd for $C_{143}H_{208}N_{36}O_{44}S_2$: 3196.55; observed: $[M+3H]^{3+}$ *m/z* = 1066.2, $[M+2H]^{2+}$ *m/z* = 1598.3.

Biotin-labeled D-XIAP$^{241-262}$ (D-6c). By the identical procedure described for the synthesis of peptide **L-6c**, thioester **D-6c** was synthesized (4.5 mg, 15% yield) from H-Rink Amide-ChemMatrix

resin (40 mg, 0.016-0.024 mmol). MS(ESI): $[M+H]^+$ Calcd for $C_{128}H_{198}N_{39}O_{42}S_2$: 3019.34; observed: $[M+3H]^{3+}$ *m/z* = 1007.3, $[M+2H]^{2+}$ *m/z* = 1510.5.

L-XIAP$^{263–299}$ (L-7)

4-Nitrophenyl chloroformate (40.3 mg, 0.2 mmol) in dry pyridine (16.1 μL, 0.2 mmol) was added to the suspension of Wang-PEG resin (0.2-0.3 mmol/g, 80 mg, 0.016-0.024 mmol) in dry DCM (1 mL) and the suspension was agitated for 80 min at room temperature. After filtration, the resin was treated with $NH_2NH_2{\cdot}H_2O$ (20 μL, 0.4 mmol) in THF for 1 h. Then, by the standard protocol for peptide synthesis, peptide **L-7** was synthesized (13.3 mg, 4.2% yield). MS(ESI): $[M+H]^+$ Calcd for $C_{195}H_{292}N_{51}O_{55}S$: 4262.84; observed: $[M+5H]^{5+}$ *m/z* = 853.4, $[M+4H]^{4+}$ *m/z* = 1066.6, $[M+3H]^{3+}$ *m/z* = 1421.6.

D-XIAP$^{263-299}$ (D-7)

By the identical procedure described for the synthesis of peptide **L-7**, peptide hydrazide **D-7** was synthesized (14.8 mg, 1.9% yield) from H-Rink Amide-ChemMatrix resin (320 mg, 0.128-0.192 mmol). MS(ESI): $[M+H]^+$ Calcd for $C_{195}H_{292}N_{51}O_{55}S$: 4262.84; observed: $[M+5H]^{5+}$ *m/z* = 853.2, $[M+4H]^{4+}$ *m/z* = 1066.3, $[M+3H]^{3+}$ *m/z* = 1421.4.

[Cys^{263}]-L-XIAP$^{241–299}$ (L-8a)

The L-XIAP$^{241–262}$ MPAA thioester (**L-6a**, 6.5 mg) and L-XIAP$^{263–299}$ (**L-7**, 6.0 mg) were dissolved in ligation buffer [6 M guanidine·HCl, 200 mM MPAA, 100 mM TCEP in PBS (pH 7.0); 170 μL] and the reaction was continued for 15 min at room temperature. The crude mixture was purified by preparative HPLC (a linear gradient of 25–55% CH_3CN in H_2O containing 0.1% (v/v) TFA over 90 min) to provide peptide **L-8a** (3.1 mg, 49% yield). MS(ESI): $[M+H]^+$ Calcd for $C_{293}H_{446}N_{83}O_{91}S_2$: 6651.40; observed: $[M+8H]^{8+}$ *m/z* = 832.5, $[M+7H]^{7+}$ *m/z* = 951.2, $[M+6H]^{6+}$ *m/z* = 1109.6, $[M+5H]^{5+}$ *m/z* = 1331.2, $[M+4H]^{4+}$ *m/z* = 1663.4.

TMR-labeled [Cys^{263}]-L-XIAP$^{241-299}$ (L-8b)

By the identical procedure described for the synthesis of peptide **L-8a**, peptide **L-8b** was synthesized (5.5 mg, 32% yield). MS(ESI): $[M+H]^+$ Calcd for $C_{330}H_{488}N_{87}O_{97}S_2$: 7290.17; observed: $[M+8H]^{8+}$ *m/z* = 912.1, $[M+7H]^{7+}$ *m/z* = 1042.2, $[M+6H]^{6+}$ *m/z* = 1215.7, $[M+5H]^{5+}$ *m/z* = 1458.6, $[M+4H]^{4+}$ *m/z* = 1823.1.

Biotin-labeled [Cys^{263}]-L-XIAP$^{241-299}$ (L-8c)

By the identical procedure described for the synthesis of peptide **L-8a**, peptide **L-8c** was synthesized (3.2 mg, 45% yield). MS(ESI): $[M+H]^+$ Calcd for $C_{315}H_{482}N_{87}O_{95}S_3$: 7104.02; observed: $[M+6H]^{6+}$ *m/z* = 1185.0, $[M+5H]^{5+}$ *m/z* = 1421.8, $[M+4H]^{4+}$ *m/z* = 1776.6.

[Cys^{263}]-D-XIAP$^{241-299}$ (D-8a)

By the identical procedure described for the synthesis of peptide **L-8a**, peptide **D-8a** was synthesized (1.9 mg, 27% yield). MS(ESI): $[M+H]^+$ Calcd for $C_{293}H_{446}N_{83}O_{91}S_2$: 6651.40; observed: $[M+8H]^{8+}$ *m/z* = 832.3, $[M+7H]^{7+}$ *m/z* = 951.1, $[M+6H]^{6+}$ *m/z* = 1109.4, $[M+5H]^{5+}$ *m/z* = 1331.1, $[M+4H]^{4+}$ *m/z* = 1663.4.

TMR-labeled [Cys^{263}]-D-XIAP$^{241-299}$ (D-8b)

By the identical procedure described for the synthesis of peptide **L-8a**, peptide **D-8b** was synthesized (2.8 mg, 31% yield). MS(ESI): $[M+H]^+$ Calcd for $C_{330}H_{488}N_{87}O_{97}S_2$: 7290.17; observed: $[M+8H]^{8+}$ *m/z* = 912.0, $[M+7H]^{7+}$ *m/z* = 1042.2, $[M+6H]^{6+}$ *m/z* = 1215.8, $[M+5H]^{5+}$ *m/z* = 1458.6, $[M+4H]^{4+}$ *m/z* = 1822.7.

Biotin-labeled [Cys^{263}]-D-XIAP$^{241-299}$ (D-8c)

By the identical procedure described for the synthesis of peptide **L-8a**, peptide **D-8c** was synthesized (3.5 mg, 34% yield). MS(ESI): $[M+H]^+$ Calcd for $C_{315}H_{482}N_{87}O_{95}S_3$: 7104.02; observed: $[M+6H]^{6+}$ *m/z* = 1184.8, $[M+5H]^{5+}$ *m/z* = 1421.4, $[M+4H]^{4+}$ *m/z* = 1776.4.

L-XIAP$^{241–299}$ (L-9a)

VA-044·2HCl (12.9 mg, 40 μmol) was added to a solution of peptide **L-8a** (5.5 mg) in desulfurization buffer [6 M guanidine·HCl, 200 mM phosphate buffer (pH 6.8), 200 mM TCEP·HCl, and 40 mM MESNa, 2 mL]. The mixture was incubated for 3 h at 37 °C. The product was purified by preparative HPLC (a linear gradient of 25–55% CH_3CN in H_2O containing 0.1% (v/v) TFA over 90 min) to provide peptide **L-9a** (4.0 mg, 73% yield). MS(ESI): $[M+H]^+$ Calcd for $C_{293}H_{446}N_{83}O_{91}S$: 6619.34; observed: $[M+8H]^{8+}$ *m/z* = 828.5, $[M+7H]^{7+}$ *m/z* = 946.6, $[M+6H]^{6+}$ *m/z* = 1104.3, $[M+5H]^{5+}$ *m/z* = 1324.7, $[M+4H]^{4+}$ *m/z* = 1655.8.

TMR-labeled L-XIAP$^{241-299}$ (L-9b)

By the identical procedure described for the synthesis of peptide **L-9a**, peptide hydrazide **L-9b** was synthesized (1.3 mg, 42% yield). MS(ESI): $[M+H]^+$ Calcd for $C_{330}H_{488}N_{87}O_{97}S$: 7258.11; observed: $[M+7H]^{7+}$ *m/z* = 1037.6, $[M+6H]^{6+}$ *m/z* = 1210.6, $[M+5H]^{5+}$ *m/z* = 1452.2, $[M+4H]^{4+}$ *m/z* = 1814.5.

Biotin-labeled L-XIAP$^{241-299}$ (L-9c)

By the identical procedure described for the synthesis of peptide **L-9a**, peptide hydrazide **L-9c** was synthesized (2.7 mg, 73% yield). MS(ESI): $[M+H]^+$ Calcd for $C_{315}H_{482}N_{87}O_{95}S_2$: 7071.96; observed: $[M+6H]^{6+}$ *m/z* = 1179.9, $[M+5H]^{5+}$ *m/z* = 1415.4, $[M+4H]^{4+}$ *m/z* = 1768.7.

D-XIAP$^{241-299}$ (D-9a)

By the identical procedure described for the synthesis of peptide **L-9a**, peptide hydrazide **D-9a** was synthesized (1.2 mg, 63% yield). MS(ESI): $[M+H]^+$ Calcd for $C_{293}H_{446}N_{83}O_{91}S$: 6619.34; observed: $[M+8H]^{8+}$ *m/z* = 828.2, $[M+7H]^{7+}$ *m/z* = 946.4, $[M+6H]^{6+}$ *m/z* = 1104.0, $[M+5H]^{5+}$ *m/z* = 1324.5, $[M+4H]^{4+}$ *m/z* = 1655.1.

TMR-labeled D-XIAP$^{241-299}$ (D-9b)

By the identical procedure described for the synthesis of peptide **L-9a**, peptide hydrazide **D-9b** was synthesized (2.0 mg, 72% yield). MS(ESI): $[M+H]^+$ Calcd for $C_{330}H_{488}N_{87}O_{97}S$: 7258.11; observed: $[M+8H]^{8+}$ *m/z* = 908.0, $[M+7H]^{7+}$ *m/z* = 1037.7, $[M+6H]^{6+}$ *m/z* = 1210.4, $[M+5H]^{5+}$ *m/z* = 1452.4, $[M+4H]^{4+}$ *m/z* = 1814.9.

Biotin-labeled D-XIAP$^{241-299}$ (D-9c)

By the identical procedure described for the synthesis of peptide **L-9a**, peptide hydrazide **L-9c** was synthesized (3.1 mg, 89% yield). MS(ESI): $[M+H]^+$ Calcd for $C_{315}H_{482}N_{87}O_{95}S_2$: 7071.96; observed: $[M+7H]^{7+}$ *m/z* = 1011.1, $[M+6H]^{6+}$ *m/z* = 1179.5, $[M+5H]^{5+}$ *m/z* = 1415.0, $[M+4H]^{4+}$ *m/z* = 1768.1.

L-XIAP$^{241–356}$ (L-5a)

An $NaNO_2$ solution (200 mM, 12 μL) was added to a solution of hydrazide **L-8a** (3.5 mg) in activation buffer [6 M guanidine·HCl, 100 mM phosphate buffer (pH 3.0), 200 μL] at −20 °C, the reaction was continued for 20 min. An MPAA solution [6 M guanidine·HCl, 200 mM phosphate buffer (pH 6.8), 200 mM MPAA, 200 μL] was then added to the reaction, and the pH of the mixture was adjusted to 7.0 immediately. The reaction mixture was stirred at room temperature for 30 min at

room temperature. Peptide **L-3a** (3.2 mg) in MPAA buffer [6 M guanidine·HCl, 150 mM phosphate buffer (pH 7.0), 200 mM TCEP·HCl, 100 mM MPAA, 400 μL] was added to the mixture and the pH of the mixture was adjusted to 7.0 immediately. The reaction mixture was stirred for 1 h at room temperature. The crude mixture was purified by preparative HPLC (a linear gradient of 25–55% CH_3CN in H_2O containing 0.1% (v/v) TFA over 90 min) to provide peptide **L-5a** (2.2 mg, 33% yield). MS(ESI): $[M+H]^+$ Calcd for $C_{592}H_{882}N_{162}O_{178}S_5$: 13276.82; observed (ESI): $[M+16H]^{16+}$ *m/z* = 830.9, $[M+15H]^{15+}$ *m/z* = 886.4, $[M+14H]^{14+}$ *m/z* = 949.7, $[M+13H]^{13+}$ *m/z* = 1022.6, $[M+12H]^{12+}$ *m/z* = 1107.7, $[M+11H]^{11+}$ *m/z* = 1207.9, $[M+10H]^{10+}$ *m/z* = 1328.8, $[M+9H]^{9+}$ *m/z* = 1476.4.

D-XIAP$^{241-356}$ (D-5a)

By the identical procedure described for the synthesis of peptide **L-5a**, peptide **D-5a** was synthesized (0.5 mg, 20% yield). MS(ESI): $[M+H]^+$ Calcd for $C_{592}H_{882}N_{162}O_{178}S_5$: 13276.82; observed (ESI): $[M+16H]^{16+}$ *m/z* = 830.9, $[M+15H]^{15+}$ *m/z* = 885.8, $[M+14H]^{14+}$ *m/z* = 949.3, $[M+13H]^{13+}$ *m/z* = 1022.5, $[M+12H]^{12+}$ *m/z* = 1107.4, $[M+11H]^{11+}$ *m/z* = 1208.1, $[M+10H]^{10+}$ *m/z* = 1328.3, $[M+9H]^{9+}$ *m/z* = 1475.9.

L-XIAP^{TMR} (L-5b)

By the identical procedure described for the synthesis of peptide **L-5a**, peptide **L-5b** was synthesized (90 μg, 15% yield) MS(ESI): $[M+H]^+$ Calcd for $C_{629}H_{925}N_{166}O_{184}S_5$: 13916.60; observed: $[M+16H]^{16+}$ *m/z* = 870.7, $[M+15H]^{15+}$ *m/z* = 928.6, $[M+14H]^{14+}$ *m/z* = 994.9, $[M+13H]^{13+}$ *m/z* = 1071.4, $[M+12H]^{12+}$ *m/z* = 1160.6, $[M+11H]^{11+}$ *m/z* = 1266.1, $[M+10H]^{10+}$ *m/z* = 1392.2, $[M+9H]^{9+}$ *m/z* = 1546.4.

L-XIAP^{biotin} (L-5c)

By the identical procedure described for the synthesis of peptide **L-5a**, peptide **L-5c** was synthesized (430 μg, 29% yield) MS(ESI): $[M+H]^+$ Calcd for $C_{614}H_{919}N_{166}O_{182}S_6$: 13730.45; observed: $[M+16H]^{16+}$ *m/z* = 859.2, $[M+15H]^{15+}$ *m/z* = 916.5, $[M+14H]^{14+}$ *m/z* = 981.9, $[M+13H]^{13+}$ *m/z* = 1057.7, $[M+12H]^{12+}$ *m/z* = 1145.6, $[M+11H]^{11+}$ *m/z* = 1249.6, $[M+10H]^{10+}$ *m/z* = 1374.2, $[M+9H]^{9+}$ *m/z* = 1527.0.

D-XIAP^{TMR} (D-5b)

By the identical procedure described for the synthesis of peptide **L-5a**, peptide **D-5b** was synthesized (450 μg, 12% yield). MS(ESI): $[M+H]^+$ Calcd for $C_{629}H_{925}N_{166}O_{184}S_5$: 13916.60; observed: $[M+16H]^{16+}$ *m/z* = 870.8, $[M+15H]^{15+}$ *m/z* = 928.6, $[M+14H]^{14+}$ *m/z* = 994.8, $[M+13H]^{13+}$ *m/z* = 1071.3, $[M+12H]^{12+}$ *m/z* = 1160.6, $[M+11H]^{11+}$ *m/z* = 1266.1, $[M+10H]^{10+}$ *m/z* = 1392.4, $[M+9H]^{9+}$ *m/z* = 1546.4.

D-XIAP^{biotin} (D-5c)

By the identical procedure described for the synthesis of peptide **L-5a**, peptide **D-5c** was synthesized (1.17 mg, 24% yield) MS(ESI): $[M+H]^+$ Calcd for $C_{614}H_{919}N_{166}O_{182}S_6$: 13730.45; observed: $[M+16H]^{16+}$ *m/z* = 858.7, $[M+15H]^{15+}$ *m/z* = 916.4, $[M+14H]^{14+}$ *m/z* = 981.8, $[M+13H]^{13+}$ *m/z* = 1057.1, $[M+12H]^{12+}$ *m/z* = 1145.0, $[M+11H]^{11+}$ *m/z* = 1249.0, $[M+10H]^{10+}$ *m/z* = 1373.9, $[M+9H]^{9+}$ *m/z* = 1526.4.

D-SMAC^{biotin} (D-10)

By the identical procedure described for the synthesis of peptide **L-10**, peptide **D-10** was synthesized (38.7 mg, 35% yield). MS(ESI): $[M+H]^+$ Calcd for $C_{46}H_{76}N_{13}O_8S$: 971.26; observed: 970.7.

L-SMAC^{FAM} [L-11; H-Abu-Arg-Pro-Phe-Lys(5-FAM)-NH_2]

By the identical procedure described for the synthesis of peptide **L-10**, peptide **L-11** was synthesized (6.4 mg, 18% yield). MS(ESI): $[M+H]^+$ Calcd for $C_{51}H_{60}N_{10}O_{11}$: 989.10; observed: 989.8.

D-SMAC^{FAM} (D-11)

By the identical procedure described for the synthesis of peptide **L-11**, peptide **D-11** was synthesized (7.9 mg, 21% yield). MS(ESI): $[M+H]^+$ Calcd for $C_{51}H_{60}N_{10}O_{11}$: 989.10; observed: 989.5.

L-SMAC (L-12; H-Abu-Arg-Pro-Phe-Lys-NH_2)

By the identical procedure described for the synthesis of peptide **L-10**, peptide **L-12** was synthesized (10.2 mg, 35% yield). MS(ESI): $[M+H]^+$ Calcd for $C_{30}H_{51}N_{10}O_5$: 631.80; observed: 631.5.

D-SMAC (D-12)

By the identical procedure described for the synthesis of peptide **L-12**, peptide **D-12** was synthesized (8.2 mg, 28% yield). MS(ESI): $[M+H]^+$ Calcd for $C_{30}H_{51}N_{10}O_5$: 631.80; observed: 631.3.

L-SMAC^{FLAG} [L-13; H-Abu-Arg-Pro-Phe-Lys(FLAG)-NH_2, FLAG: H-Asp-Tyr-Lys-Asp-His-Asp-Gly-Asp-Tyr-Lys-Asp-His-Asp-Ile-Asp-Tyr-Lys-Asp-Asp-Asp-Asp-Lys-Ahx-]

By the identical procedure described for the synthesis of peptide **L-10**, peptide **L-13** was synthesized (52 mg, 21% yield). MS(ESI): $[M+H]^+$ Calcd for $C_{151}H_{220}N_{41}O_{53}$: 3457.65; observed: $[M+4H]^{4+}$ *m/z* = 865.2, $[M+3H]^{3+}$ *m/z* = 1153.2, $[M+2H]^{2+}$ *m/z* = 1728.9.

D-SMAC^{FLAG} (D-13)

By the identical procedure described for the synthesis of peptide **L-10**, peptide **D-13** was synthesized (22 mg, 18% yield). MS(ESI): $[M+H]^+$ Calcd for $C_{151}H_{220}N_{41}O_{53}$: 3457.65; observed: $[M+4H]^{4+}$ *m/z* = 865.6, $[M+3H]^{3+}$ *m/z* = 1153.7, $[M+2H]^{2+}$ *m/z* = 1729.6.

L-SMAC^{biotin} [H-Abu-Arg-Pro-Phe-Lys(Ahx-biotin)-NH_2, L-10]

The peptide resin was manually constructed by Fmoc-SPPS on NovaSyn TGR resin (0.25 mmol/g, 360 mg, 0.09 mmol). Fmoc-protected amino acids (3 eq) were coupled by using *N*,*N*'-diisopropylcarbodiimide (DIC, 209 μL, 0.135 mmol) and HOBt·H_2O (21.2 mg, 0.135 mmol) in DMF. Fmoc-Lys(Mtt)-OH was employed for coupling of the C-terminal Lys. After Fmoc-deprotection of Abu, Boc protection at N-terminal amine was conducted by treatment with $(Boc)_2O$ (32.7 mg, 0.15 mmol) and $(i\text{-}Pr)_2NEt$ (52.2 μL, 0.03 mmol) at room temperature for 2 h. Then Mtt group was deprotected by treatment of 1% TFA in DCM at room temperature for 2 min × 3 and 30 min. Fmoc-Ahx-OH and biotin were then coupled by the identical DIC/HOBt activation. The resulting protected peptide resin was treated with TFA/thioanisole/*m*-cresol/1,2-ethanedithiol/H_2O (80:5:5:5:5) at room temperature for 2 h. After removal of the resin by filtration, the filtrate was poured into ice-cold dry Et_2O. Purification by preparative HPLC on a Cosmosil 5C18-AR300 column [Nacalai Tesque, 20 × 250 mm, a linear gradient of 10–40% CH_3CN containing 0.1% (v/v) TFA aq. over 90 min] provided the peptide **L-10** (38.2 mg, 35% yield). MS(ESI): $[M+H]^+$ Calcd for $C_{46}H_{76}N_{13}O_8S$: 971.26; observed: $[M+H]^+$ *m/z* = 970.8.

Folding of synthetic XIAP BIR3 domains

The lyophilized peptide was dissolved in urea solution (7 M urea, 20 mM Tris, 150 mM NaCl, 5 mM 2-mercaptoethanol, 0.1 mM EDTA, 0.01 mM $ZnCl_2$, pH 8.0; 0.3 mg/mL). The denatured proteins were subjected to dialysis using a Slide-A-Lyzer G2 dialysis cassette (cutoff 3.5 kDa, Thermo)

against a 200-fold volume of dialysis buffer (20 mM Tris, 150 mM NaCl, 5 mM 2-mercaptoethanol, 0.01 mM $ZnCl_2$, pH 8.0) with decreasing concentrations of urea (3, 1, and 0 M) for 1.5 h at 4 °C, and then dialyzed against the dialysis buffer overnight at 4 °C.

CD spectra of L-XIAP BIR3 and D-XIAP BIR3 domains

Refolded proteins in Tris buffer were dialyzed against PBS buffer [PBS (pH 7.0) containing 1 mM DTT]. CD spectra of L-XIAP$^{241–356}$ and D-XIAP$^{241–356}$ were recorded on a JASCO J-720 circular dichroism spectrometer at 20 °C.

Surface plasmon resonance (SPR) analysis

SPR analysis of synthetic XIAP BIR3 domain binding to mutated SMAC peptide was carried out using a ProteOnXPR36 SPR system (BioRad). After the immobilization of SMAC-derived peptides with biotin modification (SMAC^{biotin}, **L-10** or **D-10**, 5 nM, 5 min) onto a ProteOn NLC sensor chip, the analyte protein solution of synthetic XIAP$^{241–356}$, XIAP^{TMR} and XIAP^{biotin} (0–2000 nM) were flushed into the flow system in the running buffer [10 mM 4-(2-hydroxyethyl)-1-piperazineethanesulfonic acid (HEPES, pH 7.4), 150 mM NaCl containing 0.005% Tween-20] at 25 °C. For analysis of the binding affinity of the biotin-labeled XIAP BIR3 domain (XIAP^{biotin}), unconjugated streptoavidins on the SMAC^{biotin}-loaded sensor chip were protected by pretreatment with excess biotin (100 μL, 2 min). All analytes were evaluated for 60 s as contact time, followed by 600 s dissociation at a flow rate of 50 μL/min. The triplicate data were analyzed using GraphPad Prism software.

Fluorescence polarization (FP) assay

FP assays were performed in 96-well non-binding surface black assay plates (Corning) as reported previously.[20] For the binding titration analysis, the fluorescent SMAC-derived peptide (SMAC^{FAM}, 5 nM) and increasing concentrations of XIAP BIR3 domain (0–1000 nM) in 0.10 mL of assay buffer [PBS containing 100 μg/mL bovine gamma globulin, 0.02% sodium azide] were incubated for 30 min at room temperature. The K_D was obtained by nonlinear least-squares fitting to a single site binding model and Scatchard plot. For the competitive inhibition experiment, unlabeled SMAC-derived peptide (**L-12** or **D-12**) and SMAC^{FAM} were diluted five-fold with PBS in advance. The XIAP BIR3 domain (120 nM, 90 μL/well) was incubated with the unlabeled SMAC-derived peptide (5 μL) for 30 min. Then, SMAC^{FAM} (5 μL, 5 nM final) was added and the mixture was incubated for 30 min.

FP signals were detected using an EnVision Xcite plate reader (Perkin Elmer) with a 480-nm excitation filter and a 535-nm emission filter. The data were analyzed using GraphPad Prism software.

ELISA assay

A competitive binding inhibition assay by ELISA was conducted based on the protocol descried in section 1. ELISAs were conducted in HEPES buffer [20 mM HEPES (pH 7.4), 100 mM NaCl containing 0.05% Tween-20, and 0.1% BSA]. Initial blocking was performed by incubating with HEPES buffer containing 3% BSA (300 μL/well) for 1 h. After three washes, XIAP $BIR3^{biotin}$ (10 nM) in HEPES buffer (100 μL/well) was added and incubated for 2 h. After three washes, the FLAG-labeled mutated SMAC peptide (300 nM) at varying concentrations of inhibitors in HEPES buffer containing 1% DMSO (100 μL/well) was added and incubated for 1 h. After three washes, a 1:5000 dilution of HRP-conjugated anti-FLAG antibody (Sigma) in HEPES buffer (100 μL/well) was added and incubated for 1 h. After three washes, the TMB solution (Wako, 100 μL/well) was added and incubated for 1 h. Next, aqueous 1 M H_2SO_4 (100 μL/well) was added. Absorbance at 450 nm was measured for each well using the EnVision Xcite plate reader. The IC_{50} values were calculated using GraphPad Prism software (GraphPad software).

Chemical array analysis

Photoaffinity linker-coated (PALC) slides were prepared according to the protocol described in section 1 using amine-coated slides and the photoaffinity PEG or proline linker. A solution of compounds in DMSO was spotted onto the PALC glass slides with a chemical arrayer equipped with 24 stamping pins. The slides were exposed to UV irradiation of 4 J/cm^2 at 365 nm using a CL-1000L UV crosslinker (UVP, CA) for immobilization. The slides were washed successively with DMSO, DMF, acetonitrile, THF, dichloromethane, EtOH and ultra-pure water (5 min, three times each) and dried. L-XIAP $BIR3^{TMR}$ or D-XIAP $BIR3^{TMR}$ (1 μM in 1% skimmed-milk-TBS-T) was incubated with the glass slide for 1 h and the slides were then washed with TBS-T [10 mM Tris-HCl (pH 8.0), 150 mM NaCl, 0.05% Tween-20] (5 min, three times). The slides were dried and scanned at 532 nm on a GenePix scanner. The fluorescence signals were quantified with GenePixPro.

References

1. Gyrd-Hansen, M. & Meier, P. 2010, "IAPs: from caspase inhibitors to modulators of NF-κB, inflammation and cancer", *Nature Reviews Cancer,* vol. 10, no. 8, pp. 561-574.
2. Li, J. & Yuan, J. 2008, "Caspases in apoptosis and beyond", *Oncogene,* vol. 27, no. 48, pp. 6194-6206.
3. Mace, P., Shirley, S. & Day, C. 2010, "Assembling the building blocks: structure and function of inhibitor of apoptosis proteins", *Cell Death and Differentiation,* vol. 17, no. 1, pp. 46.
4. (a) Birnbaum, M.J., Clem, R.J. & Miller, L.K. 1994, "An apoptosis-inhibiting gene from a nuclear polyhedrosis virus encoding a polypeptide with Cys/His sequence motifs", *Journal of Virology,* vol. 68, no. 4, pp. 2521-2528. (b) Hinds, M.G., Norton, R.S., Vaux, D.L. & Day, C.L. 1999, "Solution structure of a baculoviral inhibitor of apoptosis (IAP) repeat", *Nature Structural & Molecular Biology,* vol. 6, no. 7, pp. 648-651. (c) Sun, C., Cai, M., Gunasekera, A.H., Meadows, R.P., Wang, H., Chen, J., Zhang, H., Wu, W., Xu, N. & Ng, S. 1999, "NMR structure and mutagenesis of the inhibitor-of-apoptosis protein XIAP", *Nature,* vol. 401, no. 6755, pp. 818-822.
5. Duckett, C., Nava, V.E., Gedrich, R.W., Clem, R.J., Van Dongen, J.L., Gilfillan, M.C., Shiels, H., Hardwick, J.M. & Thompson, C.B. 1996, "A conserved family of cellular genes related to the baculovirus iap gene and encoding apoptosis inhibitors.", *The EMBO Journal,* vol. 15, no. 11, pp. 2685-2694.
6. Deveraux, Q.L., Takahashi, R., Salvesen, G.S. & Reed, J.C. 1997, "X-linked IAP is a direct inhibitor of cell-death proteases", *Nature,* vol. 388, no. 6639, pp. 300-304.
7. Takahashi, R., Deveraux, Q., Tamm, I., Welsh, K., Assa-Munt, N., Salvesen, G.S. & Reed, J.C. 1998, "A single BIR domain of XIAP sufficient for inhibiting caspases", *The Journal of Biological Chemistry,* vol. 273, no. 14, pp. 7787-7790.
8. (a) Deveraux, Q.L., Leo, E., Stennicke, H.R., Welsh, K., Salvesen, G.S. & Reed, J.C. 1999, "Cleavage of human inhibitor of apoptosis protein XIAP results in fragments with distinct specificities for caspases", *The EMBO Journal,* vol. 18, no. 19, pp. 5242-5251. (b) Sun, C., Cai, M., Meadows, R.P., Xu, N., Gunasekera, A.H., Herrmann, J., Wu, J.C. & Fesik, S.W. 2000, "NMR structure and mutagenesis of the third Bir domain of the inhibitor of apoptosis protein XIAP", *The Journal of Biological Chemistry,* vol. 275, no. 43, pp. 33777-33781.

9. (a) Huang, Y., Park, Y.C., Rich, R.L., Segal, D., Myszka, D.G. & Wu, H. 2001, "Structural basis of caspase inhibition by XIAP: differential roles of the linker versus the BIR domain", *Cell,* vol. 104, no. 5, pp. 781-790. (b) Riedl, S.J., Renatus, M., Schwarzenbacher, R., Zhou, Q., Sun, C., Fesik, S.W., Liddington, R.C. & Salvesen, G.S. 2001, "Structural basis for the inhibition of caspase-3 by XIAP", *Cell,* vol. 104, no. 5, pp. 791-800. (c) Chai, J., Shiozaki, E., Srinivasula, S.M., Wu, Q., Dataa, P., Alnemri, E.S. & Shi, Y. 2001, "Structural basis of caspase-7 inhibition by XIAP", *Cell,* vol. 104, no. 5, pp. 769-780. (d) Shiozaki, E.N., Chai, J., Rigotti, D.J., Riedl, S.J., Li, P., Srinivasula, S.M., Alnemri, E.S., Fairman, R. & Shi, Y. 2003, "Mechanism of XIAP-mediated inhibition of caspase-9", *Molecular Cell,* vol. 11, no. 2, pp. 519-527.

10. (a) Chai, J., Du, C., Wu, J., Kyin, S., Wang, X. & Shi, Y. 2000, "Structural and biochemical basis of apoptotic activation by Smac/DIABLO", *Nature,* vol. 406, no. 6798, pp. 855. (b) Liu, Z., Sun, C., Olejniczak, E.T., Meadows, R.P., Betz, S.F., Oost, T., Herrmann, J., Wu, J.C. & Fesik, S.W. 2000, "Structural basis for binding of Smac/DIABLO to the XIAP BIR3 domain", *Nature,* vol. 408, no. 6815, pp. 1004-1008. (c) Wu, G., Chai, J., Suber, T.L., Wu, J., Du, C., Wang, X. & Shi, Y. 2000, "Structural basis of IAP recognition by Smac/DIABLO", *Nature,* vol. 408, no. 6815, pp. 1008-1012.

11. (a) Du, C., Fang, M., Li, Y., Li, L. & Wang, X. 2000, "Smac, a mitochondrial protein that promotes cytochrome c–dependent caspase activation by eliminating IAP inhibition", *Cell,* vol. 102, no. 1, pp. 33-42. (b) Verhagen, A.M., Ekert, P.G., Pakusch, M., Silke, J., Connolly, L.M., Reid, G.E., Moritz, R.L., Simpson, R.J. & Vaux, D.L. 2000, "Identification of DIABLO, a mammalian protein that promotes apoptosis by binding to and antagonizing IAP proteins", *Cell,* vol. 102, no. 1, pp. 43-53. (c) Srinivasula, S.M., Hegde, R., Saleh, A., Datta, P., Shiozaki, E., Chai, J., Lee, R., Robbins, P.D., Fernandes-Alnemri, T. & Shi, Y. 2001, "A conserved XIAP-interaction motif in caspase-9 and Smac/DIABLO regulates caspase activity and apoptosis", *Nature,* vol. 410, no. 6824, pp. 112-116.

12. Fulda, S. & Vucic, D. 2012, "Targeting IAP proteins for therapeutic intervention in cancer", *Nature Reviews Drug Discovery,* vol. 11, no. 2, pp. 109-124.

13. (a) Infante, J.R., Dees, E.C., Olszanski, A.J., Dhuria, S.V., Sen, S., Cameron, S. & Cohen, R.B. 2014, "Phase I dose-escalation study of LCL161, an oral inhibitor of apoptosis proteins inhibitor, in patients with advanced solid tumors", *Journal of Clinical Oncology,* vol. 32, no. 28, pp. 3103-3110. (b) DiPersio, J.F., Erba, H.P., Larson, R.A., Luger, S.M., Tallman, M.S.,

Brill, J.M., Vuagniaux, G., Rouits, E., Sorensen, J.M. & Zanna, C. 2015, "Oral Debio1143 (AT406), an antagonist of inhibitor of apoptosis proteins, combined with daunorubicin and cytarabine in patients with poor-risk acute myeloid leukemia—results of a phase I dose-escalation study", *Clinical Lymphoma Myeloma and Leukemia,* vol. 15, no. 7, pp. 443-449.

(c) Bunch, K.P., Noonan, A.M., Lee, J., O'Sullivan, C.C.M., Houston, N.D., Ekwede, I., Chen, J., Herrmann, M., Cao, L. & Takebe, N. 2014, "Pharmacodynamic biomarkers from phase II study of the SMAC (Second Mitochondrial-Derived Activator of Caspases)-mimetic birinapant (TL32711; NSC 756502) in relapsed platinum-resistant epithelial ovarian cancer (EOC), primary peritoneal cancer, or fallopian tube cancer (FTC) (NCT01681368)", *American Society of Clinical Oncology*, vol. 32, no. 15, pp. 5585-5585.

14. Derakhshan, A., Chen, Z. & Van Waes, C. 2017, "Therapeutic small molecules target inhibitor of apoptosis proteins in cancers with deregulation of extrinsic and intrinsic cell death pathways", *Clinical Cancer Research : An Official Journal of the American Association for Cancer Research,* vol. 23, no. 6, pp. 1379-1387.
15. Bang, D. & Kent, S.B. 2004, "A one-pot total synthesis of crambin", *Angewandte Chemie International Edition,* vol. 43, no. 19, pp. 2534-2538.
16. Fang, G., Li, Y., Shen, F., Huang, Y., Li, J., Lin, Y., Cui, H. & Liu, L. 2011, "Protein chemical synthesis by ligation of peptide hydrazides", *Angewandte Chemie International Edition,* vol. 50, no. 33, pp. 7645-7649.
17. Wan, Q. & Danishefsky, S.J. 2007, "Free-radical-based, specific desulfurization of cysteine: a powerful advance in the synthesis of polypeptides and glycopolypeptides", *Angewandte Chemie International Edition,* vol. 46, no. 48, pp. 9248-9252.
18. Luque, L.E., Grape, K.P. & Junker, M. 2002, "A highly conserved arginine is critical for the functional folding of inhibitor of apoptosis (IAP) BIR domains", *Biochemistry,* vol. 41, no. 46, pp. 13663-13671.
19. de Souza, Theo Luiz Ferraz, Sanches, D., Gonçalves, R.B., da RochaPita, S.S., Pascutti, P.G., Bianconi, M.L., de Almeida, Fabio Ceneviva Lacerda, Silva, J.L. & de Oliveira, A.C. 2010, "Conformational selection, dynamic restriction and the hydrophobic effect coupled to stabilization of the BIR3 domain of the human X-linked inhibitor of apoptosis protein by the tetrapeptide AVPI", *Biophysical Chemistry,* vol. 152, no. 1-3, pp. 99-108.
20. Nikolovska-Coleska, Z., Wang, R., Fang, X., Pan, H., Tomita, Y., Li, P., Roller, P.P., Krajewski, K., Saito, N.G. & Stuckey, J.A. 2004, "Development and optimization of a

binding assay for the XIAP BIR3 domain using fluorescence polarization", *Analytical Biochemistry,* vol. 332, no. 2, pp. 261-273.

Chapter 2. Solid-Phase Synthesis of β-Hydroxy Ketones Via DNA-Compatible Organocatalytic Aldol Reactions

One-bead-one-compound (OBOC) libraries constructed by solid-phase split-and-pool synthesis are a valuable source of protein ligands. Most OBOC libraries are comprised of oligoamides, particularly peptides, peptoids and peptoid-inspired molecules. Further diversification of the chemical space covered by OBOC libraries is desirable. Towards this end, the author reports here that the proline-catalyzed asymmetric aldol reaction, developed by List and Barbas for solution-phase synthesis, also works well for coupling immobilized aldehydes and soluble ketones. These reaction conditions do not compromise the amplification of DNA by the polymerase chain reaction. Thus, this chemistry should be useful for the construction of novel DNA-encoded OBOC libraries by solid-phase synthesis.

The important consideration in developing reactions for the synthesis of DNA-encoded libraries is to evaluate the level of chemical damage suffered by the encoding DNA that would compromise it amplifiability. For example, routine amino acid or peptoid couplings are known to degrade encoding tags to some degree (Figure 1A and B). To establish powerful methodology for the construction of DNA-encoded OBOC libraries, the author designed solid-phase synthesis of β-hydroxy ketones *via* the organocatalytic aldol reaction[1] of immobilized aldehydes and soluble ketones (Figure 1C). The mild conditions are show to be quite compatible with the presence of the DNA tags. Thus, this chemistry should be useful in the synthesis of novel DNA-encoded OBOC libraries.

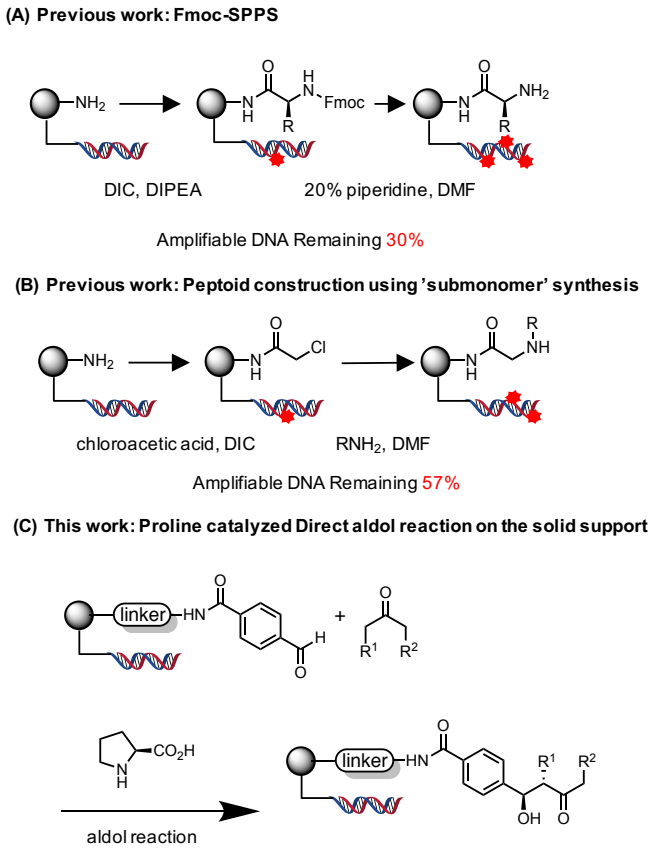

Figure 1. Chemistry Suitable for the Construction for One-Bead One-Compound Libraries by Solid-Phase Synthesis. The red stars on the DNA indicate chemical modifications that would impede amplification of the encoding tag.

TentaGel HL NH_2 resin (110 µM, 0.46 mmol/g) was modified with a disulfide-containing linker to allow the release of compounds from the solid support under mild reductive conditions (treatment with TCEP) to avoid potential dehydration following the aldol addition product under the usual acidic cleavage conditions. The amino terminal end of the linker was acylated with 4-formyl benzoic acid using Oxyma coupling conditions (Scheme 1).[2] Various solvents and conditions were then explored for the (*S*)-proline-catalyzed addition of acetone to this immobilized aldehyde. The author included in all of the reactions beads that contained an inactive control substrate made by coupling benzoic acid (with no formyl group) to the linker. This inert compound served as an internal standard to aid in the quantification of the conversion of the formyl-containing substrate.

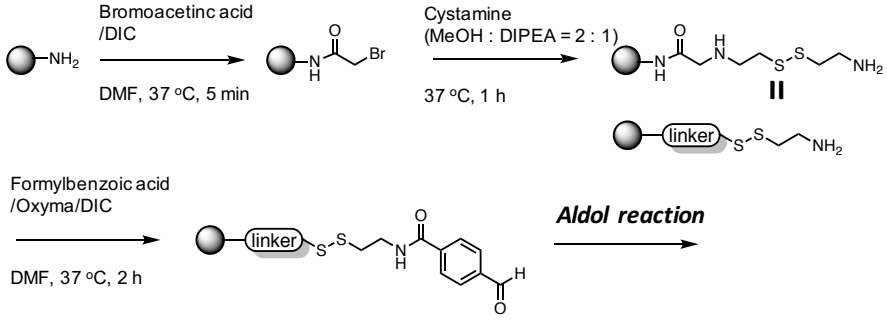

Scheme 1. Immobilization of aldehyde on the Tentagel beads.

The author found using DMSO as the solvent and incubating for 16 h at room temperature in the presence of one equivalent of proline (with respect to the aldehyde on the resin) provided the highest yield of the desired aldol product (Table 1, entry 6), as determined by liquid chromatography−mass spectrometry (LC-MS). This result was obtained using a large excess of ketone with respect to the immobilized aldehyde (100:1 molar ratio). Reactions employing lower ketone levels resulted in poor conversion. Poor results were also obtained when the amount of proline was reduced. Note that proline was used as a suspension because of its modest solubility in all of the solvents examined. The author also examined various proline derivatives such as tetrazole substituted-proline[3] 2-(methoxymethyl)pyrrolidine and prolinamide, but found that (*S*)-proline was the best choice (Table 2), which was also true for the solution-phase organocatalytic aldol reaction.[1e]

Table 1. Establishment of optimal conditions

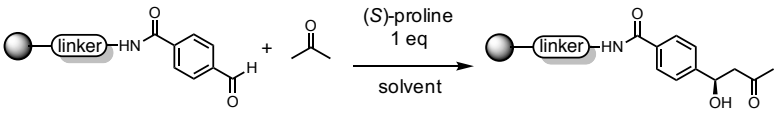

Entry	Solvent	Temp (°C)	Conversion (%)
1	acetonitrile	4	0
2	acetonitrile	20	2
3	NMP	4	11
4	NMP	20	42
5	DMSO	4	75
6	DMSO	20	95
7	DMF	4	4
8	DMF	20	35

Reaction conditions: Reactions were carried out using 1 eq of (*S*)-proline and acetone (100 eq, 44 μL) to resin loading (0.006 mmol) in 120 μL DMSO. Conversion was determined from cleaved crude mixture by monitoring LC-MS, calculated by two peak ratio between starting aldehyde and inactive benzoic ring which is used for internal standard.

Table 2. Comparison of various proline-derived catalysts

Entry	catalyst	amount of catalyst (eq)	Conversion (%)	ee (%)
1	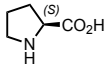	1	99	73
2[a]	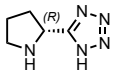	1	99	70
3	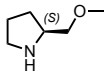	5	98	8
4	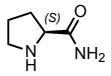	3	99	1

Reaction conditions: Reactions were carried out using organocatalyst and acetone (100 eq, 44 μL) to resin loading (0.006 mmol) in 120 μL DMSO for 16 hours. Conversion was determined from cleaved crude mixture by monitoring LC-MS, calculated by two peak ratio between starting aldehyde and inactive benzoic ring which is used for internal standard. [a] Reaction was completed in 4h.

The aldol product was formed in a modest 73% ee. The use of a variety of additives, such as chiral diols,[4] thioureas,[5] and guanidinium salts[6] or lowering the temperature (4 and −10 °C) did not improve the enantioselectivity significantly (data not shown). Hence, the conditions described above were used to explore the scope of the reaction with respect to the aldehyde and ketone components.

Table 3 shows the results of the reaction of acetone with a number of immobilized aldehydes. All of the reactions proceeded with almost quantitative conversion, even when an *ortho*-substituent was present (**1g**, **1h**). However, when the formyl group was *ortho* to the amide no reaction was observed (data not shown). A heteroaromatic aldehyde also worked well (**1i**). In general, the enantioselectivities were modest, with ee ranging from 54%−79%. A notable exception was **1f**, which was produced as a single stereoisomer. This is typical for the solution phase aldol reaction of benzaldehydes with electron-withdrawing substituents *ortho* to the aldehyde, as noted by List and co-workers.[7]

Table 3. Substrate scope of acceptor aldehyde

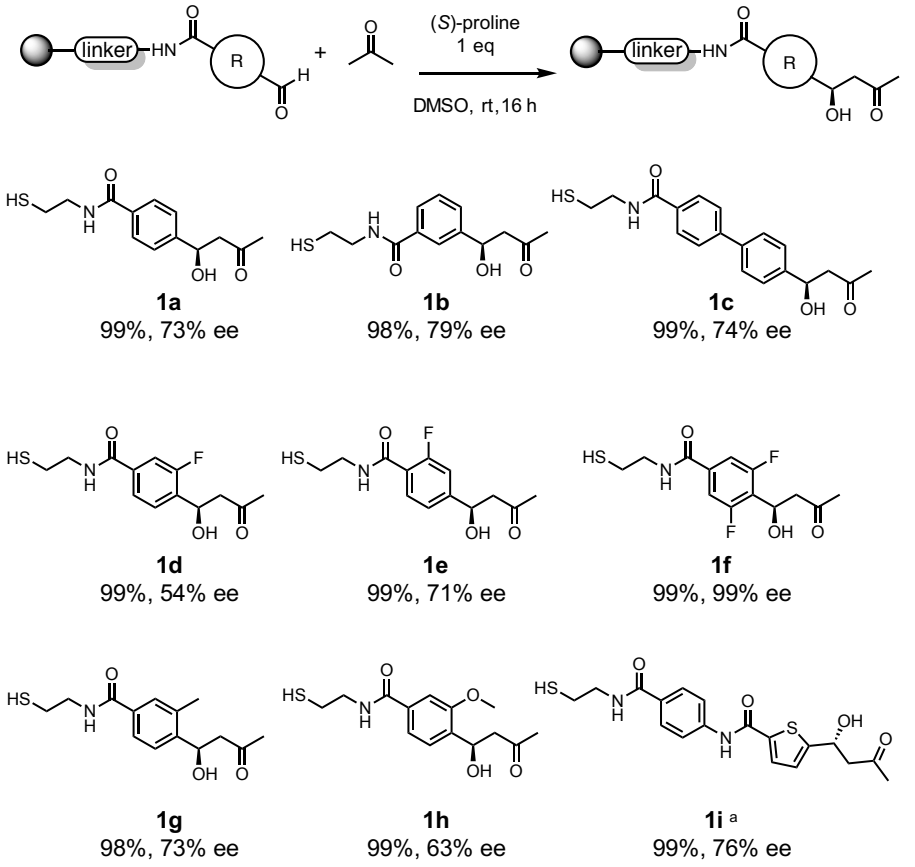

Reaction conditions: Reactions were carried out using 1 eq (*S*)-proline and acetone (100 eq, 44 μL) to resin loading (0.006 mmol) in 120 μL DMSO. Conversion was determined from cleaved crude mixture by monitoring LC-MS, calculated by two peak ratio between starting aldehyde and inactive benzoic ring which is used for internal standard. Ee were determined by chiral HPLC.[a]To monitor products by UV length of 254 nm, Fmoc-4-Abz-OH was coupled before coupling 5-formylthiophen-2-carboxylic acid.

Next, direct aldol reactions between the *p*-formyl benzoic acid-derived immobilized substrate and various soluble ketones were investigated (Table 4). The reactivity of most soluble ketones was excellent (90%−99% conversion), with the sole exception of dimethoxyacetone, which was a respectable 78%. In all cases, the anti product was favored, generally providing drs of 3:1−4:1. Hydroxyacetone was exceptional in that no detectable syn product was formed using this ketone. The enantioselectivity was improved over the reactions employing acetone. With the exception of cyclopentanone (57% ee), the major anti product was produced in 84%−98% ee. The use of nonsymmetrical ketones produced mixtures of regioisomers. For 2-butanone, there was no preference, with both regioisomers produced in equal amounts. However, for hydroxyacetone and

methoxyacetone, the regioisomer resulting from the more substituted carbon acting as the nucleophile (called the nonterminal product in Table 4) was strongly favored (>20:1). These results largely mirror those obtained in the solution-phase aldol reaction.[8]

Table 4. Substrate scope of donor ketone

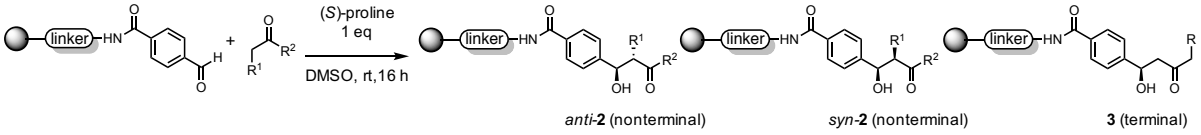

Entry	Ketone	Conversion (*anti*-**2** + *syn*-**2** + **3**) (%)	**2**		rr (**2**:**3**)	**3**
			dr (anti:syn)	ee (%) anti; (syn)		ee (%)
1	cyclopentanone	99 (*anti*-**2a** + *syn*-**2a**)	4:1	57 (69)	–	–
2	cyclohexanone	90 (*anti*-**2b** + *syn*-**2b**)	1:1	85 (80)	–	–
3	dimethoxyacetone	78 (*anti*-**2c** + *syn*-**2c**)	4:1	84 (n.d.)[a]	–	–
4	methoxyacetone	90 (*anti*-**2d** + *syn*-**2d** + trace**3d**)	3:1	98 (n.d.)[b]	> 20:1	n.d.[b]
5	2-butanone	99 (*anti*-**2e** + *syn*-**2e** + **3e**)	4:1	96 (80)	1:1	94
6	hydroxyacetone	99 (*anti*-**2f** + *syn*-**2f** + trace**3f**)	> 20:1	84 (n.d.)[b]	> 20:1	n.d.[b]

Reaction conditions: Reactions were carried out using using 1 eq (*S*)-proline (with respect to aldehyde) and 100 eq of ketones to resin loading (0.006 mmol) in 120 μL DMSO. Conversion was determined from cleaved crude mixture by monitoring LC-MS, calculated by two peak ratio between starting aldehyde and inactive benzoic ring which is used for internal standard. Ee were determined by chiral HPLC. Diastereoisomeric and regioisomeric ratios were determinend by ^{1}H NMR analysis of the crude product. [a]Not determined because the enantiomers were inseparable. [b]Not determined because not enough compound could be obtained for analysis.

With an eye toward incorporating useful functionality into the aldol products, Fmoc-protected 1-amino-2-propanone and Fmoc-protected 4-piperidinone were examined as substrates, but these reactions failed to produce the desired aldol products. This is probably due to the lower solubility of these ketones in DMSO. The same high concentration that could be achieved for the ketones shown in Table 4 was not possible with these substrates. This is likely to be a problem using any ketone containing an Fmoc-protected amine. Therefore, the author turned our attention to trying to incorporate an azido moiety into the aldol product. An azide can be further elaborated using copper-catalyzed Huisgen cycloadditions, aza-Wittig reactions or can be reduced to an amine with a phosphine. Unfortunately, under the standard conditions described above, azidoacetone provided a poor yield of the desired aldol product. However, the author found that the addition of a guanidinium-type ionic liquid, as reported by Martinez-Casteneda et al.,[9] provided the desired α-azido-β-hydroxy ketone in excellent yield as well as with high stereo-, regio-, and enantioselectivity (Figure 2A). However, a two-day incubation at 4 °C was required to obtain this result. Thus, the author also examined the possibility of displacing the alcohol in the aldol product with azide under Mitsunobu conditions (Figure 2B). After several attempts, the author found that using a large excess (50 equiv) of all the soluble reagents required for the Mitsunobu reaction provided a high yield of the desired product. Thus, using either of these protocols, a versatile azido group can be incorporated into the aldol product, allowing further elaboration of the molecule.

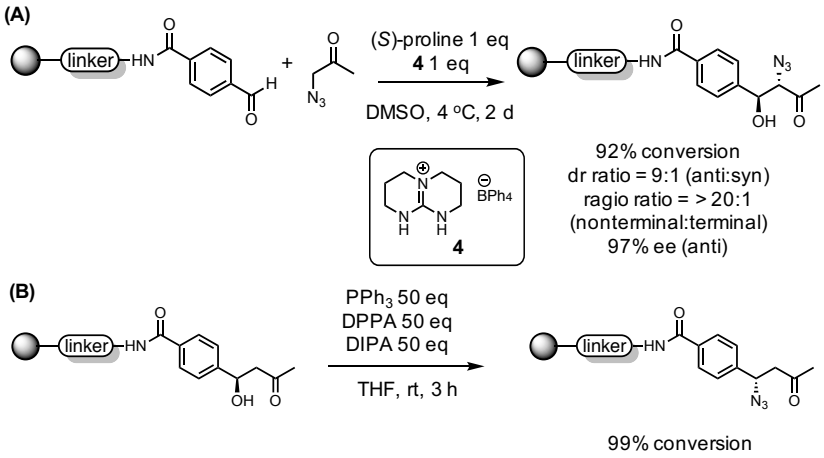

Figure 2. Incorporation of azide group to aldol product. (A) Aldol reaction using azido acetone. Diastereoisomeric and regioisomeric ratios were obtained by ^{1}H NMR of crude mixture. Ee were determined by chiral HPLC. (B) Conversion of the hydroxy group to an azide using the Mitsunobu reaction.

The author hypothesized that the mild conditions employed for the proline-catalyzed aldol reaction would be compatible with encoding DNA. To address this point, the author employed a quantitative polymerase chain reaction (qPCR) assay described by Malone and Paegel in which a 200 bp double-stranded DNA molecule is subjected to the reaction conditions and the amount of DNA that remains amplifiable by the polymerase chain reaction (PCR) is quantified. Thus, the immobilized DNA was incubated for 16 h at room temperature in the presence of acetone, immobilized aldehyde and proline. The qPCR data showed that at least 90% of the DNA could be amplified relative to a control reaction in which the DNA was not exposed to any chemical reagents (Figure 3).

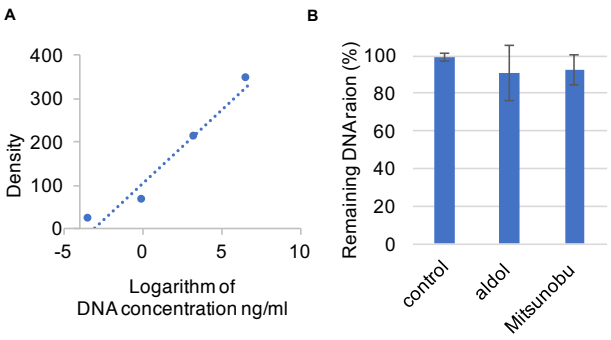

Figure 3. Quantification of amplifiable DNA remaining ratio by DNA damage assay. (A) Calibration curve made by DNA standard samples of a known concentration. R = 0.96. (B) Remaining DNA damage ratio of aldol reaction and Mitsunobu reaction. The remaining DNA ratio of aldol reaction values were 91 ± 14%. That of Mitsunobu reaction were 93 ± 8%. Results were generated from triplicate experiments.

In conclusion, the proline-catalyzed aldol reaction has been adapted to bead-based synthesis. To a large degree, the trends observed in the solid-phase reaction parallel those observed when the reaction is carried out in solution, the major difference being the need for a large excess of ketone and an equivalent of proline. As anticipated, the reaction conditions have little or no effect on the amplifiability of encoding DNA. Therefore, this process should be a valuable tool for the construction of DNA-encoded OBOC libraries. Finally, the author have employed in this study a disulfide linker that can be cleaved reductively[9] to ensure that our analysis of the intrinsic stereoselectivity of the aldol reaction was not compromised by the chemistry used to release the compound from the bead, as might be the case for acidic cleavage, for example. In subsequent work the author have found that cleavage of compounds from resins with RAM linkers by brief treatment with dilute trifluoroacetic acid does not result in detectable racemization, so there is no need to use the disulfide linker if this is not convenient.

Experimental Section

General Information

Synthetic resins were purchased from Rapp Polymere GmbH (Germany). All of the chemical reagents and solvents from commercial sources were used without further purification. HPLC and LC-MS analysis was carried out by Agilent 1100 Series equipped with ZORBAX SB-C18 Rapid Res, 4.6 × 100 mm × 3.5 μm column, PDA detector and a linear gradient of 5% acetonitrile, 0.05% formic acid/aqueous solution to 95% acetonitrile, 0.05% formic acid/aqueous solution in 1.0 mL/min flow rate, 15 min gradient.

All steps involving water utilized distilled water filtered through a Barnstead Nanopure filtration system (Thermo Scientific). ^{1}H and ^{13}C NMR spectra were recorded on a Bruker AM 400 spectrometer (operating at 400 and 101 MHz respectively) in $CDCD_3$ with 0.03% TMS as an internal standard, unless otherwise specified. Chemical shifts are reported in parts per million (ppm) downfield from TMS.

Immobilization of aldehyde on the beads

Tentagel HL NH_2 resin were swelled by DMF 2 h. The resin were acylated with solution of 1 M bromoacetic acid and 1 M DIC in DMF for 5 min at 37 °C. Halide displacement was performed by saturated cystamine dihydrochloride in MeOH : DIPEA = 2 : 1 solution for an hour at 37 °C. Formylbenzoic acid (4.0 eq to resin loading), Ethyl (hydroxyimino)cyanoacetate (Oxyma) (3.0 eq to resin loading) and *N*,*N*'-Diisopropylcarbodiimide (DIC, 3.0 eq to resin loading) were mixed together in DMF and reaction were conducted for 2 h at 37 °C.

Direct aldol reaction on the solid phase

Benzoic aldehyde on Tentagel NH_2 HL resin (0.06 mmol) were reacted with solution of (*S*)-proline (1.0 eq, 6.9 mg), soluble ketone (100 eq) in DMSO 850 μl at room temperature for 16 h. After reaction, aldol product on the resin was cleaved by 100 mM TCEP・HCl solution (pH 7.0) at room temperature for 90 min. Crude solution were purified by preparative HPLC (a linear gradient of 0–100% CH_3CN in H_2O containing 0.1% (v/v) TFA over 30 min) to afford a fraction of desired aldol product. Every compounds were extracted with DCM, then dried under vacuum.

Compound 1a

250 mg of Tentagel NH_2 HL resin (0.49 mmol, 120 µmol) was used for synthesis. Yields was 9.2 mg (29%). **^{1}H-NMR of 1a** (700 MHz; CD_3OD): δ 7.83 – 7.78 (m, 2H), 7.50 – 7.46 (m, 2H), 5.18 (dd, J = 9.0, 4.2 Hz, 1H), 3.53 (t, J = 7.0 Hz, 2H), 2.90 (dd, J = 16.1, 9.0 Hz, 1H), 2.79 (dd, J = 16.1, 4.2 Hz, 1H), 2.74 – 2.69 (m, 2H), 2.18 (s, 3H). **^{13}C-NMR of 1a** (700 MHz; CD_3OD): δ 209.4, 149.6, 128.5, 127.04, 70.62, 53.34, 49.40, 48.67, 44.46, 30.72, 24.43. HRMS (ESI-TOF MS) m/z: [M+H]+ Calcd for $C_{13}H_{18}NO_3S_1^+$ 268.10; Found 286.1016.

Procedure of DNA damage assay

Encoding tentagel beads with DNA

In a mobicol spin column10 mg of 10 µm tentagel beads were incubated in 500 µL BTPWB overnight rotating. The wells were then washed 1x with 150 µL of BTPLB and an encoding solution consisting of appropriate OP stocks 11XX[±] (60 µL, 60 µM, 1.2 nmol) and 22XX[±] (60 µL, 60 µM, 1.2 nmol), and T4 DNA ligase (171 U) was combined in BTPLB (450 µL total volume) for the resin sample and added to the appropriate wells. The plates were sealed and incubated rotating (4 h, RT). The mobicol spin column was washed 3x with BTPWB, and the process repeated for 13XX-24XX, 15XX-26XX, 17XX-28XX, 19XX-2AXX and terminating with Reverse Primer (0B01). Then, DNA encoded beads were subjected the same reaction conditions described above. Control reasin were suspended BTPLB at room temperature for 16 h.

qPCR analysis

qPCR matrix contained Taq DNA Polymerase (0.05 U/µL), oligonuclotide primers FWD-PCR1 and REV-PCR1 (0.3 µM each), SYBR Green (0.2X, Life Technologies), and PCR buffer (1X). 10 µm DNA encoded beads (1 µL, 50 beads/µL, BTPWB) were added to separate amplification wells containing qPCR matrix (20 µL). Supernatant for each resin sample (1 µL) was added to separate amplification wells (20 µL, 3 replicates). Template standard solutions (1 µL, 100 amol, 10 amol, 1 amol, 100 zmol, 10 zmol, 1 zmol, 100 ymol, and 10 ymol in BTPWB) were added to separate amplification reactions (20 µL). Reactions were thermally cycled (96 °C, 10 s; [95 °C, 8s; 72 °C, 24 s] x 30 cycles ; C1000 Touch Thermal Cycler, Bio-Rad, Hercules, CA) with fluorescence S5 monitoring (channel 4, CFX96 Real-Time System, Bio-Rad) and quantitated (CFX Manager, Version 3.1, Bio-Rad, baseline subtracted). The number of amplifiable tags per bead was calculated by dividing the qPCR result by the number of beads per well. The PCR sample (6 µL) was imaged on

gel by native PAGE (6% 1 x TBE, 6W, 30 min) and stained with SybrGold (Invitrogen). The brightness of each bands were quntified by ImageJ.

Aldol reaction with azidoacetone on the solid phase

Tentagel NH_2 HL resin were swelled by DMF 2h. Fmoc-Met-OH (4.0 eq to resin loading), Oxyma (4.0 eq to resin loading) and DIC (4.0 eq to resin loading) were mixed together in DMF and reaction were conducted for 2 h at 37 °C. After Fmoc deprotection by 20 % piperidine in DMF for 20 min at room temperature, Formylbenzoic acid (4.0 eq to resin loading), Oxyma (4.0 eq to resin loading) and DIC (4.0 eq to resin loading) were mixed together in DMF and reaction were conducted for 2 at 37 °C. Benzoic aldehyde on resin (0.06 mmol) were reacted with solution of L-proline (1.0 eq, 6.9 mg), compound 4 (1.0 eq, 27.5 mg), and 850 µl azideacetone in DMSO 850 µl at 4 ^{o}C for 2 days. After reaction, compounds were cleaved by 20 mg/mL CNBr solution in 0.2 M HCl at room temperature for 6 h. As the reaction was performed on solid phase in small scale, the author monitored the reaction conversion by measuring the ration of starting aldehyde and inactive benzoic ring which was mixed in the aldehyde resin in a certain amount.

Mitsunobu reaction on the solid phase

Tentagel NH_2 HL resin were swelled by DMF 2. Fmoc-Met-OH (4.0 eq to resin loading), Oxyma (4.0 eq to resin loading) and DIC (4.0 eq to resin loading) were mixed together in DMF and reaction were conducted for 2 h at 37 °C. After Fmoc deprotection by 20 % piperidine in DMF for 20 min at room temperature, Formylbenzoic acid (4.0 eq to resin loading), Oxyma (4.0 eq to resin and DIC (4.0 eq to resin loading) were mixed together in DMF and reaction were conducted for 2 h at 37 °C. Benzoic aldehyde on resin (0.06 mmol) were reacted with solution of L-proline (1.0 eq to resin loading, 6.9 mg), ketone (100 eq to resin loading) in DMSO 850 µl at room temperature for 16 h. Triphenylphosphine (75 mg, 50 eq to resin loading) and diisopropyl azodicarboxylate (70 ml, 50 eq to resin loading) was dissolved in THF 100 ml cooling in the ice bath. Then, Dipehnyl phosphorazidate (65 ml, 50 eq to resin loading) was added dropwisely cooling in the ice bath. This reaction mixture were added to the resin (0.006 mmol) at room temperature for 3 h. After reaction, compounds were cleaved by 20 mg/mL CNBr solution in 0.2 M HCl at room temperature for 6 h. As the reaction was performed on solid phase in small scale, the author monitored the reaction conversion by measuring the ration of starting aldehyde and inactive benzoic ring which was mixed in the aldehyde resin in a certain amount.

References

1. (a) Sakthivel, K., Notz, W., Bui, T. & Barbas, C.F. 2001, "Amino acid catalyzed direct asymmetric aldol reactions: a bioorganic approach to catalytic asymmetric carbon−carbon bond-forming reactions", *Journal of the American Chemical Society,* vol. 123, no. 22, pp. 5260-5267. (b) List, B., Pojarliev, P. & Castello, C. 2001, "Proline-catalyzed asymmetric aldol reactions between ketones and α-unsubstituted aldehydes", *Organic Letters,* vol. 3, no. 4, pp. 573-575. (c) Hoang, L., Bahmanyar, S., Houk, K. & List, B. 2003, "Kinetic and stereochemical evidence for the involvement of only one proline molecule in the transition states of proline-catalyzed intra-and intermolecular aldol reactions", *Journal of the American Chemical Society,* vol. 125, no. 1, pp. 16-17. (d) Notz, W., Tanaka, F. & Barbas, C.F. 2004, "Enamine-based organocatalysis with proline and diamines: the development of direct catalytic asymmetric aldol, Mannich, Michael, and Diels−Alder reactions", *Accounts of Chemical Research,* vol. 37, no. 8, pp. 580-591. (e) Mase, N., Tanaka, F. & Barbas III, C.F. 2004, "Synthesis of β-Hydroxyaldehydes with stereogenic quaternary carbon centers by direct organocatalytic asymmetric aldol reactions", *Angewandte Chemie International Edition,* vol. 43, no. 18, pp. 2420-2423. (f) List, B., Hoang, L. & Martin, H.J. 2004, "New mechanistic studies on the proline-catalyzed aldol reaction", *Proceedings of the National Academy of Sciences of the United States of America,* vol. 101, no. 16, pp. 5839-5842.
2. Subirós-Funosas, R., Prohens, R., Barbas, R., El-Faham, A. & Albericio, F. 2009, "Oxyma: An efficient additive for peptide synthesis to replace the benzotriazole-based HOBt and HOAt with a lower risk of explosion [1]", *Chemistry–A European Journal,* vol. 15, no. 37, pp. 9394-9403.
3. Hartikka, A. & Arvidsson, P.I. 2004, "Rational design of asymmetric organocatalysts—increased reactivity and solvent scope with a tetrazolic acid", *Tetrahedron: Asymmetry,* vol. 15, no. 12, pp. 1831-1834.
4. Zhou, Y. & Shan, Z. 2006, "Chiral diols: A new class of additives for direct aldol reaction catalyzed by L-proline", *The Journal of Organic Chemistry,* vol. 71, no. 25, pp. 9510-9512.
5. Reis, Ö., Eymur, S., Reis, B. & Demir, A.S. 2009, "Direct enantioselective aldol reactions catalyzed by a proline–thiourea host–guest complex", *Chemical Communications,* no. 9, pp. 1088-1090.

6. Martínez-Castañeda, A., Poladura, B., Rodríguez-Solla, H., Concellon, C. & del Amo, V. 2011, "Direct aldol reactions catalyzed by a heterogeneous guanidinium salt/proline system under solvent-free conditions", *Organic Letters,* vol. 13, no. 12, pp. 3032-3035.
7. Martinez, A., van Gemmeren, M. & List, B. 2014, "Unexpected beneficial effect of *ortho*-substituents on the (*S*)-proline-catalyzed asymmetric aldol reaction of acetone with aromatic aldehydes", *Synlett,* vol. 25, no. 7, pp. 961-964.
8. List, B. 2002, "Proline-catalyzed asymmetric reactions", *Tetrahedron,* vol. 28, no. 58, pp. 5573-5590.
9. Martínez-Castañeda, Á., Kędziora, K., Lavandera, I., Rodríguez-Solla, H., Concellón, C. & del Amo, V. 2014, "Highly enantioselective synthesis of α-azido-β-hydroxy methyl ketones catalyzed by a cooperative proline–guanidinium salt system", *Chemical Communications,* vol. 50, no. 20, pp. 2598-2600.
10. Fisher, K.J., Turkett, J.A., Corson, A.E. & Bicker, K.L. 2016, "Peptoid Library Agar Diffusion (PLAD) assay for the high-throughput identification of antimicrobial peptoids", *ACS Combinatorial Science,* vol. 18, no. 6, pp. 287-291.

Chapter 3. Conclusions

1-1. The author has established chemical synthesis of Src SH2 domains and application to mirror-image screening systems for isolation of Src SH2 domain inhibitors. $Src^{145-251}$ and its modified derivatives including Src^{TMR} and Src^{biotin} were prepared by the facile synthetic protocol. Several in vitro assays were developed using synthetic proteins, namely SPR analysis, FP assay, ELISA and chemical array. The primary chemical array and the secondary ELISA screening from natural products and its derivatives provided by RIKEN identified a number of chiral compounds with inhibitory activity towards target proteins.

1-2. The author has established chemical synthesis of XIAP BIR3 domain and application to mirror-image screening systems for isolation of XIAP BIR3 domain inhibitors. $XIAP^{241-356}$ and its modified derivatives including $XIAP^{TMR}$ and $XIAP^{biotin}$ were prepared by the facile synthetic protocol using conserved amino acids. Several in vitro assays were developed using synthetic proteins, namely SPR analysis, FP assay, ELISA and chemical array are developed. The primary chemical array screening from natural products and its derivatives provided by RIKEN identified a number of chiral compounds with binding activity towards target proteins.

2. The author has developed solid-phase synthesis of β-hydroxy ketones *via* the organocatalytic aldol reactions for DNA-encoded OBOC library construction. The optimized reaction condition provided desired aldol products. The reactions including a variety of aldehyde and various soluble ketones proceeded with almost quantitative conversion and modest ee. The mild reaction conditions have little or no effect on the amplifiability of encoding DNA. Azido group were successfully incorporated by using azidoaceton as a substrate or conduct mitsunobu reaction toward aldol products, allowing further chain elaboration of the molecule.

Abbreviations

Ahx: aminocaproic acid
BIR: baculovirus IAP repeat
Btl: bruton's tyrosine kinase
Dbz: 3,4-diaminobenzoic acid
DIAP: *drosophila* inhibitor of apoptosis protein
DIPCI: *N*,*N*′-diisopropylcarbodiimide
EDT: 1,2-ethanedithiol
EDTA: ethylenediaminetetraacetic acid
ELISA: enzyme-linked immunosorbent assay
FAM: carboxyfluorescein
FP: fluorescence polarization
Gu: guanidine
HBTU: 2-(1*H*-benzotriazol-1-yl)-1,1,3,3-tetramethyluronium hexafluorophosphate
HEPES: 4-(2-hydroxyethyl)-1-piperazineethanesulfonic acid
HIV: human immunodeficiency virus
HmT: Hapv middle T antigen
HOBt: 1-hydroxybenzotriazole
HRP: horseradish peroxidase
IAP: inhibitor of apoptosis protein
MDM2: mouse double minute 2 homolog
MES: 2-mercaptoethanesulfonic acid
MFD: metal-free desulfurization
MPAA: 4-mercaptophenylacetic acid:
Nbz: *N*-acyl-benzimidazolinone
NCL: native chemical ligation
OBOC: one-bead one-compound
OpIAP: IAP generated from the *Orgyia pseudotsugata* nuclear polyhedrosis virus
PBS: phosphate buffered saline
PI3K: phosphoinositide 3-kinase
PPI: protein-ptein interactions
SH2: Src homology 2 domain
SMAC: second mitochondria-derived activator of caspase
SPPS: solid-phase peptide synthesis
SPR: surface plasmon resonance
TCEP: tris(2-carboxyethyl)phosphine
Thz: thioproline
TMB: 3,3',5,5'-tetramethylbenzidin
TMR: tetramethylrhodamine
XIAP: X-linked IAP

Acknowledgements

The author wishes to express my deepest gratitude to Associate Professor Shinya Oishi, Professor Hiroaki Ohno, and Professor Nobutaka Fujii (Graduate School of Pharmaceutical Sciences, Kyoto University) for their directions and valuable discussion during this work. Their idea/thoughts always stimulated my scientific interests and enhanced my ability of logical thinking.

The author would like to express my sincere gratitude to Professor Koichiro Oshima, Professor Eiichi Yamaguchi, and Professor Dimiter Ialnazov (Graduate school of Advanced Integrated Studies in Human Survivability, Kyoto University) for the constant encouragement and perspective comments to help me move forward.

The author is extremely grateful to Dr. Thomas Kodadek (The Scripps Research Institute, Florida) for accepting my external internship and having supervised me on this study.

The author would like to show my great appreciation to Professor Hiroyuki Osada, Dr. Yasumitsu Kondoh, and Dr. Kaori Honda (RIKEN Center for Sustainable Resource Science) for their professional guidance as well as technical supports to accomplish this research.

The author is grateful to all of the previous and present-members of Department of Bioorganic Medicinal Chemistry/Department of Chemogenomics (Graduate School of Pharmaceutical Sciences, Kyoto University), Graduate school of Advanced Integrated Studies in Human Survivability, and Kodadek Laboratory (The Scripps Research Institute, Florida) for providing all the necessary information to help finishing the study.

And at the end but not least, the author would like to thank my family, though none of you have really contributed scientifically but your unceasing encouragement and support are deeply appreciated.

List of Publications

This study was published in the following papers.

Chapter 1.

Section 1. Synthesis of the Src SH2 Domain and its Application in Bioassays for Mirror-image Screening

Keitou Shu, Taro Noguchi, Kaori Honda, Yasumitsu Kondoh, Hiroyuki Osada, Hiroyuki Ohno, Nobutaka Fujii, and Shinya Oishi

RSC Advances, vol. 7, no. 61, pp. 38725-38732, 2017.

Section 2. Synthesis of XIAP BIR3 Domain for Mirror-image Screening

Keitou Shu, Kaori Honda, Yasumitsu Kondoh, Hiroyuki Osada, Hiroyuki Ohno, Nobutaka Fujii, and Shinya Oishi

Manuscript in preparation

Chapter 2. Solid-Phase Synthesis of β-Hydroxy Ketones Via DNA-Compatible Organocatalytic Aldol Reactions

Keitou Shu, and Thomas Kodadek

ACS Combinatorial Science, vol. 20, no. 5, pp. 277-281, 2018.